

STUDY OVERVIEW OF THE NEAR EARTH ASTEROID SAMPLE RETURN



An ESA Technology Reference Study

Planetary Exploration Studies Section (SCI-AP)
Science Payload and Advanced Concepts Office (SCI-A)






prepared by/préparé par	David Agnolon
reference/référence	SCI-PA/2007/004/DA
issue/édition	1
revision/révision	0
Date of issue/date d'édition	31/05/2007
status/état	Released
Document type/type de document	Public report

European Space Agency
Agence spatiale européenne

ESTEC
Keplerlaan 1 - 2201 AZ Noordwijk - The Netherlands
Tel. (31) 71 5656565 - Fax (31) 71 5656040

Study overview of the near earth asteroid
sample return

Near Earth Asteroid Sample Return Technology Reference Study – Study Team		
ESA 	David Agnolon Peter Falkner Jens Romstedt Detlef Koschny Tra-Mi Ho	NEA-SR TRS Study manager NEA-SR TRS Study Technical officer Support of in-situ engineering and science activities NEA-SR TRS Study scientist Science consultancy
Astrium Satellites UK 	Marie-Claire Perkinson Kian Yazdi Angelo Povoleri Paolo D'Arrigo Michael Wilkinson Howard Gray Simon Barraclough Dave Pecover John Shiell Graham Viney Ben Green Mark Bonnar Paolo Ponzio	Project Manager Lead systems engineer Mission Analysis engineer Mission consultant Assistant engineer Solar electric propulsion consultant Thermal architect Operations engineer Mechanisms engineer Chemical propulsion architect Data handling consultant Design engineer Cost engineer
Astrium Satellites France	Xavier Sembely Sébastien Boulade Guillaume Bodineau	Systems engineer Systems engineer GNC engineer
Astrium Space Transportation France	Jean Marc Bouilly Francine Bonnefond Jérôme Bertrand Philippe Tran	Technical manager and thermal protection expert Programme manager Design engineer Aerothermodynamics expert
Galileo Avionica 	Piergiovanni Magnani Edoardo Re Roland Gelmi Mirko Izzo	Sampling system project leader Program manager Systems engineer Systems engineer

Near-Earth Asteroid Sample Return Technology Reference Study – Mission Summary

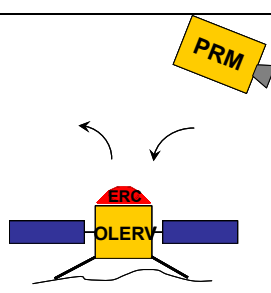
Key scientific objectives	Physical, chemical and mineralogical characterization of a primitive solar system object (NEA 1999JU3) via sample return to possibly enhance our understanding about: <ul style="list-style-type: none"> ○ The initial conditions of the solar nebulae and its evolution history, ○ The properties of the planet building blocks, ○ The link between meteorites and asteroids, ○ The nature and origins of organic compounds, ○ NEAs' possible contribution to early life and the threat they might now represent. 		
Strawman reference payload assumed for this study	<ul style="list-style-type: none"> ● NEA Orbiter-Lander-Earth Return Vehicle (OLERV) module: <ul style="list-style-type: none"> ○ During remote sensing: Narrow Angle Camera, Wide Angle Camera (also used for surface science), Radio Science Experiment, UV-visible-NIR imaging spectrometer ○ During surface operations: Sub-surface micro-camera, thermometer 		
Launch and transfer	<ul style="list-style-type: none"> ● Launch of 2335 kg into GTO by Soyuz-Fregat 2-1B (Kourou) (05-12-2016) ● Forward transfer + Insertion into asteroid orbit via dedicated chemical propulsion module ● Return to Earth of the Orbiter-Lander-Earth Return Vehicle module (04-12-2020): Low ΔV 		
Orbiting, Landing and Sampling	<ul style="list-style-type: none"> ● Preliminary 3-4 months of science orbital operations + selection of landing site ● Sampling rehearsals to increase chances of success ● Landing + sampling operations (design allows up to 3): descent ~ 40 minutes from 500 m orbit, sampling ~ 20 minutes, immediate re-ascent after completion of sampling operations ● Total stay about the asteroid: up to 8 months, possibly extended 		
Earth return vehicle	<ul style="list-style-type: none"> ● OLERV carries Earth Re-entry Capsule (ERC) back to Earth ● Hard landing with crushable energy-absorbing structure following high speed Earth re-entry (12.5 km/s) 		
S/C Modules	Propulsion Module (PRM)	Orbiter-Lander-ERV	Earth Re-entry Capsule
Stabilization	NA	3-axis	Spin
Orbit/Altitude	Forward interplanetary trajectory + insertion into orbit about the asteroid	6 km circular orbit (remote sensing) + landing + return to Earth	Descent throughout Earth atmosphere
Initial inclination	NA	90° polar terminator orbit about the asteroid	V_{∞} elevation: -45°
S/C ΔV requirements	2.55 km/s	~ 66 m/s (operations about the asteroid) + ~ 640 m/s (Earth return)	NA
Operational lifetime	~ 3 years	> 4 years	> 4 years
Dry mass (incl. subsystem, excl. system margins)	210 kg	363 kg (excl. ERC)	57
Total dry mass	756 kg (incl. 20% system margin)		
P/L mass	420 kg (OLERV+ERC)	64 kg (ERC + remote sensing suite)	6 kg (sample container)
Total wet mass	2335 kg (incl. all margins)		
Power (peak)	752 W (rendezvous manoeuvre)		
Telemetry band	NA	X/X (+Ka downlink in support of radio science)	UHF beacons for recovery
Continuous compressed science bit rate	NA	5.46 kbps (average over 24 h)	NA
Key mission drivers	<ul style="list-style-type: none"> ● Target selection ● Low gravity operations (in particular at landing) + unknown soil properties ● Surface stay time ● Earth re-entry and landing velocity 		
Key critical technologies	<ul style="list-style-type: none"> ● Sampling mechanism for autonomous short-term collection ● Navigation camera and software for autonomous soft landing ● Image processing algorithms for on-board real-time image recognition ● Ratcheting landing legs with damping capability ● Sample containment and transfer ● Earth Re-entry Capsule ● Energy absorbing material for hard landing 		

TABLE OF CONTENTS

1	INTRODUCTION	9
1.1	Study objective	9
1.2	Mission concept requirements	9
2	NEAR-EARTH ASTEROIDS (NEA)	10
2.1	NEA science and environment	10
2.1.1	Small bodies in the solar system	10
2.1.2	Near-earth asteroids: overview	11
2.1.3	NEA properties: science facts and environment	12
2.1.3.1	Composition	12
2.1.3.1.1	Chemical, mineral composition and taxonomy	13
2.1.3.1.2	Space weathering, surface gardening [Chapman04II]	14
2.1.3.1.3	Surface properties related to sampling	15
2.1.3.1.4	Magnetism	17
2.1.3.2	Global physical properties	17
2.1.3.2.1	Mass and gravitational properties	17
2.1.3.2.2	Size, Volume	18
2.1.3.2.3	Bulk density and porosity	18
2.1.3.2.4	Rotation state and shape	18
2.1.3.2.5	Binaries	19
2.1.4	Ground observations	19
2.2	Missions to Near-Earth Asteroids	20
2.2.1	Past, current and planned missions	20
2.2.2	NEA Mission concept studies	21
2.3	Scientific requirements of the TRS mission concept	23
2.3.1	Taxonomy	23
2.3.2	Science objectives	23
2.3.2.1	Remote sensing objectives	23
2.3.2.2	Sample requirements for a sample return scenario	25
2.3.2.2.1	Size/Mass	25
2.3.2.2.2	Location	25
2.3.2.2.3	Composition	25
2.3.2.3	Science objectives for an in-situ investigation scenario	25
2.3.2.4	Planetary protection aspects and scientific integrity of the sample	26
3	TRADE-OFF APPROACH	27
3.1	Overall trade-off	27
3.2	Science payload trade-off	28
4	SELECTION OF TARGET AND BASELINE ARCHITECTURE	30
4.1	Down-selected targets	30
4.2	Mission architecture trade	32
4.2.1	Mission analysis	32

4.2.2	Earth re-entry	33
4.2.3	Configuration	33
4.2.3.1	Options	33
4.2.3.2	Scenario analysis	34
4.2.3.2.1	Scenario 1 (single spacecraft)	34
4.2.3.2.2	Scenario 2 (single spacecraft + dedicated outbound propulsion module)	35
4.2.3.2.3	Scenario 3 (Orbiter-only spacecraft + lander-return vehicle)	36
4.2.3.2.4	Scenario 4 (orbiter-return vehicle + lander-only spacecraft)	36
4.2.4	Mission architecture trade	36
5	MAJOR TRADE-OFF: SAMPLING STRATEGY	38
5.1	Mission architecture summary	38
5.2	Sampling operations	39
5.2.1	Landing/sampling strategy	39
5.2.2	Sampling mechanism	40
5.2.2.1	Trade-off	40
5.2.2.2	Selected concept	42
5.3	Extended stay and in-situ science	42
5.3.1	Extended stay: Ground involvement and additional science	43
5.3.2	Additional requirements and consequences	43
5.3.2.1	Anchoring	43
5.3.2.2	In-situ instrumentation	44
5.3.3	Available options and trade-off	46
5.3.3.1	Options for an extended stay	46
5.3.3.2	Consequences for thermal, power, communication and mechanical design	47
5.4	GNC strategy during descent and landing	50
6	DESIGN OF SELECTED MISSION CONCEPT	51
6.1	Baseline scenario	51
6.1.1	mission analysis	51
6.1.1.1	Transfers to the selected target	51
6.1.1.2	Back-up launch dates and targets	52
6.1.1.3	Geometry of the transfer	53
6.1.2	1999 JU3 properties	53
6.1.3	Launch vehicle	55
6.1.4	Mission operations	56
6.1.4.1	Operations overview	56
6.1.4.2	Departure strategy	57
6.1.4.3	Target approach	57
6.1.4.4	Proximity operations	58
6.1.4.4.1	Asteroid observations from orbit	58
6.1.4.4.2	Landing, sampling and re-ascent operations	59
6.2	Design margins	61
6.3	System overview	62
6.4	OLERV Configuration and structures	64
6.5	Propulsion	65
6.5.1	Propulsion module	65

6.5.2	OLERV RCS	66
6.6	GNC and AOCS	68
6.6.1	Equipment	68
6.6.2	Simulations and performances	69
6.6.2.1	1-burn descent guidance strategy	69
6.6.2.2	Navigation for landing prior to descent	70
6.6.2.3	Navigation for landing during descent	72
6.7	Mechanisms	74
6.7.1	Landing legs	74
6.7.1.1	Design	74
6.7.1.2	Stability analysis	76
6.7.2	Sampling mechanism	76
6.7.3	Sample containment and transfer	79
6.8	Earth Re-entry Capsule	80
6.9	Thermal	82
6.10	Power	84
6.11	Data handling	85
6.12	Telecommunications	86
6.13	Ground segment and equipment	86
7	CONCLUSION	87
8	LIST OF ABBREVIATIONS	88
9	REFERENCES	90
ANNEXES		94
	OLERV dimensions and equipment accommodation	94
	Power system budget	96
	Vega launch	97
	TRL levels	97
 FIGURES		
Figure 1:	Orbits of the over 50,000 catalogued asteroids	11
Figure 2:	Space weathering [Noble05]	14
Figure 3:	Evidence of Regolith on two S-type Asteroids: Eros (left) and Itokawa (right)	15
Figure 4:	“Cigar”-shaped NEA with rotation axis along the axis of maximum inertia	19
Figure 5:	Trade-offs to be conducted for an asteroid sample return	27
Figure 6:	Propellant-to-mass ratio for most accessible targets	31
Figure 7:	Critical landing with large solar panels	35
Figure 8:	Mission concept design tree	38
Figure 9:	Selected sampling concept	42
Figure 10:	Configuration options for extended surface stay	46
Figure 11:	Spacecraft temperature variation for extended stay	48
Figure 12:	Battery mass increase with respect to stay duration	49

Figure 13: Toppling situation at landing.....	50
Figure 14: sensitivity to launch date and departure date from the asteroid for 2016 mission	52
Figure 15: Geometry of the interplanetary transfers	53
Figure 16: Spherical projection of the surface temperature distribution for asteroid at 1.06AU with a 25 hour rotation period	54
Figure 17: Heat flux on spacecraft during freefall to sub solar point	55
Figure 18: Injection into GTO with apogee raising and then escape to a 4.5km/sec V_{∞} orbit	57
Figure 19: Asteroid rendezvous manoeuvres	58
Figure 20: Orbit disturbances	59
Figure 21: Exploded view of the Spacecraft composite (left) – Spacecraft within the launcher fairing (right) (without MLI)	62
Figure 22: Spacecraft functional architecture	63
Figure 23: “Mono-block” OLERV baseline design	64
Figure 24: Alternative OLERV design - separation of the sampling module with the return vehicle.....	65
Figure 25: Propulsion Module design	66
Figure 26: RCS thrusters: functional architecture and configuration	67
Figure 27: AOCS functional architecture.....	68
Figure 28: One-burn descent strategy - trajectory	69
Figure 29: Influence of the landing latitude Figure 30: Influence of the initial orbit altitude	69
Figure 31: Final descent velocity	70
Figure 32: Position estimation via comparison with DEM model on ground	70
Figure 33: Cross-track error Figure 34: Along-track error	71
Figure 35: Velocity error - cross-track (left), along-track (right)	71
Figure 36: Shadow motion	72
Figure 37: Descent vision-controlled trajectory.....	73
Figure 38: Worst case landing scenario	74
Figure 39: Landing legs required footprint to ensure stability at landing.....	75
Figure 40: Ratcheting landing leg design	75
Figure 41: Worst case condition for bouncing-off the surface	76
Figure 46: Sampling mechanism design	77
Figure 47: Sampling - Interface design of the coring tool	77
Figure 48: Corer closing mechanism – a possible design option.....	77
Figure 49: Sampling mechanism - deployment and sampling steps.....	78
Figure 50: Sample transfer system - design and operations.....	80
Figure 51: Earth Re-entry Capsule design	80
Figure 52: Sensitivity analysis of ERC entry parameters	81
Figure 53: ERC accommodation and structure	82
Figure 54: Internal spacecraft temperature variation with baselined thermal control	83
Figure 55: Parabolic-shaped radiators for externally-mounted equipment.....	83
Figure 56: Variation of eclipse duration wrt orbit radius.....	84
Figure 57: OLERV dimensions (side view).....	94
Figure 58: OLERV dimensions (top view)	94
Figure 59: OLERV internal and external equipment accommodation	95
Figure 60: OLERV sampling and landing GNC equipment accommodation	95
Figure 61: Power budget	96

TABLES

Table 1: NEA Classification [NEOMAP05].....	12
Table 2: Asteroid spectral types, features and mineralogical interpretations	14
Table 3: Surface temperature range for assumed model asteroids.....	16
Table 4: Parameters associated to typical NEAs	17
Table 5: Overview of past, current and planned missions to small bodies.....	20
Table 6: Mission concept studies for small bodies' exploration.....	21
Table 7: Ranking of the asteroid spectral types for the study	23
Table 8: Remote sensing science objectives	24
Table 9: In-situ measurement science objectives.....	25
Table 10: Remote sensing reference payload suite.....	28
Table 11: Optional remote sensing instruments.....	30
Table 12: Selected targets - main physical and orbital parameters.....	32
Table 13: Configuration options	34
Table 14: Preliminary launch mass margins for each identified sample return scenario	37
Table 15: Sampling operations – options trade-off.....	40
Table 16: Sampling mechanism options suitable to selected sampling approach – Trade-off.....	41
Table 17: Description of optional in-situ instruments	45
Table 18: Technical features of optional in-situ instruments (do not include margins)	45
Table 19: Advantages and drawbacks of configuration options for extended stay.....	47
Table 20: GNC options for descent and landing - trade-off.....	51
Table 21: Baseline + optional transfers.....	51
Table 22: Baseline transfer with a 10 months stay about 1999JU3	52
Table 23: 1999JU3 properties	54
Table 24: Baseline launch vehicle's technical features	55
Table 25: Primary operational phases.....	56
Table 26: Descent, landing, sampling and ascent operations.....	61
Table 27: Margin overview.....	61
Table 28: System mass budget.....	63
Table 29: Propulsion Module technical features.....	65
Table 30: OLERV RCS: ΔV and thrust requirements	67
Table 31: Navigation accuracy at landing departing from 500 m orbit.....	71
Table 32: Monte-Carlo GNC simulation parameters.....	73
Table 33: Simulations results.....	74
Table 34: ERC technical features.....	81
Table 35: Power system characteristics	84
Table 36: Enabling technologies for the selected asteroid sample return mission concept.....	87
Table 37: VEGA Launch margins	97
Table 38: ESA TRL levels.....	97

1 INTRODUCTION

This document provides an overview of the Near-Earth Asteroid Sample Return system design study led by SCI-AP (Science Payload and Advanced Concept Office, Planetary Exploration Studies Section) and prime contracted by Astrium Satellites UK and largely makes use of the technical work provided by the industrial team. The Near-Earth Asteroid Sample Return (NEA-SR) is one of the Technology Reference Studies (TRS) introduced by the Science Payload & Advanced Concepts Office (SCI-A) at ESA. The overall purpose of the TRSs is to focus the development of strategically important technologies that are of likely relevance to potential future science missions. This is accomplished through the study of technologically demanding and scientifically interesting missions, which are currently not part of the ESA science programme ([SCI_A04]). The TRSs subsequently act as a reference for possible future technology development activities.

A mission concept to explore a primitive Near Earth Asteroid and return a scientifically valuable sample has been investigated in the TRS context because of the particular technology challenges related to the target selection, the landing and sampling activities on a low-gravity body and the Earth atmospheric re-entry. This activity builds on the study heritage provided by the Deimos Sample Return TRS [Renton06I]. In the NEA case, the optimal mission architecture is very much depending on the accessibility of the target, primarily because of the impact on the propulsion system, spacecraft configuration and therefore mass margins and associated sub-system technology. This is the reason why a large part of this report focuses on the various trade-offs which had to be conducted. More specifically, the asteroid environment (i.e. micro-gravity and surface properties) mainly drives the operations strategy, the guidance, navigation and control function, the sampling and transfer mechanism as well as the landing system. Most of these considerations are valid for any micro-gravity body sample return and, to a lesser extent, are also relevant to a planetary sample return. Last but not least, the return leg is a critical aspect of the concept and this study exploits the synergies with a Deimos Sample Return or a Mars Sample Return scenario.

The ultimate aim of the study is to identify the technologies which optimally enable the mission concept, and to provide requirements for the development of these technologies in a 5 year time frame. A particular effort was made so as to down-select available technologies or those which require a lesser development effort.

1.1 Study objective

The primary objective of the Near-Earth Asteroid Technology Reference Study is to establish a cost-efficient, scientifically meaningful and technologically feasible mission architecture for a near-Earth asteroid space-based mission concept. A large number of mission scenarios and designs and their related constraints are analysed with a particular emphasis on landing/sampling operations and technologies.

1.2 Mission concept requirements

The NEA exploration mission concept studied in the frame of this TRS shall primarily:

[MR1]

Perform a sample return (ASR) and/or in-situ surface investigation (AIS) of 1 or 2 NEAs: AIS is included in the top-level trade-off for completeness. However, a sample return mission concept is scientifically favoured if a cost-efficient design can be identified.

[MR2]

- Collect 100 g of asteroid material from any single sampling location in a sample return scenario [Molster03] & [Sears04II]
- Collect an amount of material which allows to identify the desired sample components in the in-situ investigation scenario
- Recover contextual information for both scenarios

[MR3]

Target a spectrally classified asteroid(s) of primary scientific interest: The scientific interest lying in the exploration of near-Earth asteroids is presented in next chapter. Exception is made for back-up targets which may be of unknown type.

[MR4]

Follow a design-to-cost, risk minimization approach: These constraints are obviously subjective. In particular, a sample return mission inherently presents many risk factors (landing, sampling, transfer, ascent, Earth re-entry). The ultimate aim of the study is to emphasize, for each identified mission option, element and technology, the particular cost and risk constraints which they are associated with and to down-select the concepts which minimize these parameters.

[MR5]

Make use of enabling technologies which development horizon is no more than 5 years (TRL 6 by 2011): TRL levels defined in Table 38

2 NEAR-EARTH ASTEROIDS (NEA)

2.1 NEA science and environment

2.1.1 SMALL BODIES IN THE SOLAR SYSTEM

During the formation of the solar system when our planets and sun accreted, a large number of small bodies (comets and asteroids) were left over as remnants of this process. These small bodies were part of the materials, building blocks, of the protoplanetary nebulae from which our solar system was formed (4.6 by years ago). Asteroids represent a large part of these primordial objects and reside throughout the solar system since its creation. Asteroid's exploration can therefore greatly enhance our understanding of the planetary formation process and constrain the related theories [CV05]. The asteroid population is highly diversified in many ways (orbital, physical, chemical and mineralogical properties, etc.). This high level of diversity is generally explained through two main mechanisms: their original accretion location in the primordial nebula and their subsequent evolutionary history. The main asteroid belt, which is believed to be the leftover of a planet formation process, is the main asteroid reservoir of the solar system but NEAs are much

more easily accessible with respect to the resource requirements of a space mission. It is to be noted that Near Earth Asteroids or NEAs are also sometimes identified with the more generic term of Near Earth Objects or NEOs due to the unclear boundary between some asteroid types and comets (some are believed to be residual dormant cometary cores such as 4015 Wilson-Harrington). In this document, we will keep the NEA definition for clarity purposes (observational definition: an object is called a comet if, and only if, a coma has been observed [DePater06]).

2.1.2 NEAR-EARTH ASTEROIDS: OVERVIEW

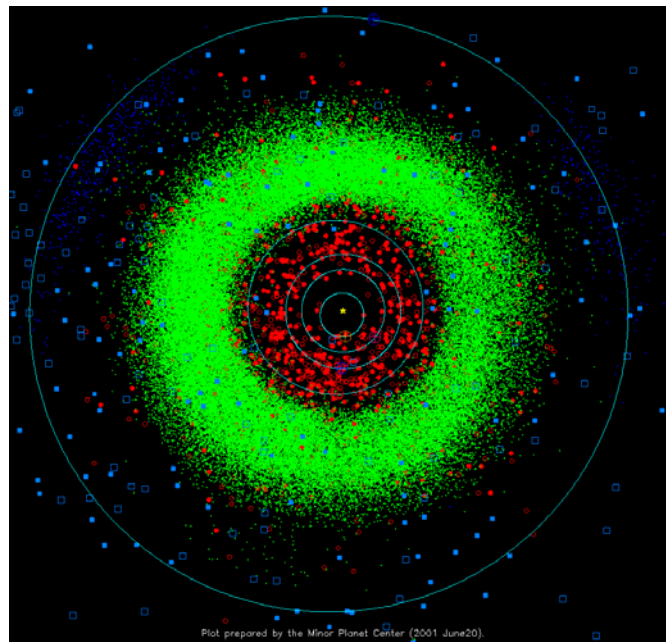


Figure 1: Orbits of the over 50,000 catalogued asteroids

*Green dots: Main belt, Red dots: Near-Earth Asteroids,
 Cloud of blue dots: Trojan asteroids, Blue circles: Orbits of
 Mercury, Venus, Earth, Mars, Jupiter*

As depicted in the previous figure, most asteroids are concentrated in a relatively flat toroidal region between the orbits of Mars and Jupiter (previously referred to as the Main Belt). However, a small number were (and still are) perturbed in their orbit (mainly via 3/1 mean motion resonance with Jupiter, collisional events, Yarkovsky effect [Bottke02], or others [Chapman04]) and can find their way inwards or outwards the solar system. A large number (~ 4000) of the asteroids which migrated to the inner solar system belongs to the so-called near-Earth asteroid population if their periastron is lower than 1.3 AU. The NEA population is itself divided into 3 sub-categories according to the orbital properties: Atens, Apollos and Amors (Table 1). For this study, the target is selected out of any of these 3 categories.

In addition to the main belt and near-Earth space, asteroids can mainly be found about Jupiter's Lagrange points (called Trojans), between Jupiter and Neptune (Centaurs) and also beyond Neptune (Trans-Neptunians).

Group	Description	Definition	Number
NEAs	Near-Earth Asteroids	$q < 1.3$ AU	~ 4000
Atens	Earth-crossing NEAs with semi-major axes smaller than Earth's (named after asteroid 2062 Aten). Spend most of their time inside the Earth's orbit	$a < 1.0$ AU, $Q > 0.983$ AU	263 (as of 23rd Feb 2005)
Apollos	Earth-crossing NEAs with semi-major axes larger than Earth's (named after asteroid 1862 Apollo). Spend most of their time outside the Earth's orbit	$a > 1.0$ AU, $q < 1.017$ AU	1676 (as of 23rd Feb 2005)
Amors	Earth-approaching NEAs with orbits exterior to Earth's but interior to Mars' (named after asteroid 1221 Amor).	$a > 1.0$ AU, $1.017 < q < 1.3$ AU	1260 (as of 23rd Feb 2005)
PHAs	Potentially Hazardous Asteroids: NEAs whose Minimum Orbit Intersection Distance (MOID) with the Earth is 0.05 AU or less and whose absolute magnitude (H) is 22.0 or brighter	$MOID \leq 0.05$ AU, $H \leq 22.0$	858 (as of 17 April 2007)
IEOs	Interior-to-the-Earth Objects having semi-major axis lower than 1 AU and aphelion lower than 0.983 AU	$a < 1.0$ AU, $Q < 0.983$ AU	3 (as of 23rd Feb 2005)

Table 1: NEA Classification [NEOMAP05]

Q : Aphelion, q : Perihelion, a : Semi-major axis,
 $Q_{Earth} = 1.017$ AU, $q_{Earth} = 0.983$ AU

The NEA population is specifically interesting in two ways.

- They most likely originated in the main belt and therefore their **intrinsic science interest** is almost entirely preserved.
- They navigate within vicinity of the Earth which makes them **easily accessible targets** for spacecraft (there are dozens of examples of NEAs for which a landing on the surface requires fewer resources than to land on the Moon).
- However, this property has a dramatic aspect in that some of them (defined as **Potentially Hazardous Asteroids**, PHA, [Chapman04], Table 1) have a non negligible probability of collision with the Earth. In order to evaluate the potential of a NEA to cause dramatic damages to the Earth biodiversity it is also necessary to understand its physical properties and its composition (e.g. interaction with the atmosphere and Earth crust at impact).

2.1.3 NEA PROPERTIES: SCIENCE FACTS AND ENVIRONMENT

2.1.3.1 Composition

Broadly speaking, asteroids can be distinguished as belonging to three major classes. Stony asteroids (70-80% of the NEA) are composed in large part of silicates with a variable content of

metals (mostly nickel & iron) and which underwent a certain degree of differentiation. Carbonaceous asteroids (20-25% of the NEA) are characterized by silicates with a high carbon and volatile content (ices and organic molecules) and with varying Iron content and which mostly remained in their primitive geological state. Metallic asteroids are likely to be the remains of the metallic cores of a fully differentiated body.

2.1.3.1.1 Chemical, mineral composition and taxonomy

Based on the available asteroid spectra determined from ground, a taxonomic system [Tholen89] has been obtained containing ~12 major classes and several subclasses, based on an early classification scheme [Chapman75]. Although some key mineral features have been identified in this way (e.g. olivine, pyroxene, metal), there are still considerable uncertainties about the exact mineralogical composition for each spectral class. Trying to make the link between meteorites and asteroids, which are thought to be their parent bodies, is an active field of research.

Class	Albedo	Brief description	Mineralogy meteorite analogues
P	< 0.06	Very dark and nearly featureless spectrum. Organic rich silicates, carbon and anhydrous silicates; interior water ice.	Organics, anhydrated silicates
D	0.04-0.09	Dark and reddish spectrum (possibly due to organics) strongly increasing with wavelength, band at 2.2 μm is possible. Organic rich silicates, carbon and anhydrous silicates; interior water ice.	Kerogen-like organic material, anhydrated silicates
C	0.04-0.09	Flat-reddish spectrum, weak UV band (shortwards of 0.4 μm), may have 3 μm band for hydrated silicates [Rivkin02]. Carbonaceous.	Phyllo silicates, carbon, organics, CI-CM chondrites
B	0.04-0.09	<u>C-subclass</u> , weak UV band, reflectance decreases with wavelength, may have 3 μm band	Hydrated silicates, carbon, chondrites
F	0.04-0.09	<u>C-subclass</u> , weak to nonexistent UV band, may have 3 μm band	Same as B-type
G	0.06-0.01	<u>C-subclass</u> , strong UV band < 0.4 μm , flat vis-near IR spectrum, bands at 0.6-0.7 and 3.0 μm	Hydrated silicates phyllosilicates, carbon, chondrites
T	0.06-0.10	Broad UV-visible absorption, flat near IR spectrum	(Troilite, metal)
K	Near 0.09	S-like visible spectrum, weak 1 μm band, flat reflectance at 1.1-2.5 μm . Eros family	Carbon, CV-CO chondrites, pyroxene
S	0.10-0.30	UV-visible band < 0.7 μm , 1.0 μm (and or no 2.0 μm) band, red slope in vis-near IR, significant spectral variations. Stony, metallic nickel-iron mixed with iron- and magnesium- silicates.	Pyroxene, olivine, metal
M	0.12-0.25	Featureless and reddish spectrum, near IR variations, high radar albedo. Metallic; nickel-iron.	Fe-Ni metal, enstatite
Q	0.16-0.21	Strong UV band, strong absorption (olivine, pyroxene) at 1 μm , no red slope, a rare class. Carbonaceous chondrites, metal.	Ordinary chondrites, pyroxene, olivine, Fe-Ni
A	0.17-0.35	Strong UV and 1 μm (olivine) bands, no 2.0 μm band, a rare class. Originated from differentiated mantle of an asteroid.	Olivine achondrites, pallasites, olivine

Class	Albedo	Brief description	Mineralogy meteorite analogues
V	0.23-0.40	Strong UV band, 1.0 and 2.0 μm bands, weak 1.5 μm feature. A rare, Vesta-like, class	Basaltic achondrites
R	0.30-0.40	Strong UV band, 1.0 and 2.0 μm bands, red slope, a rare class	Pyroxene, olivine-rich achondrites?
E	0.40-0.55	Highest albedo, featureless reddish spectrum, identical to P, M types, weak variability in near IR, inner main-belt	Enstatite achondrites, aubrites, Fe-free pyroxene

Table 2: Asteroid spectral types, features and mineralogical interpretations

Many asteroids belong to the low-albedo primitive C type, characterised by relatively neutral spectra exhibiting sometimes the signatures of aqueous alteration. The C-type asteroids are conventionally thought to be spectral analogues for carbonaceous chondrite meteorites. Some carbonaceous meteorites have suffered aqueous alteration at low temperatures, resulting in the formation of complex assemblages of hydrous clay minerals, carbonates, sulphates, and organic molecules. Few asteroids (B-, G- and F-type) show C-like spectra with minor differences at the shorter wavelengths, which may reflect degrees of metamorphism of C-like material. D-type and P-type asteroids have low albedo and are redder than the C-type ones. Their properties are less well understood than for other types but they are thought to be of most primitive origin. S-types have a higher albedo and their reddish spectra are characterised in the near-infrared side by the absorption band(s) of pyroxene and olivine. The relation between S-type asteroids and ordinary chondrites (the most common types of meteorite falls) has been debated for decades. Space weathering is a plausible explanation why S-type spectra do not properly match ordinary chondrite spectra. Some moderate albedo asteroids with very high radar reflectivity are almost certainly made out of pure metal (M type), probably a nickel-iron alloy, suggesting melting processes during the formation. More recent spectroscopy surveys have been performed. The measurement methods (use of CCDs, narrower wavelength band) lead to different and/or refined classification [Bus02].

2.1.3.1.2 Space weathering, surface gardening [Chapman04II]

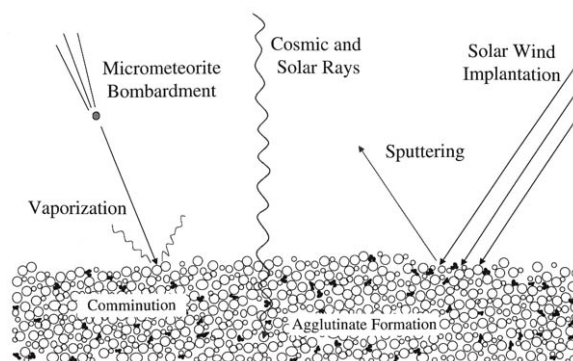


Figure 2: Space weathering [Noble05]

Present evidence suggests that space weathering (Optical alteration due to exposure to the space environment and shock) as well as surface gardening (Bombardment of the surface by small meteorites) has modified the spectral properties of asteroid surfaces, thus masking their true

compositions. The regolith top-layer, in particular, may contain particles from different parts of the asteroid, with 10 or more primary components. This is in fact one of the key reasons why sampling should preferably reach below the regolith top-layer.

2.1.3.1.3 *Surface properties related to sampling*

2.1.3.1.3.1 Mechanical and compositional properties

The basic understanding of NEA surface properties is very important for an asteroid mission which is supposed to collect surface samples. Understanding the composition, hardness of the soil and homogeneity is critical for the mission design, in particular when considering anchoring, drilling/coring or touch-and-go sample collection. Unfortunately very little is known about these properties, and this is also complicated by the differences in asteroid composition for different spectral classes.

The only two asteroid rendezvous missions to this date (NEAR and Hayabusa) were both to an S-type asteroid. Even in the two cases mentioned, a high level of diversity in the surface topography (crater vs no crater) and regolith properties (micron-sized vs coarse cm-sized particles) was found. The poor knowledge of the surface properties will certainly have an important influence on the design of the sampling system. In fact, it may have to cope with a wide range of particle sizes and different values of surface compactness. Due to the fact that a C-type asteroid has not undergone a high level of differentiation, it is however assumed for this study that no hard rock will be found on the surface. Therefore, the material is assumed to be limited to loose regolith or non magmatic compacted material.

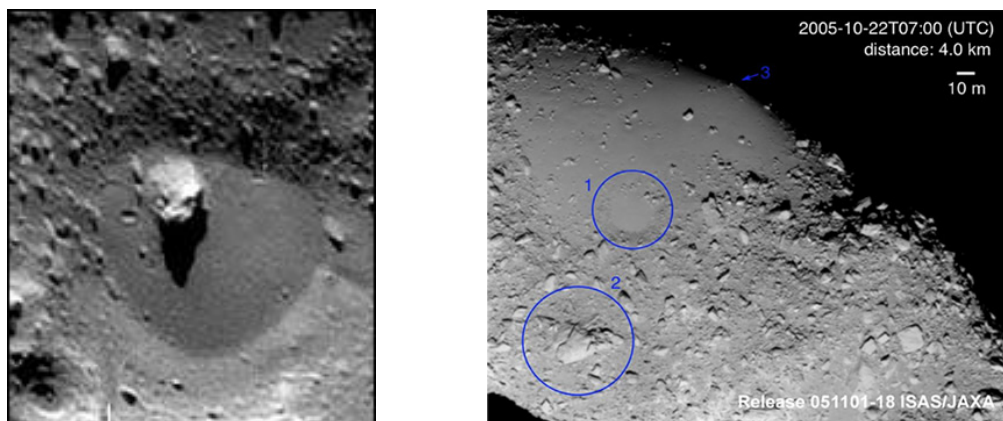


Figure 3: Evidence of Regolith on two S-type Asteroids: Eros (left) and Itokawa (right)

Blue circles show a large boulder and an area filled with regolith

A key goal of a NEA mission may also be to preserve volatiles and organics content from a regolith sample. Certain volatiles, like water ice would sublimate relatively quickly from the surface of an asteroid, but may be preserved below it, provided the regolith is not too disturbed by “gardening”. More importantly, organic compounds may be preserved in the rocks and on the surface of the grains, provided they are not heated to too high temperatures. In addition, the

regolith composition might be such that many pebbles (up to few mm diameter) are embedded within the sample (especially for small-sized fast rotators which tend to lose their “dusty” regolith), with which the sampling mechanism has to cope.

The uncertainty of the terrain properties on the surface of an asteroid represents one of the key technical challenges in designing an asteroid sample return/in situ analysis mission. The mechanical interface between the sample collection mechanism and the asteroid needs to be sufficiently flexible/adaptable to be able to penetrate the surface to the desired depth and to extract the sample without endangering the mission. The engineering constraints on a sampling mechanism are not trivial and whichever selected mechanism must undergo an extensive testing campaign.

2.1.3.1.3.2 Thermal environment

Most asteroid thermal models are based on highly idealized approximations (spherical object, zero thermal emission for night side, etc.). Nonetheless, these can give useful guides to the thermal environment that a spacecraft or lander might experience. To a first approximation, the temperature on the sunlit side follows an expression of the type [Harris98]:

$$T(\omega) = T_{Max} \cos^{1/4} \omega$$

Where ω is the angular distance to the subsolar point. T_{Max} is the subsolar temperature that is driven mostly by the asteroid distance from the Sun, its albedo, and the asteroid rotation. For a fast rotator, the temperature is approximated by:

$$T_{Max} = \left[\frac{(1 - A)S}{\pi\eta\varepsilon\sigma} \right]^{1/4}$$

Where A is the asteroid albedo, S is the solar incident flux, ε is the asteroid emissivity, η is a correction factor (close to unity) and σ is Boltzmann constant. Based on this approximation the temperature range for a site at the sub-solar point has been determined for the asteroids that have been identified as representative models for the mission concept.

Case	Spectral Class	Heliocentric distance (AU)	Rotation Rate (hours)	Min Temp (K)	Max Temp (K)	Delta (K)
1	C	0.953	2.5	223.9	383.3	159.4
2	C	0.953	20	120.4	409.8	289.4
3	C	2.02	2.5	189.1	233.5	44.4
4	C	2.02	20	117.5	279.7	162.2
5	S	0.953	2.5	253.4	340	86.6
6	S	0.953	20	147.7	395.8	248.1
7	S	2.02	2.5	194.3	216.2	21.9
8	S	2.02	20	141.3	259.1	117.8

Table 3: Surface temperature range for assumed model asteroids

The results show that the NEA surfaces can experience quite large thermal excursions, which is an important design driver for any landing element, in particular if an extended over night stay is assumed.

2.1.3.1.4 Magnetism

Magnetism was surprisingly discovered at asteroid Braille, Gaspra and Ida when flown-by by spacecraft. This suggests a remaining magnetic field from early geological evolution. Whether C-type asteroids are likely to have a weak magnetic field or not is under debate. This question would best be addressed by measuring the magnetic field in a rendezvous mission. However, the use of a magnetometer (implying a boom) has to be assessed against the mission design constraints.

2.1.3.2 Global physical properties

Scientifically interesting are the physical properties such as mass, size, shape and rotation rate. These parameters are also of tremendous importance for the mission design in particular for orbital dynamics and landing.

2.1.3.2.1 Mass and gravitational properties

The typical extremely low mass and highly non-spherical gravitational field (2.1.3.2.4) of asteroids have a major design impact. The following table draws some of the simplified features of an asteroid versus its size (for a sphere-shaped typical C-type asteroid at 1AU). The design parameters vary over a wide range, in particular V_{orbital} , V_{escape} , $R_{\text{sphere_influence}}$ and g_{asteroid} . For example, the values of V_{orbital} and V_{escape} show that bouncing on the asteroid is not desired (besides the shock aspects). In fact, a landing velocity of \sim few cm/s can be achieved if contamination-free landing using nowadays technology is assumed. Therefore, depending on the restitution coefficient (a poorly constrained and possibly close-to-1-value [Yano06]) of the asteroid's surface and the landing mechanism design, the landing could result in bouncing off the spacecraft into orbit.

Radius: R_{ast} (m)	μ_{asteroid}^* (m^3/s^2)	g_{asteroid} (g_{Earth})	$R_{\text{sphere_influence}}$ (km)	$R_{\text{Hill_sphere}}$ (km)	V_{escape} (cm/s)	V_{orbital} (cm/s)
100	0.36	3.7	0.9	14.5	8.5	6
150	1.2	5.4	1.45	21.8	12.65	8.9
200	2.9	7.5	2	29	17	12
350	15.3	13	4	51	29.6	20.9
500	45.4	19	6.2	72.5	42.6	30.1
1000	360	37	14.15	146	85	60
1500	1200	54	23	220	126.5	89.4
2000	2900	75	32.5	291	170.3	120.4
5000	45300	190	97.7	727	425.7	301

Table 4: Parameters associated to typical NEAs

*Density of 1300 kg/m^3 is assumed

μ_{asteroid} : standard gravitational parameter of the asteroid, g_{asteroid} : gravity on the asteroid surface, $R_{\text{sphere_influence}}$: Radius of the sphere of influence of the asteroid, $R_{\text{Hill_sphere}}$: Radius of the Hill sphere of the asteroid, V_{escape} : Minimum velocity required to leave the gravitational influence of the asteroid, V_{orbital} : Minimum velocity required to leave asteroid's surface and remain into orbit

Nevertheless, a clear advantage over planetary landing is that low-altitude (few km) orbits are possible and accurate mapping of the landing site as well as of hazards can be undertaken prior to

landing (nowadays cameras can easily achieve hazard mapping over the whole body from a few km at a 10 cm scale which is sufficient to relax the design on the landing legs and is much less stringent than a planetary landing).

2.1.3.2.2 *Size, Volume*

The accurate shapes and hence volumes of very few asteroids have been determined due to the difficulty of the observational techniques and the long distances. The only data which can be used to estimate the rough size for most asteroids is the visual magnitude (translated into an absolute magnitude). From there, the diameter can then be derived if we assume a visual geometric albedo. NEAs tend to be relatively small (1-2 km or less) when compared with the largest objects in the main belt partly due to the collisional events they have undergone and because the orbits of smaller fragments are altered the most. The target of the NEAR mission, asteroid 433 Eros, is very atypical, being by far the largest NEA (33x13x13 km). There are then only very few objects in the 2-10 km diameter range and the largest part in the 100-2000 m range (such as Itokawa). This has very important consequences when designing a mission to NEAs: while scientific preference is for targeting larger objects (more likely to show some surface differentiation and to develop regolith) all the more accessible targets are likely to be small (around 1 km in diameter), with extremely low gravity and largely homogeneous.

2.1.3.2.3 *Bulk density and porosity*

The bulk density is subsequently derived from mass and volume. It is thought that the bulk density of most asteroid spans from 1.10^3 kg/m^3 to 5.10^3 kg/m^3 . C-types and S-types have a low average value of $1.3.10^3 \text{ kg/m}^3$ and $2.7.10^3 \text{ kg/m}^3$ respectively but this can vary. The bulk density gives a first order indicator of the asteroid porosity. C-type asteroids have a high porosity.

Because of their different history, asteroids present also considerable difference in their internal structure. Monoliths are essentially homogeneous wholly intact units. Fractured bodies have a sufficient number of cracks or faults that their tensile strength is reduced, yet their original structure remains intact. Shattered bodies have interior structures that are even more dominated by an abundance of joints and cracks. Rubble piles are bodies that have been completely shattered and reassembled, where the new structure may be completely disorganized relative to the original. In addition to this we have to consider the possibility of substantially homogeneous bodies at a macroscopic level, which still display a high level of microporosity, decreasing the overall density of the material. All these potential structures have important implications for landing and/or collecting samples from the surface as they affect the design of anchoring and sampling systems.

To evaluate unambiguously the porosity of an asteroid, a ground penetrating radar is a desirable instrument for an asteroid mission. However it should be seen in the context of risk mitigation. It indeed places rather large constraints on mission operations and complexity and it is in particular deemed impossible to deploy it if a single platform is used for orbital, landing and return operations.

2.1.3.2.4 *Rotation state and shape*

Other important parameters of NEAs are the rotation state and asteroid shape. While the ground measurement is necessarily quite crude in estimating the shape, the rotational period and

orientation of the rotation axis can be determined reasonably well through the light curve provided a sufficiently long observation period and sensitivity of the measurements. NEAs usually rotate quite fast (2-2.5 hours rotation period are not uncommon) although some objects have much longer rotation periods (up to 15/20 hours). Although the rotation period is identified for a large number of NEAs, the determination of the spin vector is more difficult and is only known for a few targets. The data that does exist indicates that it is unlikely to find poles close to the ecliptic plane (which would be the best geometric configuration for remote sensing and landing purposes). As it is likely that no data will exist for the selected target the mission design should ensure that the spin axis is determined during asteroid approach and then used in the planning of the descent and landing strategy. Wobbling (precessional movement) is thought to be quite common, especially for small slow rotators.

NEAs are also often quite elongated – cigar-shaped (2:1 or sometimes even 3:1 ratios between ellipsoid axes are possible), indicating little re-arrangement due to self gravity. If the asteroid's shape is unknown the shape can best be approximated as an elliptical body.

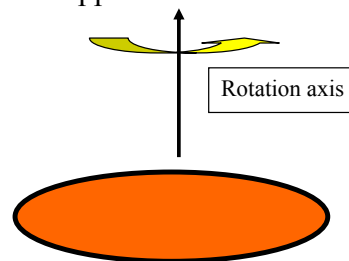


Figure 4: “Cigar”-shaped NEA with rotation axis along the axis of maximum inertia

In the case of Itokawa, it is believed that the asteroid may be formed by at least two separate bodies in physical contact (contact binary).

2.1.3.2.5 Binaries

It was suspected early that a small part of the asteroid population is constituted by binary systems. This fact has now been confirmed (see Ida and Dactyl, 1996FG3, etc.), making of this particular population a very interesting target from a science point of view but which places added constraints on the engineering side (difficulty to find a stable orbit). The detailed engineering implications of going to a binary body are to be assessed. However, because it is not a representative case of most asteroids, such objects will be avoided within this generic study.

2.1.4 GROUND OBSERVATIONS

The previous considerations show that asteroid properties (compositional and physical) are difficult to obtain systematically from the ground due to: the very large number of targets, their very small size and therefore very faint optical properties, the time limitation for a specific target of broad surveys over a large population, their position on the orbit which limits the observation opportunities for a specific target, etc. Yet, the better the target properties are known beforehand, the more chances of success the mission has (the risk factors are greatly reduced) and the most cost-efficient design can be envisaged (the technical requirements can be relaxed to the specific target properties). A lot of information can readily be obtained on ground (accurate orbital properties, spectral type, presence of a binary, rotation period, orientation of the spin axis, rough

diameter and volume, very coarse but indicative mass estimation, etc.). Therefore, any asteroid mission planning shall definitely include an intensive (ground or space-based) campaign to better characterize the target. An early characterization of the body gives a tremendous advantage during the development phase.

2.2 Missions to Near-Earth Asteroids

2.2.1 PAST, CURRENT AND PLANNED MISSIONS

In the past 30 years there have been only a few missions dedicated to asteroids science. It has been only recently that missions have been launched with the express purpose of investigating a single or multiple asteroids for more than just flyby observations. The NEA investigations will need to build upon the investigations of these spacecraft. Missions to comet are also mentioned due to the potential synergies with a NEA-SR mission concept.

Table 5: Overview of past, current and planned missions to small bodies

**For to-be-launched missions, only science objectives are listed*

Launch date	Mission	Type	Some primary achievements*
12-08-1978	ICE (NASA)	Fly-by of 2 comets via WSB transfer	In-situ analysis of Giacobini-Zinner's tail and long-range observation of comet Halley
15/21-12-1984	VEGA 1 & 2 (Soviet Academy of Science)	Fly-by of comet Halley	Analysis of ejected gas/dust and observations of comet's nucleus
07-01-1985	Sakigake (ISAS)	Fly-by of comet Halley	Particle, plasma and magnetic measurements within comet's environment
02-07-1985	Giotto (ESA)	Fly-by of comet Halley	Various remote sensing analysis (nucleus, atmosphere, coma) of comet environment
19-08-1985	Suisei (ISAS)	Fly-by of comet Halley	UV images of the hydrogen corona + solar wind measurements
18-10-1989	Galileo (NASA)	Fly-by of asteroids Gaspra and Ida (+ its moon Dactyl) on its way to Jupiter	Long-range remote sensing observations of asteroids' surfaces + discovery of an asteroid' satellite
17-02-1996	NEAR-Shoemaker (NASA)	Fly-by of Mathilde + rendezvous mission to Eros	Thorough characterization of an S-type asteroid + long-range remote sensing of a C-type + unplanned successful (short-term) landing on the surface altogether bringing about asteroid science to an unprecedented level
24-10-1998	Deep space 1 (NASA)	Fly-by of the asteroid Braille + comet Borelli. Technology demonstration.	Study of the chemical composition, geomorphology, size, spin-state, and atmosphere of the bodies. Solar wind measurements and coma composition
07-02-1999	Stardust (NASA)	Sample return of Comet Wild 2's coma material (+fly-by of asteroid Anne-Frank)	Returned samples from the comet's tail + interstellar dust for ground-based analysis. In-situ mapping and analysis of the cometary tail
03-07-2002	CONTOUR (NASA)	Fly-by of 3 comets: Encke, Schwassmann-Wachmann-3 and d'Arrest (<u>Failure</u> shortly after launch)	Close imaging, spectral mapping and gas/dust analysis of the first 2 comets. Same objectives for last comet at a longer range

Launch date	Mission	Type	Some primary achievements*
09-05-2003	Hayabusa (JAXA)	Sample return from the S-type NEA Itokawa (ongoing)	Due to failure, the possibility of returning the sample is under investigation. Remote sensing campaign brought very valuable and new knowledge to asteroid science as well as to sample return mission concepts
02-03-2004	Rosetta (incl. Philae lander) (ESA)	Rendezvous and landing on the comet (on its way) Churyumov-Gerasimenko + fly-by of Mars, asteroids Steins and Lutetia	Global characterization of the chemical, mineralogical and physical properties of the cometary nucleus and coma and of the 2 flown-by asteroids. Particularly ambitious mission incl. close orbit operations about the nucleus and dedicated landing on and analysis of the unknown comet surface
12-01-2005	Deep Impact (JAXA/ISAS)	Rendezvous + Impact mission to comet Tempel 1	Ejecta from the comet interior, after projectile impact, allowed extensive study of the physical characteristics of cometary nuclei, to determine properties of the surface layers and composition from the crater and its formation;
30-06-2007 (planned)	Dawn (NASA)	Rendezvous and orbit asteroids 1 Ceres and 4 vesta (main belt)	To characterize the asteroids' physical and compositional properties, cratering processes and magnetism to ultimately help understand the conditions and processes present at the solar system's earliest epoch and the role of water content and size in planetary evolution

2.2.2 NEA MISSION CONCEPT STUDIES

Beyond the actual missions above mentioned, a large number of mission studies were initiated in the past to investigate the feasibility of an asteroid mission. The following list is not exhaustive and focuses on sample return study but some other concepts are also listed.

Table 6: Mission concept studies for small bodies' exploration

Study/mission concept	Type	Short description	Sampling approach	Reference
Aladdin	Sample return from both Phobos and Deimos	Sample return from both Phobos and Deimos	Fly-by, impactor release and retrieval of ejecta in orbit	[Pieters99]
APIES	Swarm mission to the main belt	Fly-by and investigation of a hundred main belt asteroids	NA	[Darrigo031]
Bering	Asteroid detection mission to the main belt	To detect and study sub-km asteroids from an orbit within the asteroid Main Belt	NA	[Andersen03]
Champollion – Deep Space 4	Sample return from a comet	Sample return (1 m deep) from the cometary surface	Drilling and retrieval via rendezvous and docking	[Gorevan06]
Comet Nucleus Sample Return	Comet sample return	In-situ investigation of comet nucleus + sample return of the cometary deep surface. Later became Rosetta (in-situ only). Difficult implementation in particular due to cryogenic storage requirements	Full long-term landing/deep drilling + cryogenic storage	[Huber90]

Study/mission concept	Type	Short description	Sampling approach	Reference
Deimos Sample Return	Sample return from the Mars' moon Deimos	Sample return of up to 1 kg of Deimos material. Basic remote sensing science focusing on sampling site selection and context information. Soyuz-launch and chemical propulsion	Touch and go. Pneumatic sample mechanism	[Renton06I]
Don Quijote	NEA deflection	Deflecting and accurately measure the semi-major axis change	NA	[DonQuijote03]
EVE	Rendezvous mission	Aim to understand the formation and evolution processes to which the outer main belt (target is Hygiea) has been exposed since solar system formation. Re-fly of Dawn	NA	[Sykes06]
Gulliver	Sample return from the Mars' moon Deimos	Collect up to 2 kilograms of Deimos regolith and return it to Earth. Basic remote sensing science focusing on sampling site selection and context information	Hovering with rotating teether-wheel attached at the tip of a ~ 5 m boom.	[Britt05]
Hayabusa II (JAXA)	Primitive NEA sample return	Sample return from the primitive Cg-type 1999 JU3. Proposed re-fly of enhanced Hayabusa spacecraft	Touch and go (projectile firing + horn retrieval)	[Yoshikawa06]
Hayabusa Mark II (JAXA)	Primitive NEAs sample return	Sample return from one or more primitive objects such as Wilson-Harrington incl. extensive in-situ analysis (orbiter+lander)	Unknown. Likely full landing/sampling	[Yoshikawa06]
HERA	NEA sample return	Sample return from 3 NEA (incl. primitive type). Focus on sample return	Touch and go with tether retrieval	[Sears04I]
Ishtar	In-situ multiple asteroid mission	Multiple visits to NEAs focusing on the study of asteroid interior (incl. radar tomographer)	NA	[Darrigo03II]
Leonard	In-situ asteroid mission concept	Cost-efficient NEA surface and orbit mission to binary asteroid 1996FG3	Contact instruments only	[CNES06]
OSIRIS (NASA)	Primitive NEA sample return	Sample return from the primitive B-type 1999 RQ36. Proposed as a discovery-class mission. Study ongoing	Hovering. Tether retrieval (conceptual)	[Goddard07]
Phobos-Grunt (RSA/CSA)	Sample return from the Mars' moon Phobos (planned launch 2009)	Investigation of ancient matter pertinent to asteroid class bodies with remote sensing, in situ techniques and sample return from Phobos	Soyuz launch and SEP propulsion. Full long-term landing/sampling	[Marov04]
Simone	Multiple rendezvous mission to NEAs	Fleet of low-cost microsatellites to rendezvous with and study a	NA	[Ball02]

Study/mission concept	Type	Short description	Sampling approach	Reference
		sample of NEAs		

2.3 *Scientific requirements of the TRS mission concept*

2.3.1 TAXONOMY

Among the various spectral classes of NEAs as defined in 2.1.3.1.1 a priority list can be established. The main priority is given to the **C, P and D-class** asteroids [CV05] which are thought to be the most primitive objects. Even though B, F and G type asteroids can be related to some extent to C-type asteroids due to their spectral properties they are less representative of the carbonaceous family than C-types which compose most of this population. In addition, the Q-type presents evidences of metamorphism but remains an interesting target since it is spectrally the most similar to ordinary chondrites than any other asteroid type. Thus, a medium priority is given to the classes **B, F, G and Q**. The classes **A, E, R, T, V and S** are of lowest priority since they somehow underwent a certain degree of differentiation. The spectral class **M** shall be totally excluded because it is generally interpreted as the metal-rich core of a differentiated body and will provide little information on the History of the solar system.

Table 7: Ranking of the asteroid spectral types for the study

Priority	High	Medium	Low	Excluded
Types	C, D, P	B, F, G, Q	A, E, R, T, V, S	M (D, P from sample return, see section 2.3.2.4)

2.3.2 SCIENCE OBJECTIVES

The primary goal of this mission concept study is the development of a scenario in which sample material from a near-Earth asteroid will be returned to Earth. A sample returned to Earth permits the use of the utmost sophisticated technologies in the laboratory analysis. As an alternative mission concept, an in-situ investigation scenario (i.e. no return) is also studied in order to evaluate the main drivers and differences of both concepts. For both scenarios, a non-exhaustive list of possible science goals has been set which builds upon the science facts drawn in 2.1. However, due to the limited resource availability and because the focus is placed on sample return, they will not be all addressed within this study.

2.3.2.1 *Remote sensing objectives*

To safely land on and to identify a single or multiple interesting landing site(s) is the first operational objective of both scenarios. Therefore, a set of common remote sensing science objectives can be derived.

Table 8: Remote sensing science objectives

Science category	Science goals	Possible instruments
General	<ul style="list-style-type: none"> • Size and coarse shape • Regolith characteristics (thickness, physical and chemical properties, presence of boulders) • Rotation, precession and nutation rates • Angular momentum vector and spin axis • Surface temperature 	Camera, thermal radiometer
Mass and internal structure	<ul style="list-style-type: none"> • Mass and internal mass distribution • Gravity field • Moment of inertia • Volume and bulk density 	Camera, radio science, laser altimeter, radar tomographer
Geomorphological description and geology	<ul style="list-style-type: none"> • Searching for satellites or binaries • Global determination of topographical features • Large-sized structures (several 10 m) and stratification, i.e. homogeneous, layered or composed of accreted blocks, gaps and voids • Global determination of surface morphology • Investigating craters and ejecta e.g. number, size, distribution, structure and age • Mapping of possible sampling sites → determining if rocky or porous material • Determining photometric characteristics (colour, albedo) • Search for orbiting dust • Characterization of possibly icy fractions 	Camera, laser altimeter
Mineralogy	<ul style="list-style-type: none"> • Global mapping of spatial surface variation • Evidence for carbonate minerals • Evidence for organic hydrocarbons • Evidence for water → OH bearing minerals (e.g. hydrated silicates, oxides, salts) • Large-scale mineralogical characteristics and heterogeneity, e.g. Nickel-iron metal, olivine, pyroxene, feldspar, spinel-bearing Allende inclusion • Petrology • Characterization of surface roughness on various scales for whole surface • Surface area fraction of exposed volatiles • Search for activity → Presence of low-level gas? • Investigating space weathering effects on surface properties (sputtering and radiation damage), physics of the solar wind – asteroid interaction 	UV-VIS-IR imager
Chemical composition	<ul style="list-style-type: none"> • Large-scale chemical characteristics and heterogeneity, e.g. Fe, Mg, Si, Al, S, Ca, O, K • Search for water ice 	X-ray spectrometer, gamma-ray/neutron spectrometer
Magnetic field	<ul style="list-style-type: none"> • Magnetic field measurement 	magnetometer

2.3.2.2 *Sample requirements for a sample return scenario*

2.3.2.2.1 *Size/Mass*

The amount of material that will be brought back will influence the science that can be performed. Most instruments require only a very limited amount of material ($\ll 1$ gram) for investigations and those that require more, need only a few grams. The sampling size required for analysis is therefore, only several grams. However, a greater amount is required to get a good overview of the sampled area and minimize the influence of disturbing phenomena such as gardening, space weathering, etc. To achieve primary science objectives, it is required to bring back at least 100 g of material from any single location [Sears04II].

2.3.2.2.2 *Location*

For non-homogenous surfaces, the composition of the sample could vary depending on sample location. In this case, remote sensing measurements should be made prior to landing to identify sampling sites of interest and the specific context with which it is associated. Also, mobility shall be considered. Samples will be obtained from the top surface layer and from the subsurface at a minimum depth of 10 cm at a single site location. 10 cm is a compromise between science merit of the sample and engineering constraint. Anchoring/drilling or a mole design is a mean to get a sample from a meaningful depth (> 1 m). But they both have engineering constraints which are discussed in 5.2.2.1. In any case, the landing location may eventually be constrained by the need to land on a safe area (no boulders, no extreme temperature).

2.3.2.2.3 *Composition*

The sample will likely consist of regolith material from the top surface layer. Optimally this should also include several small pebbles with a diameter of a few millimetres. In addition, the sample should not be composed entirely of ‘surface dust’ and should have some subsurface material, providing a good mix of regolith. The sample should also retain “pristine” state of each sample during return. In order to preserve most organics, the maximum temperature that the sample should withstand has been set at 40°C throughout the mission lifetime (sampling, transfer, re-entry, recovery).

2.3.2.3 *Science objectives for an in-situ investigation scenario*

These science objectives describe investigation which can be performed on the surface of the asteroid. It is to be noted that for an in-situ mission concept, there are no requirements on the sample mass as long as it is within the detection limit of the science instruments. The sampling location requirements (depth, multiple sites and/or targets) as well as the sample composition requirements (2.3.2.2.2 and 2.3.2.2.3) are also valid for an AIS mission concept.

Table 9: In-situ measurement science objecives

Science category	Science goals	Possible instruments
General	<ul style="list-style-type: none"> Characterization of the nucleus surface and subsurface to a depth > 10 cm 	Sampling mechanism or contact instrument

Science category	Science goals	Possible instruments
Texture and grain size distribution	<ul style="list-style-type: none"> • Microscopic properties of regolith • Size distribution of dust grains in the near-surface and subsurface material • Organization of ices, organics and silicates on a microscopic scale • Determining size distribution of pores and cavities; length and width of capillaries • Micro-roughness 	microscope
Chemical and mineralogical composition	<ul style="list-style-type: none"> • Mineralogical composition • Chemical analysis • Isotopic abundances 	XRF-PIXE, laser mass spectrometer, Mössbauer spectrometer, IR spectrometer
Organics, volatiles, gases and isotopic composition	<ul style="list-style-type: none"> • Organics and chemical analysis • Volatile ices and chemical analysis • Molecular composition • Isotope ratios: D/H, nitrogen, carbon, oxygen, noble gases, 	mass spectrometer
Physical properties	<ul style="list-style-type: none"> • Surface temperature and temperature profile with depth • Determining thermal conductivity of the surface material and its dependence on temperature, porosity and the ice/dust mass ratio • Specific heat capacity of near-surface material • Near-surface material: ice and dust mantle thicknesses, porosity → Difference between dust mantles and ice/dust mixtures (signs of sintering or solidification) • Compressive, shear and tensile strengths of near-surface material 	sub-surface penetration device, thermometric measurements

2.3.2.4 Planetary protection aspects and scientific integrity of the sample

It is acknowledged that the planetary protection rules established in [NRC98], [COSPAR05] recommend a case-by-case assessment of the handling and containment requirements for sample from C, D and P-type asteroids in the mission planning phase. This is clearly out of scope of this study. C-types are classified as category V unrestricted return. However, D and P-type have been classified as category V restricted return (mainly because little is known about their properties). Even though this is to be reviewed in later stages, these latter are excluded from the current study. Clearly, the requirements associated with such a category (bio-sealing) do not fit with the low-risk and cost-efficiency objectives of the envisaged mission concept (based on [MSRCDF03] and [Vrancken06]). The outbound leg to a carbonaceous body is classified in category II.

3 TRADE-OFF APPROACH

3.1 Overall trade-off

Above all trade-offs, the decision to whether study a sample return or in-situ investigation mission concept is paramount. Yet, as [MR1] indicates (1.2), a sample return is to be selected if a cost-efficient design is considered feasible within the available resources. Both concepts may also be combined. This latter option is discussed in 5.3. Beyond this issue, the following schematic shows that an unusual large number of critical trade-offs must be performed.

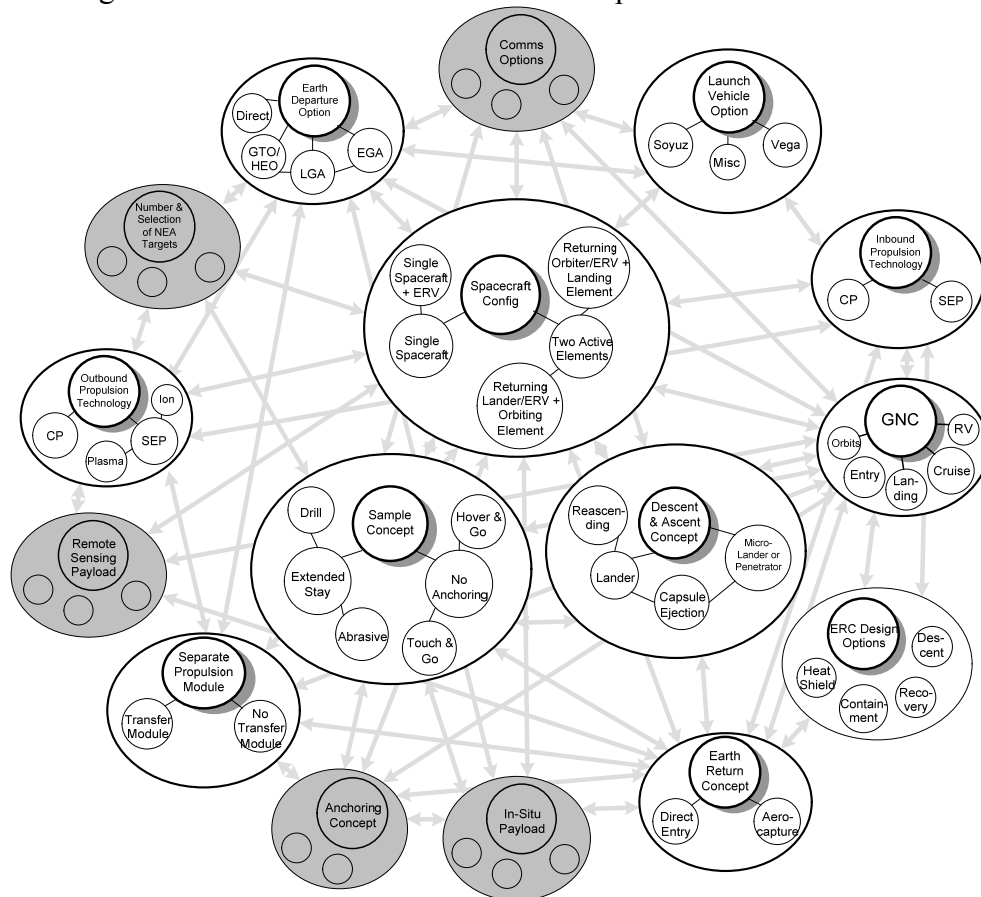


Figure 5: Trade-offs to be conducted for an asteroid sample return

Some of them have to be timely addressed in the early stages of the design, are interrelated and take into account many parameters. This is in particular the case of:

- **Sample return vs in-situ investigation**
- **Target selection**
- **Transfer propulsion**
- **Spacecraft configuration**
- **Earth return and re-entry**

For instance, target selection must account for: the physical and spectral properties/types of the targets, the environment (single or binary, accessibility, available solar power), the number of

targets (depending on ΔV capability and acceptance of much higher risk), etc. Due to the defined technology development horizon, only chemical and electrical propulsion can be envisaged for a NEA mission concept. In this particular case, the trade-off between chemical and electrical propulsion is fundamental because it drives the target selection and the type of mission (e.g. in-situ vs sample return). Clearly, a limited number of targets (a few dozens) are within reach of a chemically propelled spacecraft (assuming a low-cost launcher) while Solar Electric Propulsion (SEP) opens up many more opportunities. The spacecraft configuration is clearly dependent on the mission type (sample return vs in-situ scenario) and on the propulsion system, among others. Even though a number of Earth return and atmosphere re-entry scenario can be derived from the initial requirements, the strategy is here dictated by the low-risk approach. A number of criteria and a weighting scheme were tailored towards the need of the study and are applied to help down-select a nominal scenario. Cost, risk, science and mass were in particular used.

It is paramount to note that all trades are directly or indirectly influenced by the selection of the target. However, will be addressed in the next chapter the most critical trade-offs (propulsion, Earth re-entry, configuration, etc.) which can be closed-out along the discussion about target selection. The major trade-off related to the sampling strategy is not directly related to the target selection (orbital mechanics-wise) and is addressed separately in chapter 5.

3.2 Science payload trade-off

Due to the impossibility to down-select an extensive payload suite prior to selecting the target and mission concept, a minimum remote sensing payload suite has been defined with the aim to fulfil the primary objectives of the mission concept, namely: safely landing on and sampling of the surface of the asteroid (and of course return the sample). The preliminary reference payload which is selected in this context is highlighted in Table 10:

Table 10: Remote sensing reference payload suite

Instrument	Primary objective and characteristics	Average/ Peak compressed data rate (kbps)	Dimensions (mm ³)	Field of View (°)	Power incl. margins (W)	Mass incl. margins (kg)
Radio Science Experiment* (X/X band up/downlink + Ka downlink)	Mass and gravity field determination	NA (part of telecomm budget)	150x150x100	NA	16.5	1.65
2 Narrow Angle Camera** (APS sensor, [400-1100] nm + 4 filters (TBC))	Physical properties and landing site characterization.	2.78/4.5	150x100x50	4	0.9	1.2
2 Wide Angle Camera (APS sensor, [400-700] μm)	Physical properties of the asteroid	0.3/4.5	70x80x75	53x53	0.9	0.3
UV-Vis-NIR spectrometer*** (Imaging spectrometer [300-3200] nm)	Surface mineralogy (in particular of the landing site)	1.4/4.6	50x80x200	3.67x0.014 (instantaneous)	8.4	2.28
TOTAL		4.48/>14			26.7	5.43

*X/X up/downlink and Ka-downlink are part of the RSE. However, the X/X band transponder and related equipment is

included in the telecommunication budget. The RSE equipment is based on the KaTe experiment of SMART-1 and RSE of Bepi-Colombo

***2 NAC are used in cold redundancy (and 2 WAC also)*

****The Field of View is instantaneous and the instrument is used in the push-broom mode*

The laser altimeter may not be a strict requirement in order to construct a DEM model of the asteroid and one NAC through ground processing or the 2 NACs used in stereo mode can reconstruct a model accurate enough. The DEM model is mandatory in order to determine the accurate volume of the asteroid and therefore its density and is also used by the navigation system to enhance the position estimation of the spacecraft during descent. Nevertheless, a laser altimeter can become a requirement if the orientation of the spin axis of the asteroid is such that part of the asteroid is always in the shadow during observations. Additional scientifically meaningful remote sensing instruments are listed hereafter while additional in-situ instruments are discussed in chapter 5.3. The possibility of including this extra instrumentation is not further looked into in the frame of this study. Yet, chapter 6.3 shows that quite a large amount of payload could be embedded from a pure mass margin standpoint in the baseline scenario. However, power, operational, configuration and thermal requirements have to be thoroughly assessed (e.g. deployment and high power of a ground penetrating radar, SNR of an X/ γ -ray spectrometer, deployment of a magnetometer, etc.). The detailed characteristics of all instruments (including baseline and optional remote sensing and in-situ instrumentation) are found in [Agnolon07I].

Table 11: Optional remote sensing instruments

Instrument	Primary objective and characteristics	Average compressed data rate (kbps)	Dimensions (mm ³)	Parameter of interest	Power incl. margins (W)	Mass incl. margins (kg)
Laser altimeter (bi-static emission/detection)	Topography model of the asteroid + terrain roughness	0.046	150x150x150	PRF=4 Hz, FOV= 400 μ rad	12	4.8
Thermal radiometer ([5-40] μ m)	Surface temperature	0.086	60x40x40	1 K accuracy, GSR = 10 m	0.6	1.2
Reflective Radar Tomographer (30 MHz)	Internal structure of the asteroid	3.2	500x20 (stowed), 2x2500 (deployed)	100 Hz PRF, accuracy: 5% of the asteroid diameter	24	7.32
X-ray spectrometer ([0.5-10] keV)	Surface chemical composition	TBD	210x210x260	200 eV resolution @ 5.9 keV, GSR = 10 m	3.6	1.8
Solar X-ray/Particles Monitor	Calibration of X-ray fluxes	0.1	50x50x50	[0.5-10] keV for X-ray, [0.5-30] MeV for protons, [0.1-3] MeV for electrons	1.98	0.33
γ -ray/Neutron Spectrometer ([100 keV-10 MeV] for γ -rays, [0.2 eV-10 MeV] for neutrons)	Surface and shallow sub-surface chemical composition	TBD	110x110 (diameter)	10 keV @ 10 MeV, GSR = 500 m	3.6	4.08
Magnetometer	Magnetic field measurements	0.014	100x50x100 (excl. boom)	Range = 500 nT, accuracy = 0.1 nT	1.65	1.6
TOTAL		>3.45			47.4	21.1

PRF: Pulse Repetition Frequency, FOV: Field Of View, GSR: Ground Spatial Resolution

4 SELECTION OF TARGET AND BASELINE ARCHITECTURE

4.1 Down-selected targets

More than 3000 asteroids orbit within the near Earth space. Therefore it is clear that a preliminary selection must be performed through quick design tools and simple ranking scheme. A target is selected and considered for further mission analysis (according to the requirements) if:

- It is of identified taxonomy class as defined in section 2.3.1 (It is to be noted that Nereus was initially thought to be a related C-type while it is indeed a Xe type). The target types and orbital parameters are derived from [JPL07]
- It is not of D or P-type (for a sample return)
- Ranks among the least ΔV demanding targets

Preliminarily, the accessibility of an asteroid is evaluated analytically according to a ΔV figure computed as the sum of an in-plane ΔV (based on a simple Hohmann transfer) and a plane change manoeuvre. On the following graph, the propellant-mass ratio is shown for the most promising targets for a sample return (A mass of ~ 200 kg (dry spacecraft) is used for reference and comparison purposes).

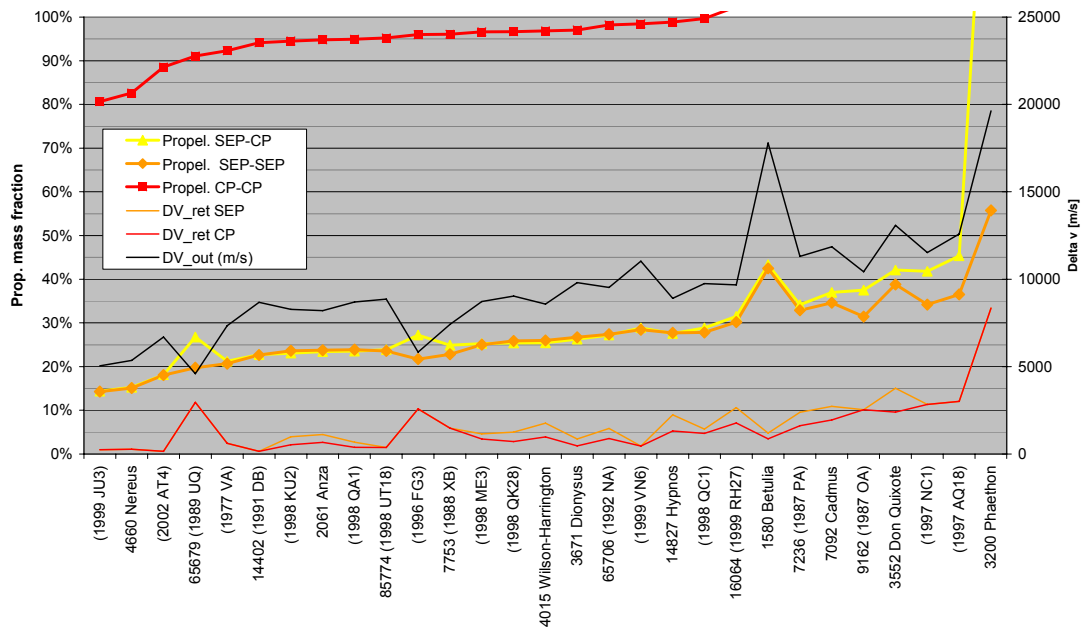


Figure 6: Propellant-to-mass ratio for most accessible targets

The selected targets are presented in Table 12.

Table 12: Selected targets - main physical and orbital parameters

target parameter	4660 Nereus	1999JU3	1996FG3	2002AT4	1998KU2	1998QA1	4015 Wilson- Harrington
a (AU)	1.4885	1.1890	1.0542	1.8664	2.2528	2.1040	2.6381
e	0.3600	0.1900	0.3498	0.4469	0.5521	0.5322	0.6237
i (deg)	1.4323	5.8847	1.9902	1.5056	4.9205	8.1642	2.7854
Ω (deg)	314.5227	251.6965	299.8887	323.7150	120.1277	332.8879	91.2628
W (deg)	157.9018	211.2962	23.916	202.7757	205.9639	299.1500	270.5730
Rp (AU)	0.95264	0.9630	0.6854	1.0323	1.0088	0.9842	0.9927
Ra (AU)	2.02436	1.4149	1.4229	2.7005	3.4965	3.2238	4.2834
Class	APO	APO	APO	AMO	APO	APO	APO
Diameter* (km)	0.95	~0.7	1.6	~0.3	2.6	0.8	4
Rot. Period (h)**	15	---	3.6	---	---	---	6.1
Tax. Type***	Xe	Cg	C	D	Cb	C?	C, F?

*The size of the object is based on measurements of the visual magnitude and therefore is dependent on the assumed albedo.

**If available, the given rotation period has a low uncertainty to its actual value since it is based on direct temporal light curve measurements.

***The taxonomy class is based upon spectral information obtained during ground spectrometric observation campaign and has a degree of uncertainty linked to the surface properties of the asteroid (e.g. gardening, space weathering, etc.).

It is interesting to mention that all the objects except 1996FG3 have perihelion very close to 1 AU, which is potentially a good characteristic to minimize the ΔV . The last three objects have a quite high aphelion. In addition, the longer orbital period might result in a reduced number of mission opportunities due to phasing issues. The targets have in general a small inclination, usually inferior to 6 deg excluding 1998QA1. This ranking does not take into account the actual transfer possibilities (phasing issues, apses position, etc.).

4.2 Mission architecture trade

Since a design-to-cost approach is required, both ASR and AIS mission concepts are initially looked into before a mission architecture can be selected.

4.2.1 MISSION ANALYSIS

Mission analysis is performed as follows:

- Opportunities for transfers to the pre-selected targets are looked for
- Combining the previous results with analysis on the inbound trip allows to identify roundtrip sample return opportunities
- For the most interesting opportunities the impact of using SEP system is investigated

The launch window to be considered is in the 2015-2025 timeframe. Both Soyuz and VEGA launches are considered for both ASR and AIS concepts. Due to the large number of possible targets and transfer options, a large set of transfers is analysed and presented in [Agnolon07II]. Due to the transfer similarities between 1998KU2, 1998QA1 and 4015 Wilson-Harrington, only transfers to 1999JU3, Nereus, 2002AT4, 1996FG3 and 4015 Wilson-Harrington are used in the following mission architecture trade-off.

Mission analysis showed that multiple asteroid visit is not desirable because it requires SEP and the subsequent transfer duration (minimum 7.2 years for a 1999JU3-Nereus mission) is not beneficial to the design-to-cost approach. The second conclusion which can be drawn is that among the down-selected targets, only 1999JU3, Nereus and 2002AT4 (not for sample return) are accessible via chemical propulsion as it is confirmed by Table 14. Missions to difficult targets (4015WH) are more than 11 years long [Agnolon07II].

4.2.2 EARTH RE-ENTRY

Two main scenarios are possible for the Earth return and re-entry:

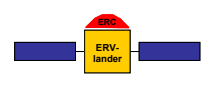
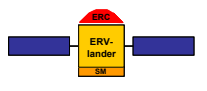
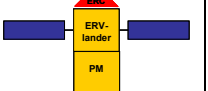
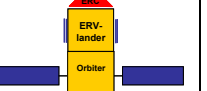
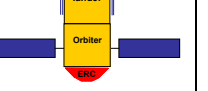
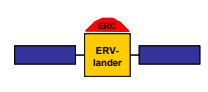
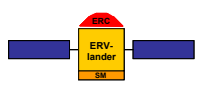
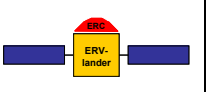
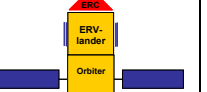
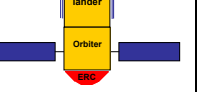
- The ERC can directly enter the Earth atmosphere at very high speed (Mars Sample Return scenario) in the range of 12.5 km/s
- It can also be inserted into LEO parking orbit via propulsive manoeuvre to undertake a lower speed re-entry (~7.6 km/s to build upon ARD demonstration). As mission analysis shows, all return atmospheric velocities are high (~12 km/s) and the ΔV needed to break requires a large amount of propellant which is either a showstopper for most of the transfers or too highly constraining
- Other scenarios such as aerocapture, ISS rendezvous, Lunar or Lagrange point orbit insertion are discarded due to their greater complexity and associated cost

In addition to the drawbacks of the second option, development is ongoing in Europe towards ablative materials to cope with a high speed Earth re-entry (V_{atm} up to 12.5 km/s) which is therefore selected.

4.2.3 CONFIGURATION

4.2.3.1 Options

Propulsion system drives the configuration selection. Only sample return configuration options are shown since they also cover the AIS case. The following configurations can be envisaged.

Phase	Scenario 1	Scenario 1'	Scenario 2	Scenario 3	Scenario 4
Transfer					
Pre-sampling asteroid orbit					

Phase	Scenario 1	Scenario 1'	Scenario 2	Scenario 3	Scenario 4
Descent and surface stay					
Ascent					
Post-sampling asteroid orbit					
Departure and transfer					
Comments	All operations performed by a single spacecraft	Sampling module remains on the surface	Dedicated propulsion module used for forward transfer	Orbiter remains in orbit. Only ERV returns	Lander remains on surface. Orbiter returns

Table 13: Configuration options

It is to be noted that Scenario 1' is a derivative of scenario 1 but can be also adapted for the other scenarios. This option will be discussed in a later section as its implications are not dramatic at this stage.

4.2.3.2 Scenario analysis

4.2.3.2.1 Scenario 1 (single spacecraft)

4.2.3.2.1.1 Chemical propulsion

This option clearly is the most cost-efficient approach but it has the drawback of being only applicable to 1999JU3 and Nereus. Another issue may be the lack of a communication relay during landing but it depends on the landing site geometry and stay time on the surface. This option was analysed in the frame of the baseline scenario presented in chapter 6.1 which showed that the launch mass would be slightly increased up to 2426 kg due to the higher mass to return to Earth.

4.2.3.2.1.2 SEP propulsion

This option is attractive since it is the most mass-efficient of all (identical to Hayabusa) because there are no system duplications and because SEP is more efficient. It also gives access to a much larger number of targets. A clear drawback is the cost of SEP equipment with respect to a chemical solution and the operational cost due to the typical long transfers. A minimum of 6-7 years is needed for a sample return from 1996FG3 and ~ 12 years for WH4015 for instance. SEP transfer durations to 1999JU3 and Nereus remain of the same order of magnitude as for Chemical Propulsion (CP). However, the main technical drawback is the landing of a spacecraft equipped with SEP, implying large solar panels. In fact, it is identified in mission analysis that the minimum

SEP thrust to be used is 50 mN/ton to achieve a reasonable compromise between needed ΔV and transfer time. In a first approximation, the peak power requirement for the engine and therefore the solar panel size would thus be similar to SMART-1 if we assume operations at 1AU (optimistic case) and triple junction GaAs cells. Solar panels span over 14 m. Therefore, we can reasonably assume that the solar panels for a 2m high spacecraft can cope with a total inclination of the spacecraft with respect to the local surface of $\sim 16^\circ$.

The maximum angle that the spacecraft shall have with the local surface at landing has been constrained to 10° which is controlled by the lander ACS and selection of the landing site. In addition to that, hazards up to 10 cm are assumed to be present on the landing site (larger boulders can be mapped from orbit and hence avoided), which adds up about 3° uncertainty. In theory, the total maximum angle that the spacecraft will have with respect to the local surface is therefore 13° . This gives only 3° margin with respect to the solar panels clearance angle.

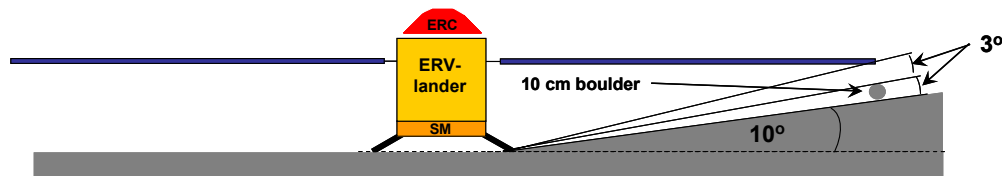


Figure 7: Critical landing with large solar panels

From these considerations, it is clear that landing with large solar panels on an asteroid surface largely increases the risk factor. Taking into account the added risk and cost with respect to the same architecture using a chemical engine, this option is discarded. Another possibility would be to hover above the surface so that landing can be avoided. However, this approach is discussed in section 5.2.1 and is discarded due to major GNC issues.

4.2.3.2.2 Scenario 2 (single spacecraft + dedicated outbound propulsion module)

4.2.3.2.2.1 Chemical propulsion

This scenario is slightly more mass efficient than scenario 1 since the jettisoning of the propulsion module at arrival allows a mass reduction of the return vehicle. The interfaces between propulsion module and lander are as limited as possible so that the gain in mass is optimized. This scenario is only possible for 1999JU3 and Nereus and for these two targets the use of the lander RCS thrusters for the return trip is possible and more mass-efficient than an extra main chemical engine. This propulsion approach is therefore recommended due to the very low return ΔV for these two targets. The drawback with respect to Scenario 1-chemical is the added cost associated to the propulsion module, but the impact is likely to be low due to the maturity achieved in developing chemical propulsion modules in Europe.

4.2.3.2.2.2 SEP propulsion

Such an option combines the advantages of scenario 2-chemical with the advantages of scenario 1-SEP. However, 2 options have to be considered. The return is achieved via chemical (which is only possible for 1999JU3 and Nereus) or SEP. The return with SEP can be discarded for the same reasons as for scenario 1-SEP. The SEP-forward and CP-return is attractive because it gives more

flexibility than chemical forward transfer and more mass margins. However, the added cost of forward SEP engine remains a drawback.

4.2.3.2.3 *Scenario 3 (Orbiter-only spacecraft + lander-return vehicle)*

4.2.3.2.3.1 Chemical propulsion

This scenario does not provide a clear advantage with respect to scenario 1 because the minimum stay time (up to 10 months without a large impact on the return ΔV) at the asteroid is long enough to allow an extensive remote sensing campaign even in scenario 1. However, it would allow the accommodation of instruments such as ground penetrating radar, magnetometer, etc. The main technical drawback in the chemical case is that the mass margins associated with launch of one composite made of 2 heavy modules are low (Analysis showed that the launch mass would be 2838 kg in the baseline scenario). Another aspect is the cost of developing 2 self-sufficient spacecraft, clearly less efficient than scenario 1 in that respect.

4.2.3.2.3.2 SEP propulsion

In the case of SEP, the mass margins are certainly better than with chemical propulsion and give access to many more targets. Again, two alternatives are possible: chemical or SEP return. The SEP return is discarded because it implies the use of two SEP engines which, cost-wise, is not compatible with the framework of this mission concept. In fact, a chemical return option has some similarities to scenario 2 with outbound SEP-inbound chemical. A full SEP orbiter certainly increases cost. However, besides the additional remote sensing equipment that it allows, this configuration could give access to a second target (for AIS only) due to the flexibility provided by SEP once the Earth return chemical vehicle has returned from the first target.

4.2.3.2.4 *Scenario 4 (orbiter-return vehicle + lander-only spacecraft)*

Based on Mars Sample Return CDF study [MSRCDF03], the complexity of the GNC operations (rendezvous) and hardware (capture mechanism) to retrieve the free-flying sample container in orbit by the orbiter necessitates an aggressive technology development schedule which is not compliant with the technology development horizon requirement for this study. The cost associated to the hardware is also a clear showstopper. This scenario can therefore be discarded for these considerations.

The conclusions of the above assessment rule out all scenarios in which return can only be achieved via electric propulsion. Therefore a sample return from 1996FG3, 4015 Wilson-Harrington, 1998QA1, 1998KU2 is selected-out and will only be considered again if Scenario 1 with chemical propulsion is not feasible.

4.2.4 MISSION ARCHITECTURE TRADE

The mission architecture trade-off timely exploits the previous targeting options and configuration options. For each target, a sample of configurations together with the propulsion options are analysed and a summary of the preliminary calculated mass margins is presented hereafter. A launch mass of 2165 kg has been taken for SEP since it is the Soyuz-Fregat capability for a Lunar

Crossing Orbit. A dedicated chemical propulsion module to raise the apogee can also be used and would show slightly better performances (2197 kg) but the fact that the mass margins in the case of SEP are not critical and the cost associated with it do not justify its use. A launch mass of 3023 kg has been assumed for a Soyuz-Fregat launch into GTO (excluding launch adaptor).

Table 14: Preliminary launch mass margins for each identified sample return scenario

Targets		199Ju3 C	+Nereus C	+2002AT4 D	+1996FG3 C (binary)	+Wilson C
SAMPLE RETURN	C1 LSC-SEP	Capacity, kg 2197 Margin 63% Mass Score 5	2197 63% 5		2197 53% 5	2197 59% 5
	C2 LSC-CP	Capacity, kg 3023 Margin 61% Mass Score 5	3023 34% 4		NP 0	NP 0
	C3 CPM/ERV	Capacity, kg 3023 Margin 61% Mass Score 5	3023 35% 4		NP 0	NP 0
	C4 SEPM/ERV	Capacity, kg 2197 Margin 58% Mass Score 5	2197 57% 5		2197 -179% 0	2197 -264% 0
	C5 pSEPM/ERV	Capacity, kg 2197 Margin 55% Mass Score 5	2197 54% 5		2197 -182% 0	2197 -267% 0
	C6 aSEPM/ERV	Capacity, kg 2197 Margin 53% Mass Score 5	2197 53% 5		2197 -183% 0	2197 -269% 0
	C7 OSC/ERV	Capacity, kg 2197 Margin 47% Mass Score 4	2197 47% 4		2197 -189% 0	2197 -275% 0

LSC: Landing Spacecraft, SEP: Solar Electric Propulsion, CP: Chemical Propulsion, ERV: Earth Return Vehicle (propelled by CP), CPM: Chemical Propulsion Modules, SEPM: SEP Propulsion Module, pSEPM: passive SEPM, aSEPM: active SEPM, OSC: Orbiting S/C

A large number of similar analyses was performed for double targets, in-situ missions, VEGA launches, etc. This table confirms that only 1999JU3 and Nereus (as interesting targets) are accessible with an outbound and inbound chemical propulsion system (2002AT4 has been discarded for sample return). Other targets require the use of SEP for both legs of the transfer, which has been discarded due to reasons mentioned in above section.

Since Table 14 clearly shows that a sample return mission to a scientifically interesting target (1999JU3 being a C-type related asteroid) is compatible with a launch with Soyuz and a cost-efficient fully chemical transfer system (best fulfilling thereby [MR1], [MR3] and [MR4]), it is selected for further detailed design. Despite the fact that a SEP orbiter-CP ERV configuration would be more flexible and may give access to a second asteroid for remote-sensing operations, the launch margins for a 1999JU3 mission are such that electrical propulsion becomes unnecessary (too high cost-to-mass margin ratio wrt chemical propulsion) and extension to a second target would expand mission operations cost.

5 MAJOR TRADE-OFF: SAMPLING STRATEGY

5.1 Mission architecture summary

The following design tree can be defined in order to cover the whole spectra of possible mission options.

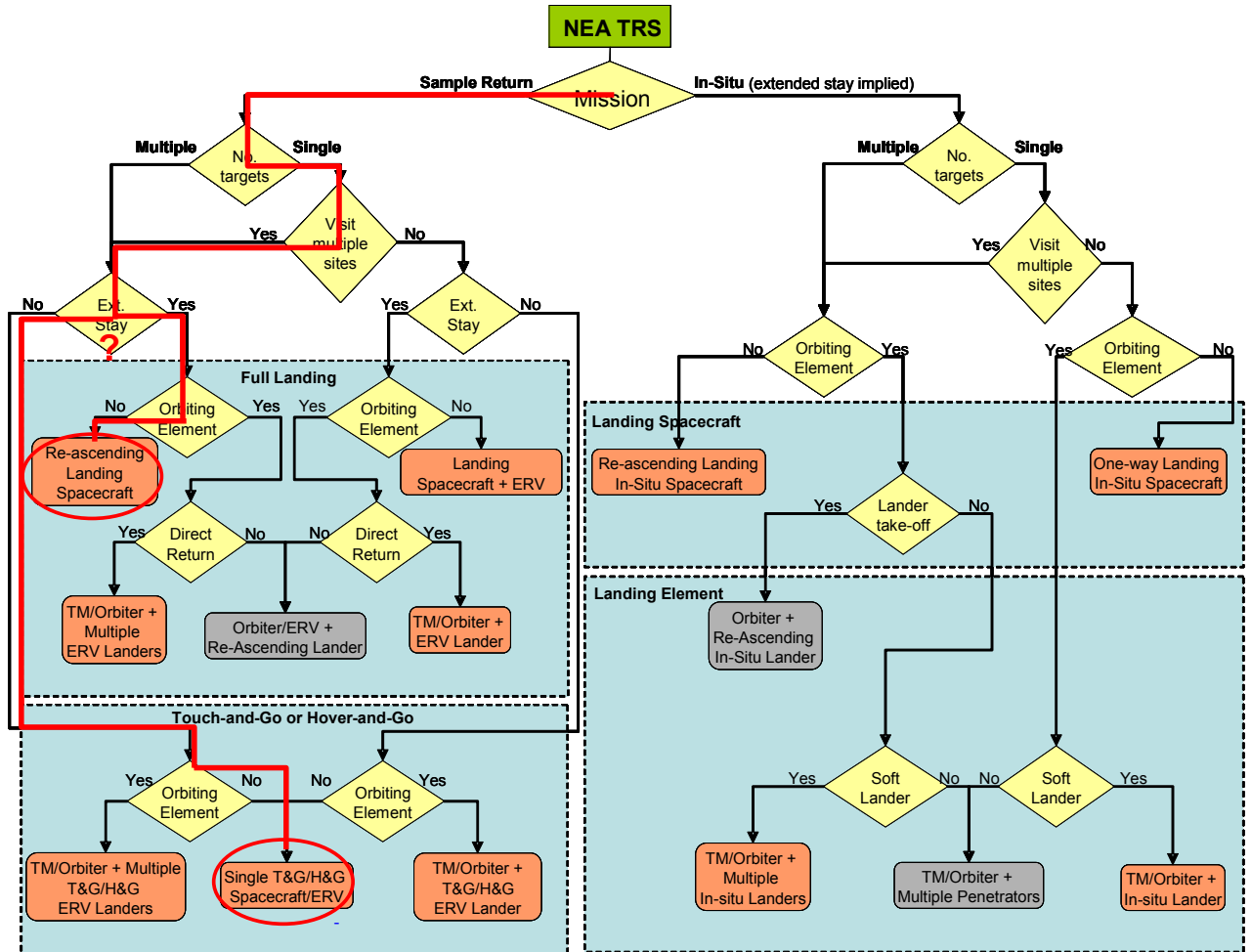


Figure 8: Mission concept design tree

The red path shows the decisions made up to this point. Nevertheless a critical trade-off remains to be done between a short-term stay/touch&go/hover&go and an extended stay. Since this particular choice depends on the landing operations, these considerations are covered in this chapter. The selection of the sampling strategy, the landing strategy, the sampling mechanism is also based on the criteria used for the main architecture which were tailored towards the specific need.

5.2 Sampling operations

5.2.1 LANDING/SAMPLING STRATEGY

Many different strategies can be thought of to obtain a sample from the asteroid surface and/or sub-surface. More than for any other sub-systems, the sampling approach and mechanism selection is driven by a well-thought balance of cost, technology readiness and risk. Table 15 tries to present all possible generic sampling strategies. A thorough trade-off was conducted at system level. Only main advantage, drawback and showstopper are listed here. The mechanisms which are illustrated below are just some examples related to the mentioned sampling strategy. Many others were considered and are not illustrated.

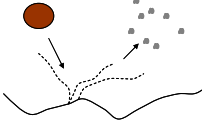
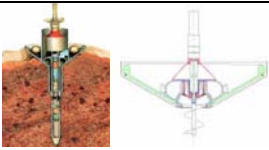
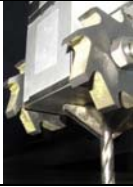

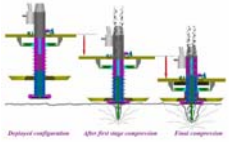



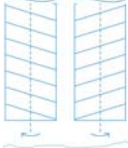
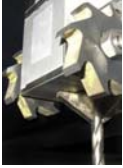


Strategy	Short description	Example of sampling and collection mechanism	Reference	Comment
1. Hover-Fire projectile-orbit retrieval	S/C hovers above the surface, fires a projectile. Ejectas are retrieved in orbit via a capture mechanism		[Pieters99]	Too low mass of material (dust)
2. Hover-sampling and retrieval with tether	S/C hovers above the surface at ~ 10m, fires the sampling mechanism attached to a tether, retrieves the sample via the tether		[Nygren00]	High risk for the penetrator or harpoon to remain stuck into the surface
3. Hover-sampling and retrieval with shaft/telescope	S/C hovers above the surface at ~ 1m, deploys the sampling mechanism attached onto a shaft, collects sample and retracts the shaft		[Rafeek00]	GNC design too challenging (required lateral - vertical velocity control ~ mm/s) + large torques on S/C
4. Sampling-retrieval of sample container in orbit	S/C lands, collects sample, transfers it into sample container which is ejected in orbit where it is retrieved by orbiter	Any sampling mechanism + capture mechanism	[Gorevan06]	High complexity, risk and cost
5. Touch&go with projectile and horn	S/C touches the surface, fires a projectile collected into a horn and takes off (short duration)		[Kubota05]	Too low mass of material (mg)
6. Touch&go with impulsive rebound	S/C touches the surface, directly collects the sample within the contact time (~few seconds) and takes off		[Renton06]	Risk of breaking the pneumatic lance upon contact + risk of toppling over + risk for pebbles to get stuck in the pipe

Table 16: Sampling mechanism options suitable to selected sampling approach – Trade-off

Name	Concept	Advantages	Drawbacks
1. Simple corer	 [Jeffrey06]	Very simple, light and robust design. Reasonable development time and cost. Easily cope with 100 g of material. Sampling verification possible. Keep stratigraphy. Cope with 10 cm depth	Requires large down thrust (~100 N). Not possible to keep loose regolith within core chamber. Not compatible with hard rock
2. Petal sampler		Same as 1. Also keeps loose regolith	Same as 1.
3. Rotating corer	 	Same as 1. Less down-thrust is needed.	Still low down thrust required (10-20 N). Slightly more complex than 1 due to rotating mechanism. Not compatible with hard rock
4. Rotating blades		May cope with rocks (TBC). Cope with 100 g material (TBC). May not require down thrust (TBC)	Lose the stratigraphy of the sample. Complex transfer of the sample. Requires substantial development. Possibility of jamming blades with pebbles. Difficult verification of sampling. Shallow sampling (unlikely compatible with 10 cm depth TBC)
5. Scoop		Reasonable development time and cost. Can easily cope with 100 g of material. Sampling verification possible. Cope with 10 cm depth. Keep stratigraphy	Not compatible with hard rock. Requires low down thrust. Closing may be prevented by pebbles. Transfer may be complex.
6. Projectile	Projectile + collector	Can cope with hard rock	Can only collect low mass of material. Risky as the main SM. Lose the stratigraphy of the sample
7. Sticky pad		Very light, robust and simple. Reasonable development time and cost. Almost certain to get a sample	Can only collect little mass of material. Not compatible with hard rock. Low down thrust required (20-50 N). Does not cope with a 10 cm depth
8. Sticky film	Large surface of sticky film material	Simple sampling. Almost certain to get a sample	Only dust, little mass of material can be collected. Complex transfer, accommodation in S/C and handling on ground. Not compatible with hard rock. Does not cope with a 10 cm depth

Re-attempt is possible with all mechanisms (all devices can be duplicated). Since thrusters are required and used to maintain the spacecraft on the ground, the frictions with the soil should prevent any sliding of the spacecraft (TBC) after a steady thrusting state is reached. Thus, no transversal torques should be created which prevents the risk of breaking the tip of the mechanism.

5.2.2.2 Selected concept

None of the above sampling mechanisms is faultless. The selected concept tries to combine the advantages of the most suitable ones. A roto-translation corer decreases the required forces needed to keep the spacecraft on ground and help sampling operations (less thrust required). Multi-appendixes can be used to enable multi-sampling. It can easily collect 100 g to 300 g of material (with properties as defined in 2.3.2.2) down to 10 cm and keeps the pristine state and stratigraphy of the sample. It does not overheat the sample beyond the required maximum temperature of 40°C. No complex mechanisms have been identified, except the rotating device which is not critical. The development time and cost of such a device are estimated to be reasonable even though the current TRL is low. The rotation mechanism can build upon the rotation mechanisms already or being developed for Philae-SD2 and ExoMars' drill. In order to keep loose regolith within the sample compartment, a closing lid should be envisaged. In addition, the inner part of the SM receives a layer of sticky material to ensure that a minimum amount of material will be collected (in the gram range) in case regolith is too loose and the lid fails to close. Nevertheless, it cannot cope with hard rock (which is very unlikely on a C-type) and a projectile would have to be implemented.

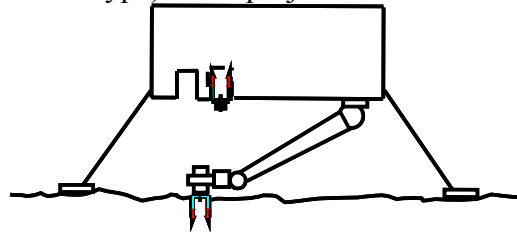


Figure 9: Selected sampling concept

Limited testing was performed on a similar tool (commercial corer + augered corer developed for space) with regolith simulant (60% olivine and 40% pebbles (diameter up to 5 mm), compression strength up to 20 kPa) on one hand and simulant of a non-magmatic compacted regolith on the other hand (gas concrete of 2 MPa). These tests showed that the required down thrust and power are respectively limited to 2.5 N (at 10 cm depth for regolith + pebble simulant) and 5 W. The material is well retained in the sample chamber due to compactness. Sampling depth of 10 cm can easily be achieved. In addition, the torques created by the rotation are limited to 0.005 Nm, which is believed to be well below the threshold which would make the spacecraft turn around its vertical axis when thrust is applied.

5.3 Extended stay and in-situ science

This section discusses the available options for an extended stay on the surface and what would be the consequences for the baseline design presented in next chapter. However, the approach is quite generic in that most conclusions are valid for any mission design or landing approach.

5.3.1 EXTENDED STAY: GROUND INVOLVEMENT AND ADDITIONAL SCIENCE

From a science and risk standpoint, it would be desirable to control from the ground the exact location of the sampling after close-up pictures of the landing area have been taken. This limited ground-interaction calls for a strict minimum surface stay of about 3 hours 30 minutes due to time required for:

- Close-up pictures and possibly conduct other in-situ analysis (temperature, etc.): 30 minutes,
- Back and forth communications (At 2.4 AU during proximity operations in 2019): 40min,
- Ground data analysis, TC implementation, check and upload: at least 2 h assumed,
- Sampling (20 minutes)

The asteroid rotation period has to be minimum 7h in order for the spacecraft to avoid the asteroid night, which excludes a large number of NEA targets. The first conclusion is that the part of the spacecraft which has to stay longer has to survive the asteroid night. In addition, longer stay on the surface would give the possibility to include a minimum in-situ science surface package which would mitigate risk in case of sample failure. Yet, its feasibility highly depends on instrument integration time. This payload analysis is out of scope of the present study but the possibility of staying longer is investigated further.

5.3.2 ADDITIONAL REQUIREMENTS AND CONSEQUENCES

In order to meet the primary mission objectives (cost-efficiency and risk minimization), the following requirements are defined with respect to an additional in-situ surface package:

- [MR6] *In case sample return + in-situ surface science is considered, the primary objective of the in-situ surface science package shall be to mitigate the failure of a sample return*
- [MR7] *An additional in-situ surface science package shall not place any constraints which have a critical impact on the sample return spacecraft design and operations*
- [MR8] *An additional in-situ surface science package is to be considered only if the added information that can be gained on the asteroid scientifically is of primary interest and necessary in case of sample return failure*

5.3.2.1 Anchoring

The choice to discard anchoring is based on [MR6] and [MR7]. The primary objective of the ISS package being to mitigate a SR failure, it was estimated that anchoring the ISS package would not favour this approach. This decision has the following impact:

- Since down-thrust has a limited capability (large mass of propellant), only contact instruments can be envisaged for the ISS package (no reaction force is created on the surface).
- Landing legs design has to be adapted to the extended stay. When thrusters stop firing, the landing legs may still have some internal elastic energy which would be released and make the S/C leave the surface.

5.3.2.2 In-situ instrumentation

A sample (not exhaustive) of in-situ instruments and mechanisms which could be envisaged for an ISS package is given here after along with their characteristics:

System	Primary objective	Description	Heritage
Mobility element			
Robotic arm	Mobility around the landing area (coverage area limited to a few m)	Robotic arm can include contact instruments as well as a shallow surface grinder/corer. Torques on the S/C to be evaluated (might require anchoring). Do not require down-thrust.	Beagle2, MER
Mole/penetrometer	Deep surface sampling (down to 5 m)	Sampling head linked to the S/C by a tether to provide power and data transfer. The instrument can include a limited number of instruments mounted within the mole head. Can achieve great depth.	Beagle2
Deep drill/corer	Deep surface sampling (down to 1-2 m).	Drilling instrument to achieve meaningful depths. Requires anchoring	SD2, ExoMars
Shallow surface corer or grinder	Shallow (few cm) surface analysis	Shallow corer or grinder to analyse the top regolith layer. Could be mounted on a robotic arm	Beagle2, MER
Science instruments			
APXS	Chemical composition of soil samples	Low-resource instrument. Integration time varies between 15 minutes to 2 hours or more. Requires calibration source	Philae, MER, Pathfinder
Mossbauer spectrometer	Analysis of Fe-bearing elements	Low-resource instrument. Integration time can be up to 12 hours. Requires calibration source	MER
Micro-camera	Surface morphology and texture	Low-resource instrument for close-up pictures and possibly compositional information.	[SCI_A04]
Laser mass spectrometer	Elemental, chemical and isotopic composition	Low-resource instrument. Laser illumination of the sample with further measurement of the ionised elements. Integration time of ~ 1-4 s.	[SCI_A04]
Temperature sensor	Temperature measurements	Temperature copper sensors/heaters	Mercury Surface Element, [Spohn01]
Densitometer	Density measurements	Density measurements via gamma-ray scattering. Requires gamma-ray source	Mercury Surface Element, [Spohn01]
IR spectrometer	Mineralogy of soil samples	Low-resource IR illuminating instrument.	
Sub-surface imager	Grain morphology of the regolith	Low-resource micro-camera mounted on a sub-surface instrument	
Gas chromatographer/ Mass spectrometer	Chemistry of organic molecules	Samples are fed through an over for gas-chromatography and time-of-flight mass-spectrometry. Requires a sample acquisition and distribution unit. Resource-demanding instrument	Philae COSAC instrument, ExoMars

System	Primary objective	Description	Heritage
LIBS/Raman spectrometer	Determine vibrational state of molecules and identify anorganic and organic species	Chemistry measured via emitted light of a collapsing plasma. Resource-demanding instrument	ExoMars
XRD	Charaterization of solid matter	Identification of crytstalline species by X-ray illumination and diffraction on a powdered sample. Resource-demanding instrument	ExoMars

Table 17: Description of optional in-situ instruments

System	Mass (g)	Volume (mm ³)	Power _{peak} (W)	Power _{average} (W)	Data volume ¹ (kbps)
Mobility element					
Robotic arm	2000	TBD	TBD	1.5	NA
Mole ²	1478	236x298x170	11	11	212
Deep drill/corer ³	4800	150x150x760 (excl. carousel)	11	<5W	NA
Shallow surface corer or grinder ⁴	350	TBD	TBD	6	TBD
Science instruments					
APXS	180	40x41x51	1.15	1.15	64
Mossbauer spectrometer	300	41x41x80	2	2	1200-4000
Micro-camera	100	19x40x96	<1	<1	8192
Laser mass spectrometer	300	40x40x70	5	0.5	4096
HP ³⁽⁵⁾	248	25x25x160	5.7	2.2	1000
IR spectrometer	300	25x25x160	<3	<3	TBD
Sub-surface imager ⁶	10	5x5x20	<1	<1	6000
Gas chromatographer/ Mass spectrometer	>4000	480x275x270	30	8	TBD
LIBS/Raman spectrometer	>3000	190x130x115	TBD	8	TBD
XRD	>6000	220x220x120	TBD	>12	TBD

Table 18: Technical features of optional in-situ instruments (do not include margins)

¹ Given for one measurement cycle

² For 1 h operations

³ Including distribution system

⁴ Many options are possible (e.g. simple grinder or sampling mechanism similar to the one used for sample return, etc.), with budgets extending over a wide range.

⁵ HP³: Package including the temperature sensor, the densitometer and another tool providing depth, accelerometry and tilting measurements (data is given for 12 h operations)

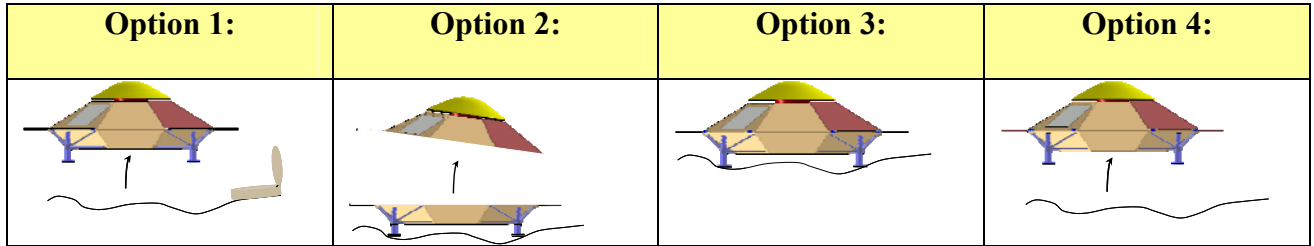
⁶ Electronics included in IR spectrometer

5.3.3 AVAILABLE OPTIONS AND TRADE-OFF

5.3.3.1 Options for an extended stay

4 options are available to envisage in-situ science and/or ground involvement in sampling operations for SR.

Figure 10: Configuration options for extended surface stay



Option	Description	Advantages	Drawbacks
1. Separate in-situ science package	Main S/C designed for short-term stay. Independent ISS package is released on surface for in-situ investigation.	<ul style="list-style-type: none"> ▪ Only ISS package is designed to withstand night conditions. ▪ Design of the ISS package relatively independent from the main spacecraft design. Impact on the baseline design is low ▪ SR failure is optimally mitigated. ▪ Main S/C can act as data relay. ▪ Design of the ISS package can be relatively simple (i.e. simple box with highly integrated P/L suite). ▪ Early release is possible to characterize soil properties before attempting sample return. ▪ Opportunity for collaboration (i.e. ISS = piggy-back P/L). ▪ Heritage from Philae & Beagle 2. ▪ No impact on the landing legs design of main S/C 	<ul style="list-style-type: none"> ▪ Ground decision-making impossible for sampling operations (for sample return). ▪ 2 different S/C have to be operated. ▪ Only contact instruments are possible for a simple design, otherwise, down-thrust also has to be used (i.e. duplication of thrusters). ▪ Sampling mechanism has to be duplicated. ▪ For a mass constrained design, option 2 should be preferred. ▪ Duplication of GNC system might be mandatory depending on the release strategy. ▪ For an extended stay, power and thermal requirements may turn out to be too demanding for such a small S/C. ▪ Limited resources will limit possible science operations.
2. Extended stay of sampling module only (incl. science package)	ERV designed for short-term stay. Lower part of S/C (Sampling module + ISS) is left on surface for in-situ investigation.	<ul style="list-style-type: none"> ▪ Only sampling module is designed to withstand night conditions. ▪ Single sampling mechanism for both SR and ISS. ▪ ERV can act as a data relay. ▪ Reduced duplication of S/C subsystems wrt option 1 (in particular GNC and landing legs are no longer duplicated). 	<ul style="list-style-type: none"> ▪ Ground-decision making impossible for sampling operations (for sample return). ▪ Requires instantaneous sampling verification and transfer. ▪ ISS can only be performed at the last SR attempt. ▪ Landing legs design of the S/C has to be adapted for extended stay if down-thrust cannot be used after main S/C departure, otherwise, thrusters have to be duplicated. ▪ Duplication of some subsystems will anyway

Option	Description	Advantages	Drawbacks
			<p>be needed (communication, power, thermal, maybe propulsion, OBDH).</p> <ul style="list-style-type: none"> ▪ SR failure is not optimally mitigated since the sampling and landing approach is about the same as for sample return. ▪ The impact on the baseline design is medium-high
3. Extended stay of the whole spacecraft	Whole S/C remains on surface for an extended stay	<ul style="list-style-type: none"> ▪ Allow ground decision-making for sampling operations. ▪ No sub-system duplications at all. ▪ Build on the same sampling approach as the sample return (but see drawbacks). ▪ Only 1 S/C to operate. 	<ul style="list-style-type: none"> ▪ Whole S/C is designed to withstand night conditions. ▪ Impact on baseline design is high ▪ No data relay during surface stay (but this is the case for the baseline design anyhow) ▪ SR failure is not optimally mitigated since the sampling and landing approach is about the same as for sample return. ▪ No mole can be envisaged (mole could remain stuck in depth and return would not be possible)
4. Orbit analysis of collected sample	No extended stay on the surface. S/C collects sample and analyse it into orbit	<ul style="list-style-type: none"> ▪ No sub-system duplications at all. ▪ Build on the same sampling approach as the sample return (but see drawbacks). ▪ Only 1 S/C to operate. ▪ No impact on the landing/sampling operations (in particular no night stay). 	<ul style="list-style-type: none"> ▪ Ground decision-making impossible for SR and ISS. ▪ Impact on baseline design is high (the whole transfer chain and distribution system has to be accommodated within the main S/C) ▪ Impact on baseline design is high-very high ▪ Analysis of the sample while in-orbit in a microgravity environment is deemed very complex. ▪ SR failure is almost not mitigated at all since the sampling and landing approach are exactly the same as for sample return (only return leg is mitigated). ▪ Very short-term stay, therefore mobility is limited to the number of attempts the main S/C can perform.

Table 19: Advantages and drawbacks of configuration options for extended stay

From this top-level analysis, it is clear that an extended stay would have large implications over the baseline design, unless an independent ISS package is embedded on the main S/C. The following highlights the major engineering constraints of option 3 to point out the sensitivity of the baseline design (chapter 6) against an extended stay. The discussion is also valid for most options.

5.3.3.2 Consequences for thermal, power, communication and mechanical design

From a thermal viewpoint two issues appear for a long stay: the increased duration of exposure to the asteroid flux on the day side and the long duration spent on the night side. The heating providing by additional in-situ instruments would increase the heat rejection requirement and therefore would lead to an increased radiator area which, in turn, would increase the power requirement on the night side to keep the equipment within the specified temperature. For the baseline scenario mainly due to the heat leaks through the radiators, this power is ~ 359 W.

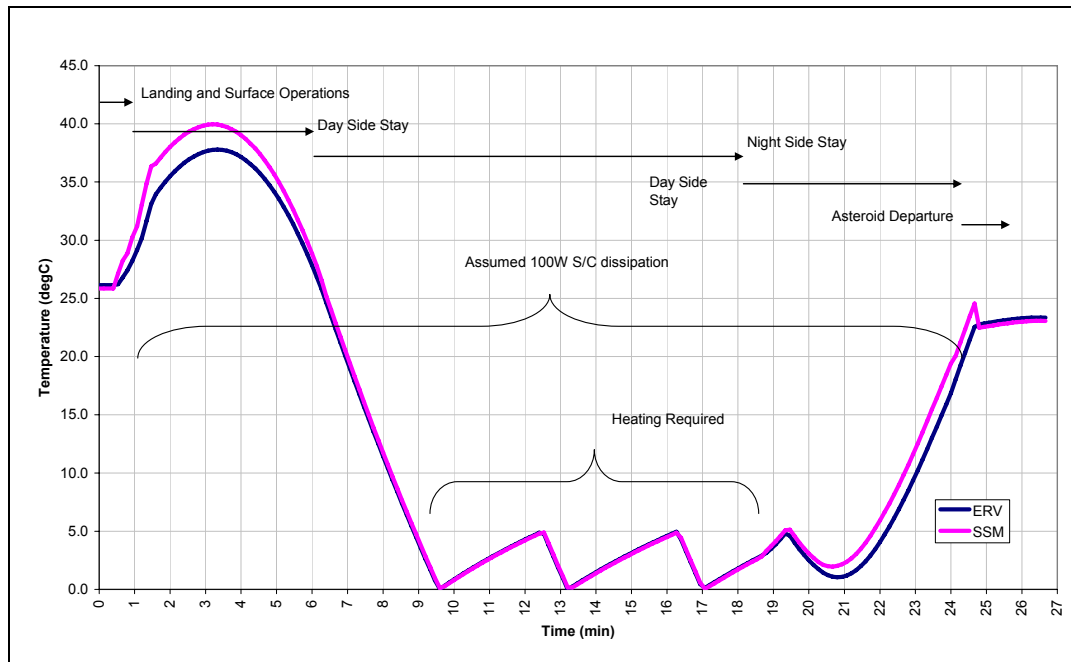


Figure 11: Spacecraft temperature variation for extended stay

Alternatives to reduce the heater power required for night side stay are:

- Allowing the spacecraft units to hibernate (all equipments turned off and allowed to go cold until solar power is available), however due to the relatively high allowable minimum temperature of the propulsion system it would not be possible for the propulsion system to survive without heating during the night so that the spacecraft can return to earth
- Implementation of large RHUs (much larger than those planned for ExoMars)
- Install louvers over radiators (Rosetta) to reduce rejected heat at night, the downside being a significant mass increase

For the baseline scenario all surface operations are powered by a 25 kg battery, allowing for 2.5 hours on the surface. For every extra hour spent on the surface, the battery mass increase is 5 kg. From a power viewpoint, the random surface geometry of the asteroid may also be such that solar power is not available. As mentioned above, a 359 W heating power is required on the night side.

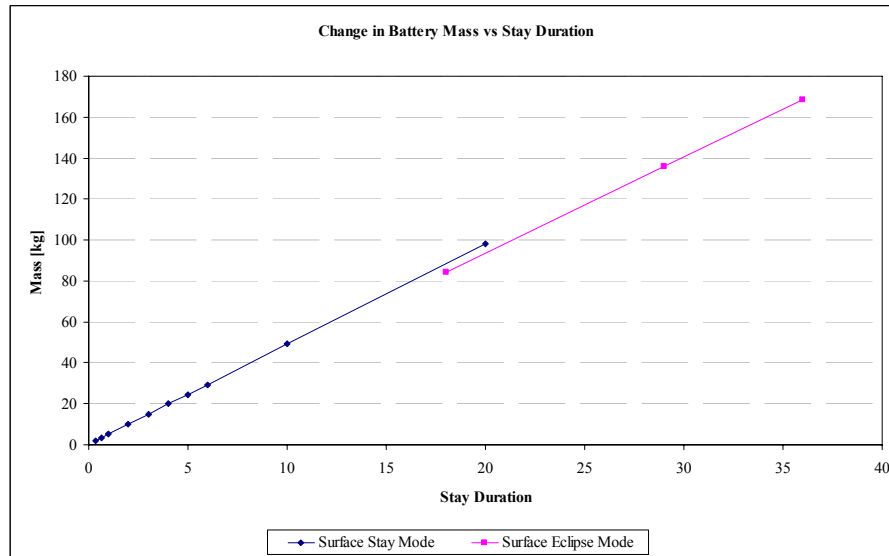


Figure 12: Battery mass increase with respect to stay duration

The battery for a night stay on a 20 h rotating asteroid would need to be ~125 kg and this would only allow staying over one night. Any requirement for a multiple night stay (days to weeks) would in addition require battery charging via the solar arrays which area would need to be increased to 10 m² at 0° latitude and 20 m² at 65°, assuming steerable arrays. Even then, this does not guarantee that the Sun can be seen at all time due to the unknown landing geometry and landscape. Beyond 65° latitude, the solar arrays are mostly inefficient due to the poor illumination conditions.

Even if a steerable HGA antenna is used, communications may also be difficult depending on the landing site landscape and the Earth-Sun relative positions. From this point of view a relay satellite would clearly be preferred if an extended stay is necessary.

This scenario presents another engineering challenge in the design of the landing system. Any landing system needs to absorb the inertial energy that the lander delivers at landing. In that respect, the landing device requires damping of the loads on the spacecraft. Any damping device has an elastic behaviour. It is to be noted that this is one of the reasons why a hold-down thrust is baselined in order to keep the spacecraft on the ground after impact. The downside of this approach is that after off-switching the thrusters (necessary for an extended stay) the elastic energy stored in the landing device has to be released which turn into a vertical impulse which can lead to a large jump/bouncing over the surface or toppling of the lander if the bouncing is not symmetric. In the leg design described in 6.7.1.1, the inertial energy is stored in a spring which is kept compressed after landing thanks to a ratcheting device. This minimizes the upwards reaction force. However, as explained in 6.7.1.1, the system is discrete (assumed to be made of 4 mm steps). Therefore, the energy stored in one ratchet pitch (1.44 J) could be released. The energy stored in this pitch by the 4 legs is thus 5.76 J and would lift the lander up to 58.8 m when the thrusters are switched off if the 4 legs store the same amount of energy.

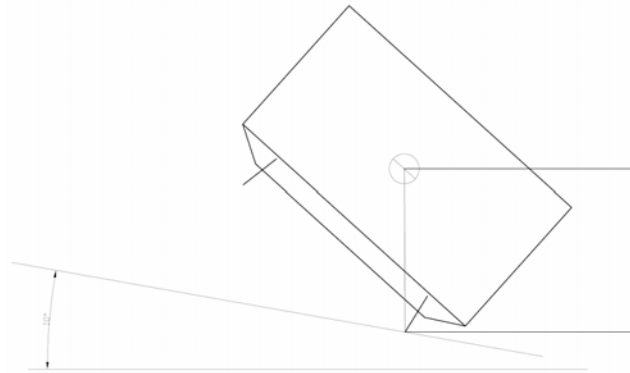


Figure 13: Toppling situation at landing

As illustrated on the above schematic, the worst-case toppling situation will occur if two legs store the maximum pitch energy which is then equal to 2.88 J. The lander will topple over if the height of the CoG increases by ~ 15.5 cm when thrusters are off. This translates into an energy of 0.015 J which is well below 2.88 J. It is clear from this preliminary analysis that switching-off the thrusters may easily lead to large bouncing of the spacecraft and possibly toppling over. This analysis is valid for this particular design but since any multiple-landing leg system would necessarily have an elastic behaviour (pure plastic behaviour would prevent multiple landing or would lead to prohibitive leg length), similar conclusions can be drawn for other landing systems. Only anchoring could prevent this behaviour but is not recommended for landing on unknown surface.

In addition to the thermal, power, communication and mechanism issues, neither is the night stay favourable from a GNC viewpoint. On the surface, the STR may be occulted by the asteroid itself. The S/C states are therefore determined prior to ascent via propagation on gyroscopes only. A long duration is prohibitive because the gyrometers have a long-term drift which would endanger the navigation during ascent trajectory.

In any case, an extended stay would make the design more complex and greatly increase the cost of the baseline configuration and is no longer envisaged in the frame of this study.

5.4 GNC strategy during descent and landing

The main requirements that the GNC system has to cope with in this phase are:

- Maintain an attitude of 10° with respect to the surface
- Keep landing vertical and horizontal velocities lower than respectively: 30 and 5 cm/s (to enable a soft landing and lightweight landing legs design and limit bouncing on the surface)
- Prevent contamination of the surface
- Engage re-ascent as soon as an FDIR is triggered

Strategy	Description	Needed equipment	Advantages	Drawbacks
1. Open-loop GNC	Pre-calculated, Open-loop descent starting at radio-navigation altitude	IMU (possibly WAC for FDIR)	Most cost-efficient and less complex approach	High landing lateral velocity. Large lateral error up to ~ 200 m. Large attitude alignment error (≥ 30 deg).

Strategy	Description	Needed equipment	Advantages	Drawbacks
	(ROSETTA/Philae): automatic and direct descent to specified location, touch-down and ascent			High constraints on landing legs and solar arrays but could use WAC to detect possible hazards or large errors to trigger immediate re-ascent
2.Navigation + Control closed-loop GNC	Navigation [Polle03] and control loop closed; guidance pre-calculated with ground support using rehearsal.	IMU + WAC (+ radar/laser altimeter)	Complies with all attitude and velocity requirements at landing. Can easily use rehearsals to help define pre-calculated trajectories. Build on European development for ExoMars	Heavier and higher cost than 1
3.Full closed-loop GNC	Navigation and control loop closed; plus autonomous real-time guidance	IMU + WAC + radar/laser altimeter + processing requirements for autonomous scene analysis	Compared to 2, can provide real-time hazard avoidance but hazard mapping can easily be done from orbit for hazards > 10 cm	Same as 2 + Largely increased mode failures due to increase processing loads

Table 20: GNC options for descent and landing - trade-off

Rehearsals are possible for all cases. The GNC strategy using WAC and thrusters for closed-loop navigation and control (and possibly radar/laser altimeter for altitude control and robustness) is selected.

6 DESIGN OF SELECTED MISSION CONCEPT

6.1 Baseline scenario

6.1.1 MISSION ANALYSIS

6.1.1.1 Transfers to the selected target

The following two transfers have been selected for detailed design of the spacecraft. The 2016 launch opportunity is selected as a baseline but the return ΔV requirements cope with the 2020 launch opportunity to ensure the design is feasible and compatible with both launch dates.

Target	launch dd/mm/yyyy	arrival dd/mm/yyyy	ΔV from GTO (m/s)	Return dd/mm/yyyy	arrival dd/mm/yyyy	ΔV_{return} m/s	v_{entry} m/s	ΔV_{total} (m/s)	ΔV with margin (m/s)
1999ju3	05/12/2016	11/07/2019	2055.5	11/11/2019	04/12/2020	6.9	12001.3	2062.4	2165.6
1999ju3	03/12/2020	11/02/2022	1745.9	20/07/2023	04/12/2024	593.0	12180.6	2338.9	2455.9

Table 21: Baseline + optional transfers

It is of interest to analyse the launch windows both for the outbound and inbound trip and the effect on the stay time.

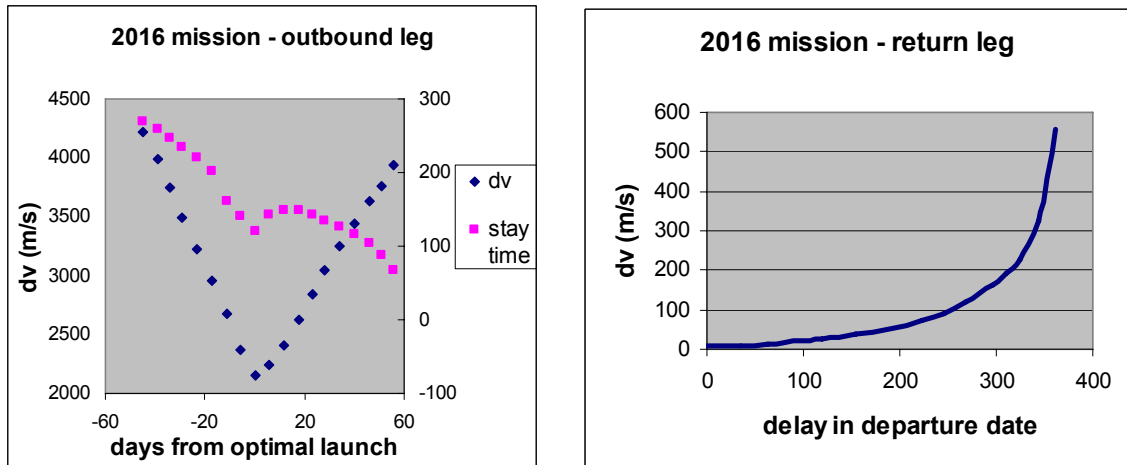


Figure 14: sensitivity to launch date and departure date from the asteroid for 2016 mission

The above graphs show that the launch window is narrow. The launch date corresponds to the last final burn to inject the spacecraft onto the escape trajectory. The departure ΔV is updated so that the injection is robust to a burn failure. The graph also shows an extended stay about the asteroid almost has no penalty and that it is more interesting to delay the departure from the asteroid. Eventually, the selected transfer is modified to account for an extended stay of 10 months and is shown hereafter.

Table 22: Baseline transfer with a 10 months stay about 1999JU3

launch dd/mm/yyyy	Departure ΔV (m/s)	DSM ΔV (m/s)	Arrival V_{inf} (m/s)	Total outbound ΔV (m/s)	Arrival at the asteroid dd/mm/yyyy	Stay time (days)	Return ΔV (m/s)	Arrival at Earth dd/mm/yyyy
05/12/2016	1645.2	29.4	385.9	2165.6	11/07/2019	309	51.1	04/12/2020

The same analysis can be done for the 2020 opportunity. In that case, it is interesting to note that for the same launch date, the anticipation of the arrival date at the asteroid by more than 1 year does not require more ΔV and is the best way to extend the stay time.

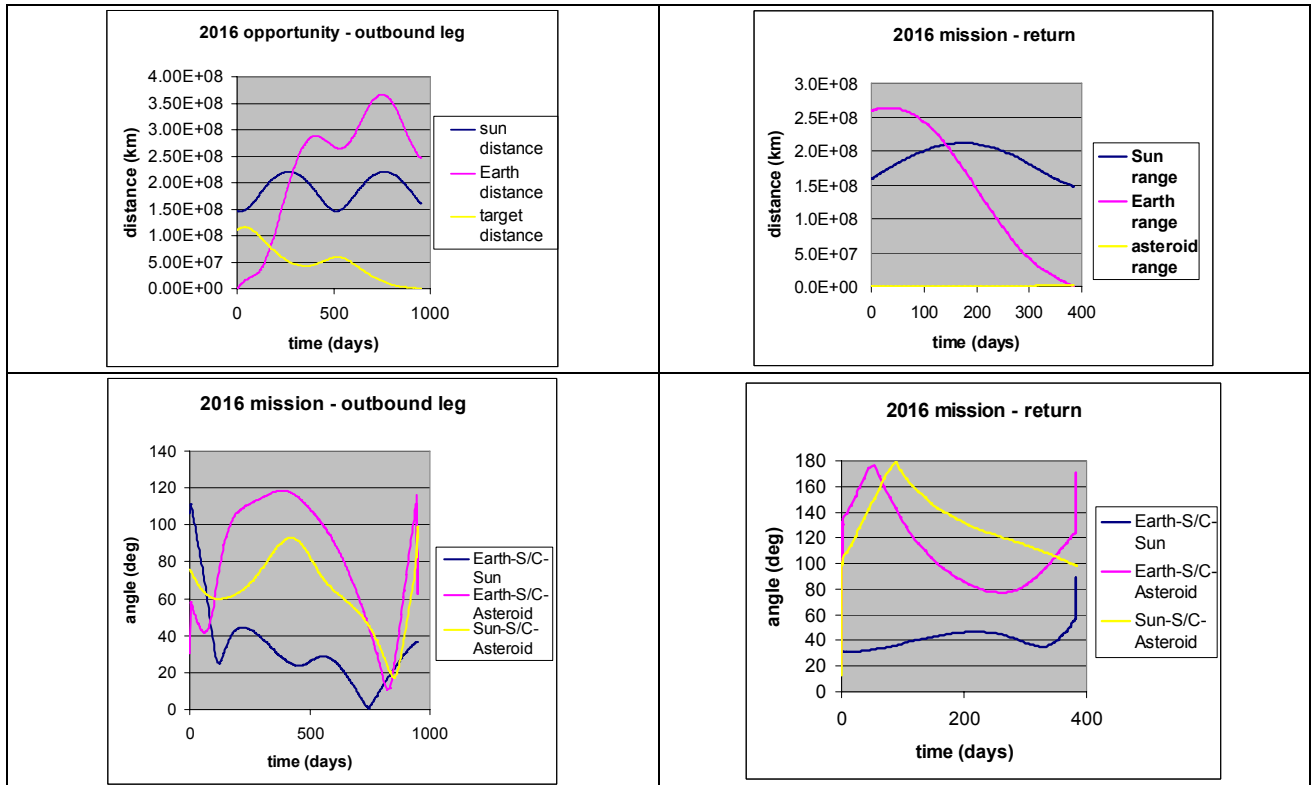
6.1.1.2 Back-up launch dates and targets

Two launch date opportunities were identified. However, it does not provide any contingency plan in case the 2016 launch window is missed by a few months due to technical problems such as launch delay, etc. A back-up date reasonably close to December 2016 is required. Mission analysis shows that no such opportunity exists for 1999JU3 and the 2017 opportunity to Nereus (2.76 km/s) is very close to the baseline launch date (January 2017). Therefore mission analysis was performed ([Agnolon07II]) to determine whether there is a target which has ΔV requirements similar to 1999JU3. According to analytical analysis about 10 targets are more accessible than 1999JU3. All of them are either of unknown type or of S-type. The conclusion is that a sample of these targets has good transfers in the range 2.3-3.5 km/s with return ΔV compatible with the use of RCS thrusters. However, only two of them (to 2002NV16) are lower than 2.8 km/s and depart in 2020

while the others are all above 2.9 km/s. Therefore, if the mission concept is to be compatible with one of these targets launch mass margins will be drastically reduced but the mission would still be feasible.

6.1.1.3 Geometry of the transfer

Figure 15: Geometry of the interplanetary transfers



Communications will not be possible between Earth and the spacecraft for a few weeks because ESS is close to 0°.

6.1.2 1999 JU3 PROPERTIES

Parameter	Value	Comment
Taxonomy class	Cg	SMASS II classification
Size	700 m x 350 m x 350 m	Assumed Prolate spheroid (cigar-shaped)
Volume	4,5.10 ⁷ m ³	
Density	1300 kg/m ³	Assumed density for a C-type
Mass	5,85.10 ¹⁰ kg	
μ	3.9 m ³ /s ²	
Semi-major axis	1.189 AU	
Orbit perihelion	0.96 AU	
Orbit aphelion	1.42 AU	

Parameter	Value	Comment
Inclination	5.88°	
Orbital period	473.6 days	
Diameter of sphere of influence	4.4 km (perihelion) – 5.5 km (aphelion)	
Diameter of Hill sphere	62 km (perihelion) – 76 km (aphelion)	
Orbital period	1.3 years	
Rotation period	Unknown	Large constraint on design. Assumed worst cases (20 h for thermal design, 2.5 h for GNC)
Spin axis orientation	Unknown	No assumptions
Assumed solar constant	1400 W/m ²	At rendezvous
Surface temperature range	[120-410] K	Day-Night. 20 h Rotation period assumed

Table 23: 1999JU3 properties

The thermal properties of the asteroid have a large impact on the mission design. Below is presented the surface temperature distribution for the envisaged 2019 arrival year and for a spherical asteroid with a 25 h rotation period (assuming a typical regolith specific heat capacity).

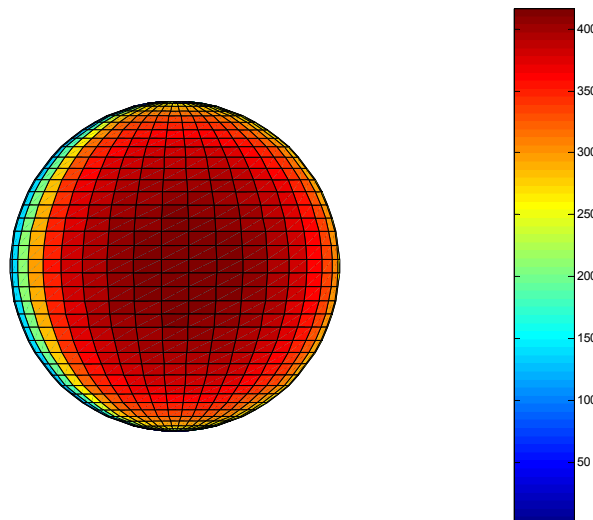


Figure 16: Spherical projection of the surface temperature distribution for asteroid at 1.06AU with a 25 hour rotation period

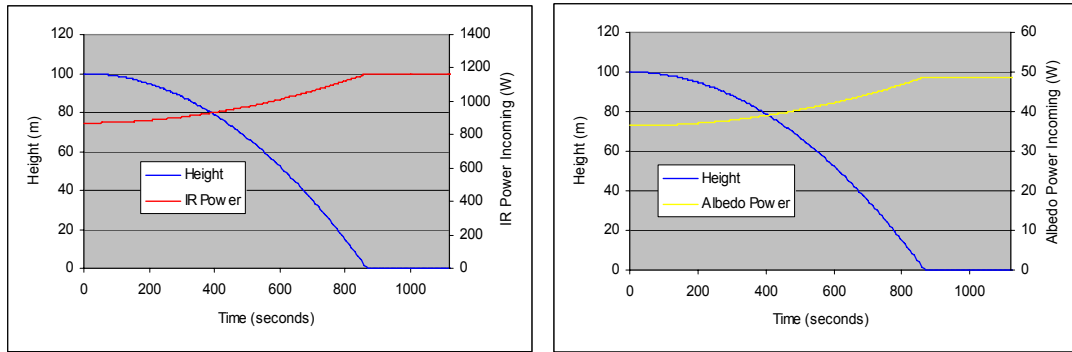


Figure 17: Heat flux on spacecraft during freefall to sub solar point

Above simulations have been performed for a spacecraft free-falling at the sub-solar point. The thermal flux mainly comes from the asteroid IR flux and visible flux ($\sim 1378 \text{ W/m}^2$ at 1AU). Similar simulations have been conducted for landings at higher latitudes and showed a much more favourable case at 45° and 70° latitude (for the latter, IR and albedo power are 3 times lower than at the sub-solar point). The sizing of the thermal system has been done for a landing at sub-solar point.

6.1.3 LAUNCH VEHICLE

Cost-efficient European launchers are favoured. Preliminary analysis showed that launch margins achieved with VEGA were negative for either AIS only or ASR scenario (see annex). For this reason, a Soyuz-Fregat 2-1B launch from Kourou has been selected as the baseline for the NEA-SR TRS. The key specifications of the launch vehicle are summarized in Table 24.

Table 24: Baseline launch vehicle's technical features

Parameter	Value	Notes	ST-type Fairing volume
Launch site	Kourou	Guiana Space Centre (CSG)	<p>The technical drawing shows a cross-section of the ST-type fairing. Key dimensions include a total height of 11.105m, a top diameter of 8.543m, a side angle of 1.4°/30', a main body diameter of 3.800m, a total length of 25.00m, a base diameter of 2.700m, and a bottom diameter of 2.710m. Components labeled include the fairing, adapter or dispenser, inter fair plane with fregat, fregat, and interstage.</p>
Launch vehicle	Soyuz-Fregat 2-1B		
Launch performance into GTO	3023 kg	35622 km x 200 km. (~ 3100 kg including 75 kg launch vehicle adaptor)	
Fairing dimensions	Diameter: 3.8 m, Height: 5.0 – 9.5 m	ST-Fairing (S-fairing not available at CSG)	
Cost	~ 40 M€	FY2007	

6.1.4 MISSION OPERATIONS

6.1.4.1 Operations overview

Table 25: Primary operational phases

Phase name	Orbit	Main events	Duration
Launch into GTO	GTO	Launch into GTO by Soyuz	60 min
S/C Acquisition	GTO	<ul style="list-style-type: none"> ▪ Separation from Fregat upper stage ▪ Deployment of SA and HGA 	60 min
Orbit raise up to sub-lunar orbit	Successive highly elliptical orbits	<ul style="list-style-type: none"> ▪ 2 perigee PRM burns provide required ΔV (final orbit of this phase is a sub-lunar orbit 300*300000 km) ▪ Possible P/L checkout and commissioning 	4-5 weeks
Injection into Earth-1999JU3 transfer	NA	PRM provides required C_3 (8 % gravity losses)	Minutes
Interplanetary cruise	Interplanetary	<ul style="list-style-type: none"> ▪ Some DSMs to change semi-major axis, eccentricity or inclination ▪ ~20 days with Sun-Earth angle < 5° ▪ Hibernation mode 	2.4 to 2.6 years
1999JU3 rendezvous	Approach trajectory	<ul style="list-style-type: none"> ▪ 3 PRM burns to cancel out the spacecraft V_{inf} relative to target starting 1.2 millions km before arrival ▪ NAC acquisition of target ▪ Initial characterization of target (RSE, imaging, etc.) ▪ PRM separation and disposal 	70 days
Orbit insertion	NA	Using main S/C RCS thrusters	A few hours
Orbital operations	Circular 6 km orbit	<ul style="list-style-type: none"> ▪ Nadir pointing instruments ▪ Minimum RSE campaign to precisely determine asteroid gravity field (1^{1/2} month) ▪ Remote sensing campaign for global characterization of the target + building-up of an accurate DEM model + local characterization of a number of landing sites (+descent and landing planning) 	Nominally 3 months (At least 1 ^{1/2} month for RSE)
Landing rehearsals	Successive low elliptical or hyperbolic orbits	<ul style="list-style-type: none"> ▪ Landing sites fly-bys ▪ Autonomous manoeuvres, rehearsals and asteroid model verification ▪ Hazard/Thermal mapping on selected landing area ▪ Final landing site selection 	10 to 20 days
Landing & sampling operations	Same as rehearsals + actual descent, landing and re-ascent	<ul style="list-style-type: none"> ▪ Autonomous descent ~ 40 min ▪ Sampling operations + coverage of contextual information ~ 20 min ▪ Pre-programmed re-ascent (thruster impulse) ~ 50 min 	~ 2 hours
Extended orbital operations	Circular 6 km orbit	Same as Orbital operations	Up to 6 ^{1/2} months
Earth return transfer injection	NA	ΔV provided by main S/C RCS thrusters	Few minutes
Interplanetary return cruise	Interplanetary	<ul style="list-style-type: none"> ▪ Hibernation mode ▪ Few DSMs 	1 to 1.4 years
Direct Earth re-entry	NA	<ul style="list-style-type: none"> ▪ ERV spin-up and ERC ejection ▪ High speed Earth re-entry and ground hard-landing of ERC (15-20 minutes) 	hours

Phase name	Orbit	Main events	Duration
Retrieval operations	NA	Locating and retrieval of capsule via beacons	Minutes to hours

6.1.4.2 Departure strategy

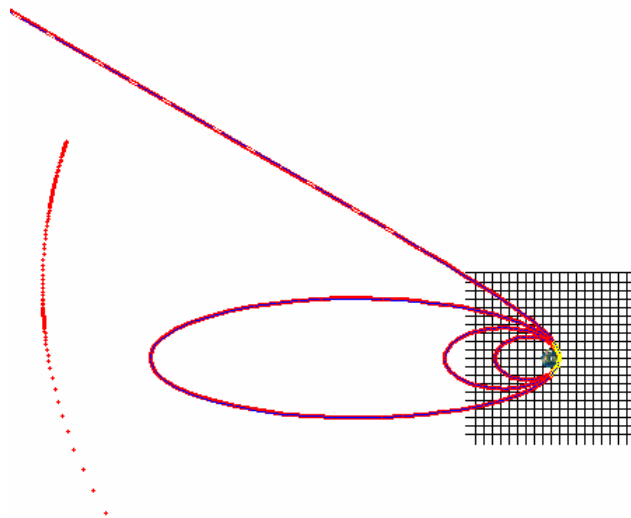


Figure 18: Injection into GTO with apogee raising and then escape to a 4.5km/sec V_{∞} orbit

The departure strategy is depicted above. The inclination required for the baseline transfer is -51° to achieve the necessary declination ([Agnolon07II]). Since Soyuz from Kourou optimally launches with a 0° degrees inclination (up to 20° without large mass penalty), a solution has to be envisaged. There are basically two options. One is to perform an EGA, which has no ΔV penalty but adds one year of operations. The other is to launch into a 20° inclined orbit and then perform the inclination change at the apogee of a HEO orbit. This typically requires 300 m/s extra ΔV . In addition, 40 m/s is added to account for one burn failure. The outbound ΔV is therefore increased to **2515 m/s**. Lastly, the apogee raising manoeuvre has to be optimized taking into account constraints such as eclipses, ground station coverage (which is found to be good with Perth), radiation minimization, etc.

6.1.4.3 Target approach

The rendezvous with the target requires a final burn which in practice is split into 4 manoeuvres as illustrated in below picture. This slightly increases the outbound V to **2550 m/s** if the burns are 23 days away from each other to allow for long and precise ground tracking. The camera is needed since the ephemeris may add a few 100 km error in the asteroid trajectory. Therefore the NAC typically looks for and acquires the actual target position right before or after the 2nd burn.

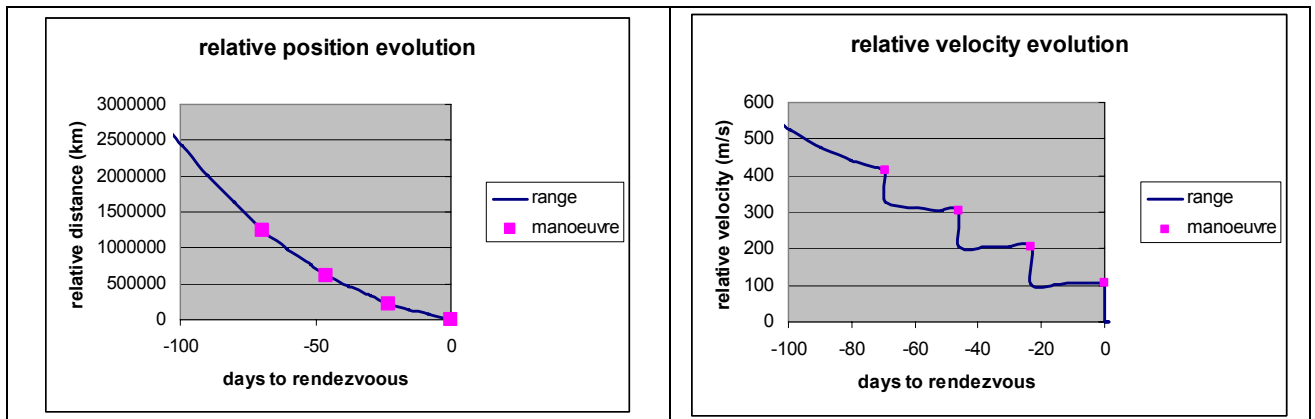


Figure 19: Asteroid rendezvous manoeuvres

The low-gravity environment about the asteroid is a major environmental driver. Orbital, landing and sampling operations are further described below.

6.1.4.4 Proximity operations

The manoeuvres during orbital, landing and return operations are managed by the RCS thrusters of the OLERV which characteristics are described in chapter 6.5.2.

6.1.4.4.1 Asteroid observations from orbit

6.1.4.4.1.1 Disturbances

The main disturbances in orbit are high orders of the gravity field and the solar radiation pressure (Sun's influence is rather low at envisaged altitudes).

- The high orders of the harmonic gravity field (J_2 , J_{22} , etc.) will mainly be felt at low altitude as slow secular rates, etc. The orbit low-limit can be selected such that these terms have a tiny influence over the orbit stability [Scheeres97].
- Solar radiation pressure tends to make the orbit non-Keplerian (by shifting the spacecraft orbital plane out of the asteroid plane containing the centre of gravity) which is clearly not desired in particular if one wants to achieve high degree of accuracy for gravity field determination and also in order to remain on a stable orbit. A maximum semi-major axis should be selected below which the influence of the SRP is negligible [Scheeres02]. In the case of 1999JU3, this maximum distance is larger than the sphere of influence of the body.

Remark: A body which is assumed to be a dormant comet could still present some form of outgassing which would have to be taken into account for the selection of a stable orbit. The selection of the main orbital parameters can be performed so that the trajectory remains stable over a number of orbits.

The following graph illustrates the contribution of each disturbance against the orbit altitude. The central gravity force is the dominant term at intermediate altitude within the sphere of influence. This does not allow to conclude on the long-term stability of the orbit which requires a more detailed analysis.

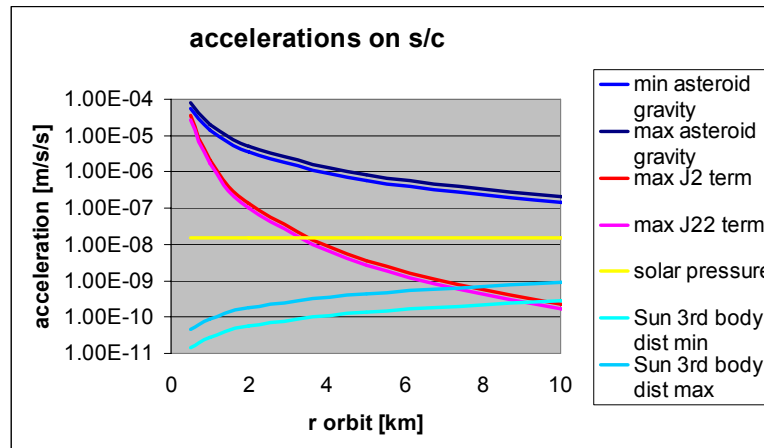


Figure 20: Orbit disturbances

6.1.4.4.1.2 Orbit selection

There are basically three types of orbits that could be envisaged:

- Elliptical orbit within the SoI
- Orbit about gravitationally compensated points (Lagrange points are specific examples of such locations) out of the SoI but within the Hill's sphere
- Non-Keplerian orbit

The three strategies were analysed. The last one turns out to be most demanding in terms of ΔV and operations (high-frequency station keeping). It is clear from a science viewpoint that staying in polar close orbit has many advantages (camera resolution, radio science accuracy, hazard mapping, etc.). A parking orbit which would be located at a constant location (out of the sphere of influence but within the Hill sphere) would yet have some design advantages (permanent asteroid-spacecraft-Sun angle, power, communications, orbit maintenance, etc.). However, analysis has shown that stable and eclipse-free polar orbits which allow full coverage of the asteroid can also be found within the SoI at 2-4 km altitude. Little ΔV is needed to maintain this type of orbit.

Radio science can be performed in the early stages of the orbit operations to preliminary determine mass and gravity field of the asteroid during the first fly-overs. In parallel, the asteroid is characterized by the WAC, NAC and UV-vis-NIR spectrometer. This allows constructing maps such as topographical map (DEM), mineralogical map, features, etc. This is followed by a period when rehearsals down to 500 m are performed to confirm the asteroid gravity and topography model and acquire close-up images (\sim cm resolution) of potential landing sites and therefore map potential hazards.

6.1.4.4.2 Landing, sampling and re-ascent operations

The sequence of this particularly critical phase of the mission is described in Table 26. T refers to the touch-down time. This sequence is meant to be representative of a typical descent with the earlier selected GNC and sampling strategy and parameters such as timeline, number of burns,

acquisition frequencies, etc. are only indicative. For attitude control, the gyroscopes are always on and the STRs are used to the greatest extent possible (when exclusion angles are small enough).

Timeline (start of event)	Altitude	Event description	
		GNC	Sampling chain
T₀ – TBD h	6 km		Robotic arm picks a corer head and place it in the right position, ready for sampling
T₀ = T – 48 h	6 km	1 st burn (Hohmann transfer) to an intermediary orbit. Commanded and monitored by ground. Only radio-navigation	
T – 24 h	6 km <H<500 m	2 nd burn (Hohmann) to a 2 nd intermediary orbit. Only radio-navigation	
T – 12 h	6 km <H<500 m	WAC takes 2 pictures at 100 s interval and sends them to ground (provides relative positioning)	
T – 9 h	6 km <H<500 m	Phasing burn commanded by ground	
T – 4 h	6 km <H<500 m	WAC takes 2 pictures at 100 s interval and sends them to ground (relative positioning)	
T – 1 h	500 m	S/C receives from ground time-tagged TC for initiation of descent. From then on, operations are entirely autonomous up until T + 22 min	
T – 40 min	500 m	Descent is initiated via descent burn. WAC active in feature point tracking mode (velocity estimation) with an image rate of 0.1 to 1 Hz. A few lateral correction burns are autonomously implemented over the descent.	
T – 39 min	500 m <H<100 m	1 image is analysed through image recognition (e.g. correlation with pre-stored images) for real-time positioning	
T – 26 min	500 m <H<100 m	1 image is analysed through image recognition (e.g. correlation with pre-stored images) for real-time positioning	
T – 15 min	100 m	Braking burn before final free-fall (<u>Optional</u>)	
T – 13 min	< 100 m	1 image is analysed through image recognition (e.g. correlation with pre-stored images) for real-time positioning	
T	0 m	Touch-down detection by contact sensors. Hold-down thrust initiated for the duration of the sampling.	
T + 2 s	0 m		Lowering of sampling mechanism down to soil + start of sampling.
T + 19 min	0 m		Sampling mechanism back in its folded position
T + 20 min	0 m	Down-thrust stopped. Ascent burn initiated (small impulse)	
T + 22 min	> 100 m	1 st burn to intermediate position. Ground resumes control of the S/C	
T + 12 h	few km – 6 km	2 nd burn to go back on the initial orbit	
T + 20 h	6 km		Verification of sample acquisition

		Event description	
T + 30 h	6 km		Corer head incl. sample is transferred to sample container

Table 26: Descent, landing, sampling and ascent operations

In red are the autonomous phases while in blue are the ground-controlled phases. The last 500 m of the descent use a one-burn descent strategy. The touch-down conditions are such that $V_{\text{Vertical}} < 30$ cm/s and $V_{\text{Horizontal}} < 5$ cm/s. V_{Vertical} is guaranteed by the choice of the initial descent altitude and $V_{\text{Horizontal}}$ is guaranteed by the lateral velocity determination via the navigation WAC and subsequent lateral control of the S/C. This latter is based upon vision-based navigation which allows to determine the lateral velocity of the S/C through features tracking (boulders, shadows, crater rims, etc.). The fact of having a vertical landing velocity limited to 20-30 cm/s by design means that even in case of major failure during autonomous final descent, the landing shall be safe, providing the attitude is not dramatically changed. Chapter 6.6.2 present more detailed simulations where the rationale for the descent parameters and the descent strategy can be found.

6.2 Design margins

During the spacecraft design study, the margins listed in Table 27 have been used. The margins largely comply with the ESA margin philosophy for assessment studies [Atzei05]. The nominal mass and power budgets are determined after application of the subsystem margins. All subsystems are sized to accommodate any other subsystem with subsystem margin applied (e.g. the re-entry probe is sized to accommodate the sample container with subsystem margins; the propulsion module is sized to accommodate the OLERV including subsystems margins).

Table 27: Margin overview

Item	Margin
<i>Subsystem mass margin</i>	
Off-the-shelf equipment	5%
Off-the-shelf equipment requiring minor modifications	10%
New designs/major modifications	20%
<i>Power subsystem margin</i>	
Off-the-shelf equipment	5%
Off-the-shelf equipment requiring minor modifications	10%
New designs/major modifications	20%
<i>Data processing</i>	
On-board memory capacity margin	50%
Processing peak capacity margin	50%
<i>Communications</i>	
Communication link	3 dB
Telecommand and telemetry data rates	3 dB
<i>System level</i>	
System level mass margin	20%
System level power margin	20%

6.3 System overview

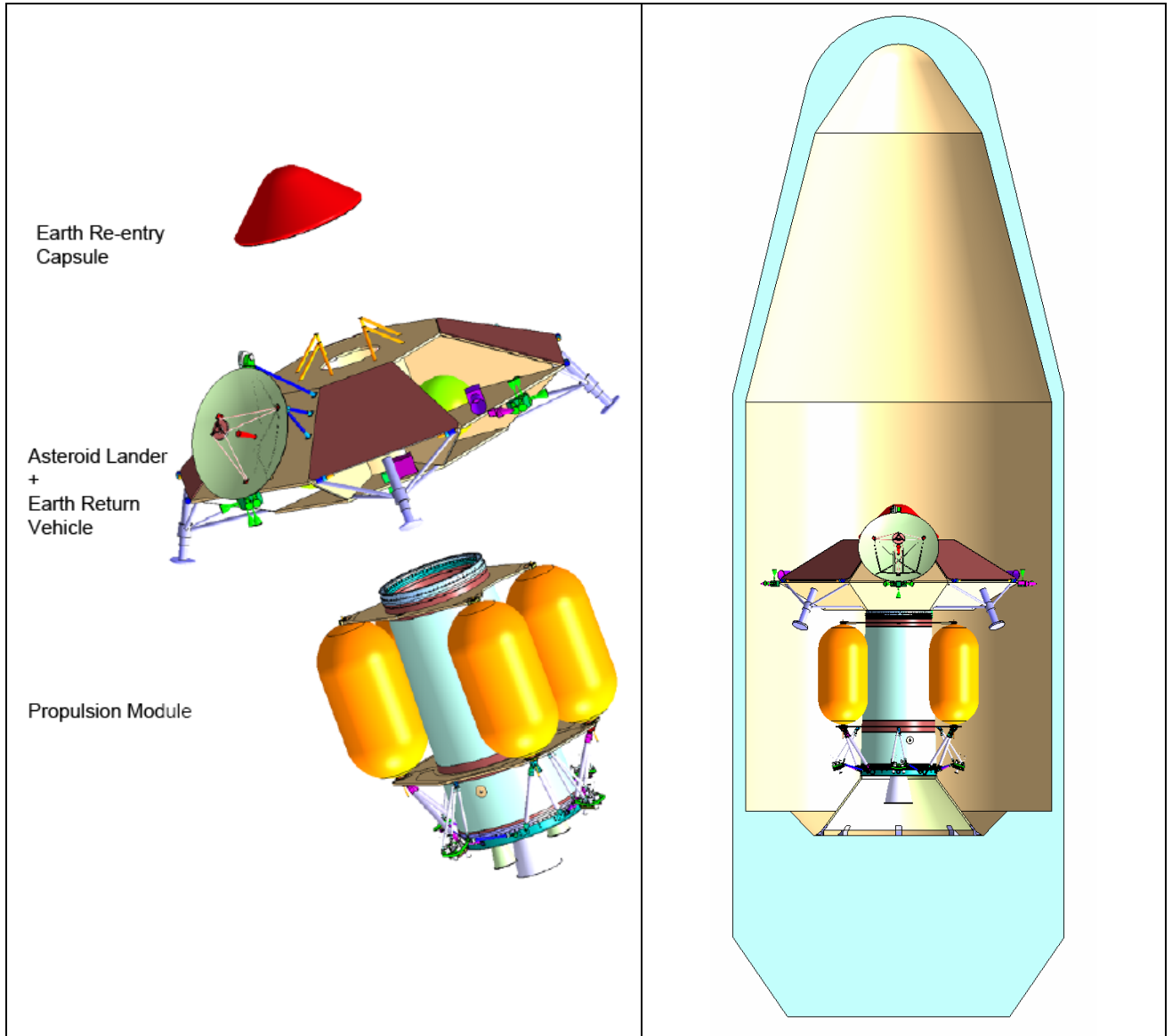


Figure 21: Exploded view of the Spacecraft composite (left) – Spacecraft within the launcher fairing (right) (without MLI)

As shown on the figure above, the launch composite is composed of the propulsion module, the OLERV and the ERC. These elements are described further in below sections. The system mass budgets are presented in the following tables.

Element or equipment	Basic dry mass in kg (incl. subsystem maturity margin)
PRM module	
PRM	210
OLERV	
AOCS	35
Communications	37

Element or equipment	Basic dry mass in kg (incl. subsystem maturity margin)
Data handling	19
Harness	20
Mechanisms	65
Payload	6.9
Power	53
Propulsion	42
Structure	59
Thermal	24
ERC	57
OLERV Total (incl. ERC)	420
OLERV + PRM total	630
Total system mass incl. 20% system margin	756
Element	Propellant mass in kg incl. 2% residual margins
PRM	1380
OLERV	199
Total	1579
Element	System mass in kg (incl. 20% system margin on dry mass for each element)
PRM	1632
OLERV	703
Total	2335
Launcher capability in GTO (not including adaptor)	3023
Launch margin (additional to system margin)	29.5%

Table 28: System mass budget

This mass budget suggests a substantial launch margin. The extra mass capability can for instance be used to carry more payload (Table 11) or a separate in-situ science package. Up to 200 kg (if the extra payload is returned to earth) or 270 kg (if the extra payload is jettisoned at the asteroid, for instance in-situ science package) could be added on the OLERV in terms of dry mass. The pure payload mass will likely be more limited than that due to required strengthening of the structure, increased power needs, etc. The functional architecture of the baseline S/C is provided below.

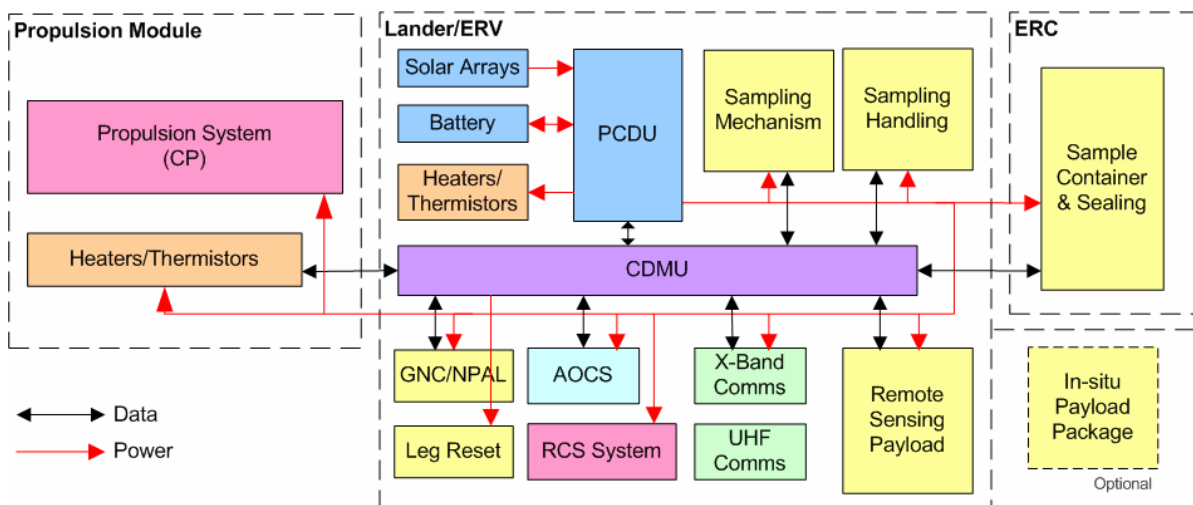


Figure 22: Spacecraft functional architecture

6.4 OLERV Configuration and structures

The main dimensions of the OLERV are illustrated in Figure 53 and Figure 54.

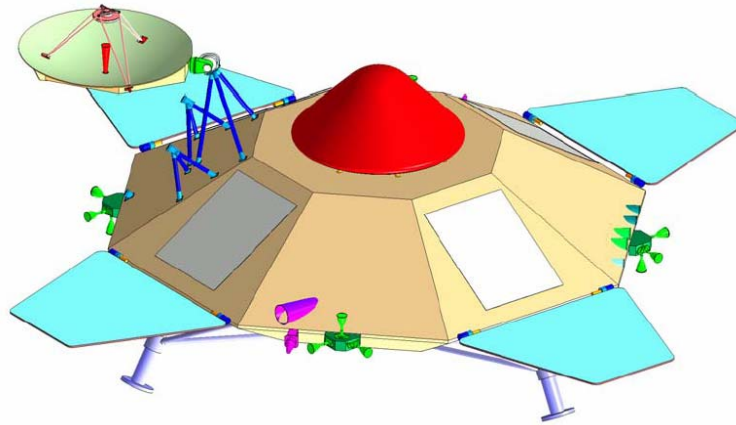


Figure 23: “Mono-block” OLERV baseline design

The OLERV is octagonal-shaped, fully integrated (i.e. orbiter and lander) and fits within the Soyuz fairing when the SA and the HGA are folded. Splitting the OLERV in two parts and jettisoning a Surface Sampling Module (including equipment which is not required for return) would save mass and is an alternative configuration. However, decoupling the SSM of the main S/C has disadvantages from a thermal viewpoint and complicates operations hence the selected mono-block concept. The spacecraft structure is made of 8 shear walls and a central floor (honeycomb aluminium) which carry the loads. The central part of the spacecraft is an 800 mm diameter cylinder which is left free for the sample transfer mechanism. This UFO-shaped design allows to have a low CoG which is highly beneficial at landing. In addition, the shape selection is also driven by the fact that such a design has advantages from a thermal viewpoint. The radiators are less exposed to the IR flux from the asteroid surface with respect to a classical box-shaped configuration and even though the bottom area is larger than for a classical design, the overall thermal budget is favourable to this configuration. The following alternative is also possible and leads to a reduced total mass budget of 2237 kg (because less mass has to be brought back to Earth) but was discarded due to thermal drawbacks (decoupling of the two stages leads to heavy heating of the SSM) and increased complexity (SSM jettisoning).

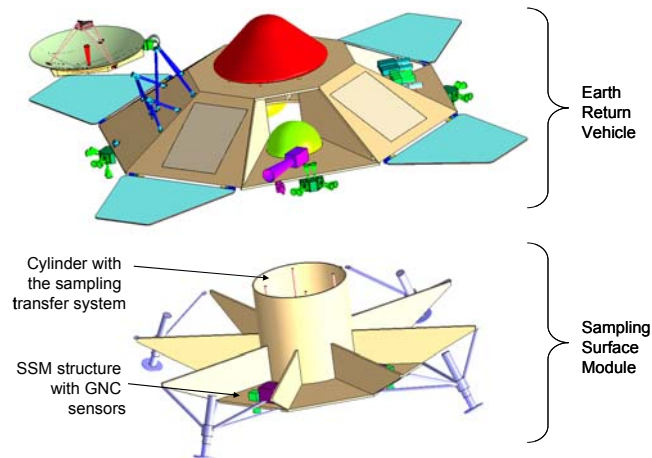


Figure 24: Alternative OLERV design - separation of the sampling module with the return vehicle

6.5 Propulsion

6.5.1 PROPULSION MODULE

Since the PRM's main task is to provide high-thrust and large ΔV to the orbiter-lander-ERV module, its design is entirely tackled in this section. In view of keeping both cost and development time at a low level, the LISA-Pathfinder PRM, under development, is considered. Its characteristics seem to adequately fit with the needs of this application and are depicted below. It has to be strengthened though due to the increased wet mass of the OLERV (703 kg) with respect to the LISA-PF design specification of 500 kg. The main equipment of LISA-PF PRM is suitable for an interplanetary transfer since it is initially based on the Rosetta orbiter.

Table 29: Propulsion Module technical features

Characteristics	Value	Comment
Dry mass	210 kg	Incl. 5% mass margin
Size	2m (height) x 2m x 1.7m (transversal)	
Total propellant mass	1380 kg	
Wet mass incl. all margins	1595 kg	Without 20% system margin
ΔV requirement	~ 2550 m/s	Total outbound ΔV (see chapter 6.1.4)
Engine configuration	Main 440 N EADS-ST EAM + 2x200N ATV thrusters	Main engine in development. Available by 2010
Maximum thrust	840 N	To limit gravity losses to 8-9 %. This high thrust leads to strengthening of the SA and HGA attachments
Isp of the main engine	323 s	300 s for the ATV thrusters
AOCS system	3-axis stabilized with 8 x 10 N reaction thrusters	
ΔV capability	3100 m/s	For a 500 kg payload
Tank resizing capability	Up to 2500 kg of propellant	

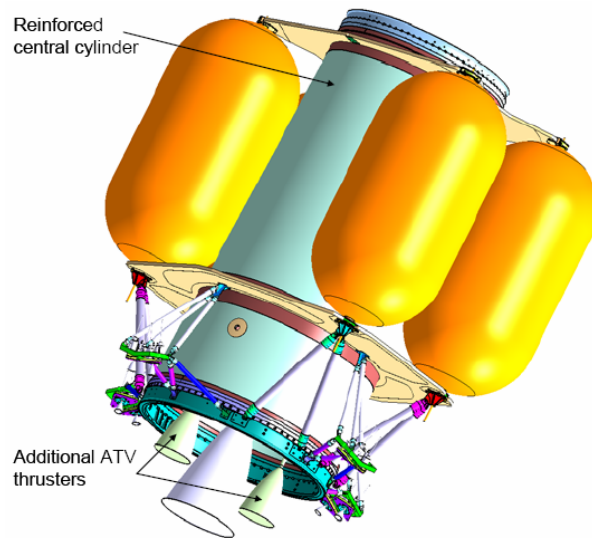


Figure 25: Propulsion Module design

6.5.2 OLERV RCS

For the reaction control system of the OLERV, three options were investigated: Hydrazine mono-propellant, MMH/NTO bi-propellant, Hybrid bi-propellant + Helium cold-gas systems. The total mono-propellant mass ($I_{sp} = \sim 220$ s) which is required is 199 kg, broken down into 22.26 kg for proximity operations (~ 70 m/s) and 176.74 kg for return ΔV (~ 640 m/s). It is the heaviest solution in terms of propellant. Nevertheless the CPS total wet mass is 23 kg heavier than a bi-propellant system and 65 kg lighter than the hybrid solution. Contamination analysis on the bi-propellant option showed that there is a risk of contaminating the landing area, therefore, it is selected-out even though, for a mass-constrained design, this option could be traded again (by choosing the proper last burn altitude). The hybrid solution is the most complex and heavy one. Therefore, the mono-propellant option is selected as a good compromise between low-mass, cost, reliability and low or no contamination (no organic compounds in the exhaust plume). Its architecture is shown below (number of thrusters is not representative).

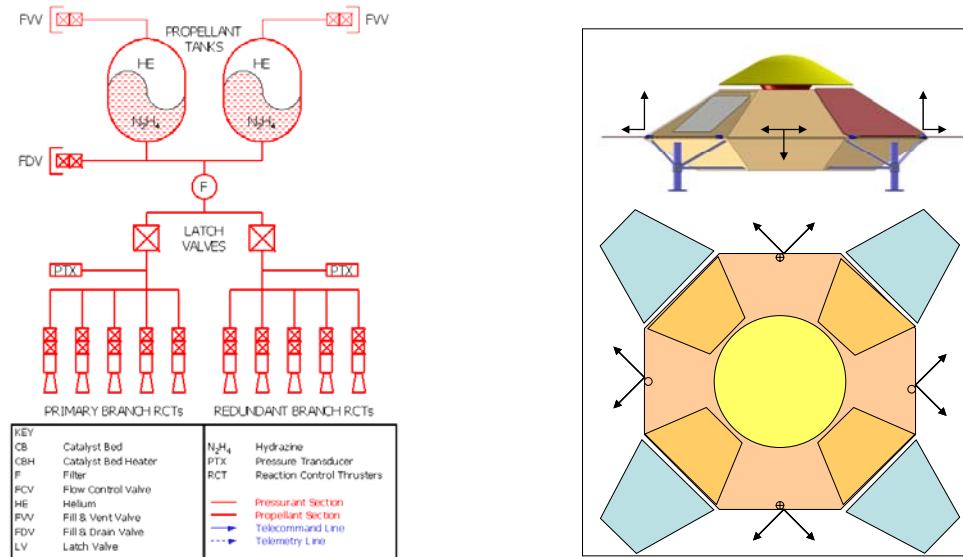


Figure 26: RCS thrusters: functional architecture and configuration

The RCS system must have a minimum configuration of 8 thrusters for the envisaged operations. However, to avoid limitations due to the required very small ΔV , the baseline propulsion system has 12 x 10N RCS nozzles (plus a fully redundant branch) used for orbit and attitude control and return-to-Earth burn. The two thrusters pointing towards zenith are switched on when one of the legs detects impact in order to prevent bouncing and to counter-act the reaction forces created by the sampling itself (therefore providing 20 N). The originality of these thrusters is that they are also used to provide the return ΔV (low ΔV but long thrust-time due to the low thrust). Given these characteristics, the requirements on the OLERV CPS system are as follows:

Scenario	OLERV (2016+2020 opportunities)			
	ΔV	Isp (s)	Thrust (N)	Burn time
Observation	15.75	220	20	0 h 6.5 m
Landing, Sampling and Ascent	52.5	220	20	0 h 21.3 m
Return	593	220	20	3 h 27.7 m
Re-target	20	220	20	0 h 6.1 m
Total return ΔV	613			4 h 1.6 m
Total return + 5% margin	643.65			
Total OLERV ΔV requirement (incl. 5% margin)	715			

Table 30: OLERV RCS: ΔV and thrust requirements

The RCS mass budget is ~ 42 kg, 26.46 kg being required for the propellant tanks, 8 kg for the thrusters and the rest for latch valves, pressure transducers, pipes, filters, etc.

6.6 GNC and AOCS

6.6.1 EQUIPMENT

While the AOCS system for the interplanetary transfer and orbital operations is quite classical and benefits from past ESA planetary missions (MEX, VEX, Rosetta), the peculiar navigation hardware and software needed for landing is quite innovative with respect to Philae for example, mainly due to the required closed-loop navigation and control as presented in chapter 5.4. The OLERV must be equipped with a 3-axis stabilized AOCS system. It is to be mentioned that hazards (bigger than 10 cm) mapping is performed on ground based on NAC data and therefore so is defined the required landing accuracy and trajectory (guidance function) on ground in order to avoid them (no need for real-time hazard avoidance). Reaction wheels of 2.5 Nms momentum capacity are used for attitude stabilization needed for HGA pointing, platform stability during science observations, descent attitude control, and potentially to provide stiffness to the spacecraft at landing and avoid torques to be created on the S/C due to rotation of the SM. Full control of the S/C is therefore guaranteed by RW and the RCS system described in above section. Attitude may also be controlled on the surface through electro-mechanical adjustment of the legs extension. The AOCS equipment consists of: 2 STR, IMU, 2 WAC, 4 RW, 2 Sun sensors, 2 radar altimeters (baselined but not strictly mandatory). The IMU have classical specification and a limited drift which is compatible with a 3 h STR outage (descent and surface operations). The total mass of the AOCS equipment is 34.9 kg and the maximum power peak is 162 W mainly coming from the wheels (104 W) and the IMU (41 W).

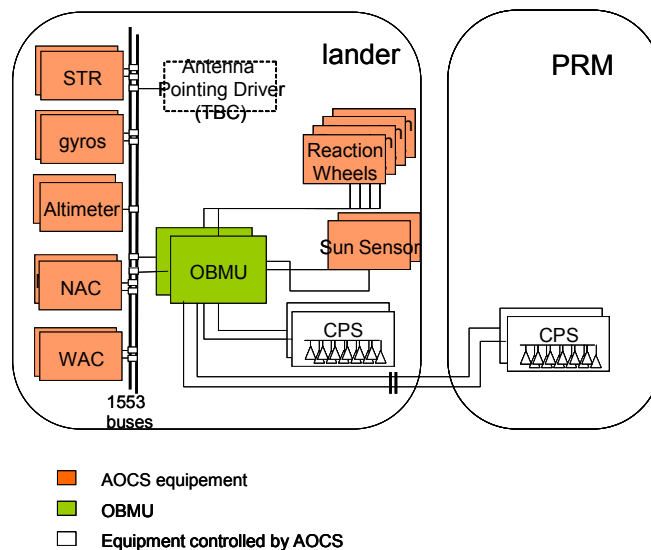


Figure 27: AOCS functional architecture

NAC is considered to be part of the science payload but is used as a GNC element for long-range target detection and approach and hazard mapping from orbit. All along the mission, the S/C can enter various AOCS modes. In addition to classical S/C AOCS modes, a number of mission-specific modes have been defined: the Collision Avoidance Mode (with the asteroid), the Descent and Landing Mode (corresponds to the autonomous descent trajectory), the Escape Mode (ascent

operations to put the S/C on a surface escape trajectory), the Surface Idle Mode (Surface Operations), the Take-Off Mode (initial impulse at surface take-off). In case an FDIR is triggered close to ground, the Escape mode is engaged before Safe hold mode.

6.6.2 SIMULATIONS AND PERFORMANCES

Taking into account the defined descent strategy and the AOCS and propulsion system, a number of simulations has been performed.

6.6.2.1 1-burn descent guidance strategy

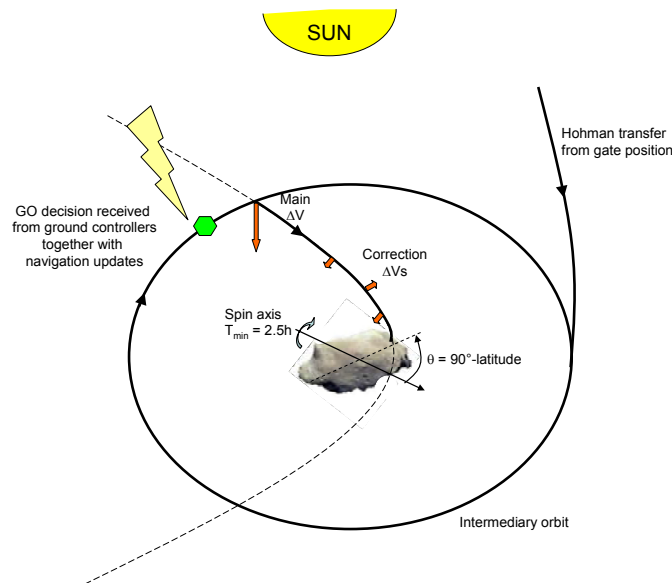


Figure 28: One-burn descent strategy - trajectory

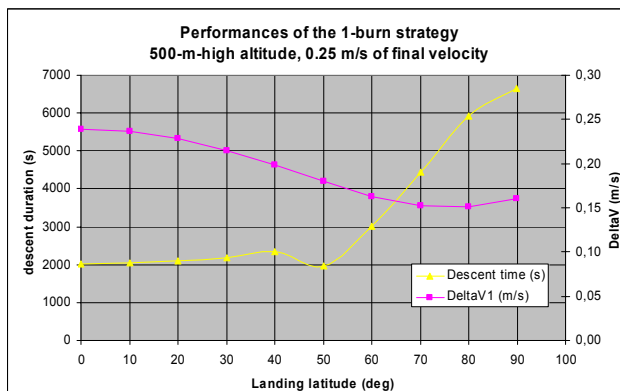


Figure 29: Influence of the landing latitude

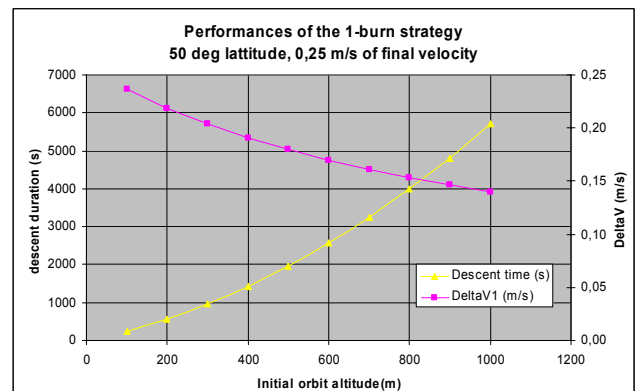


Figure 30: Influence of the initial orbit altitude

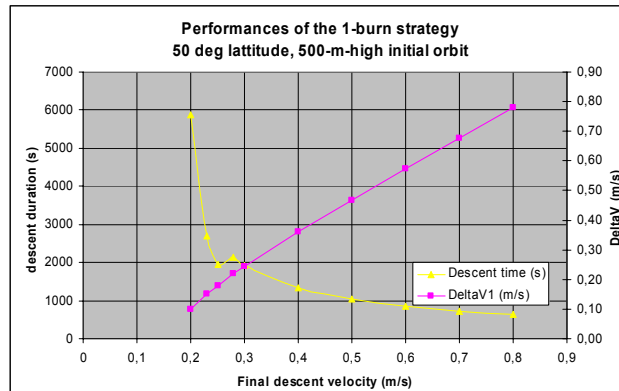


Figure 31: Final descent velocity

These three graphs show that a 500 m altitude and latitude limited to $\sim 60^\circ$ (Any value between -60 and 60° lead to reasonable descent duration) are the best compromise from a GNC standpoint in order to limit ΔV , descent duration and touch-down vertical velocity to 25 cm/s. The intermediary orbit has to be stable for at least 2 or 3 orbits (this leads to about 23 hours for a 500 m altitude orbit of a 700 m asteroid) so that the ground can feed the navigation loop appropriately. A too low altitude would lead to a rapidly unstable intermediary orbit. If the option of a last braking burn at 100 m is selected, the final vertical velocity would then become 15 cm/s.

6.6.2.2 Navigation for landing prior to descent

Prior to the descent, an asteroid terrain model is built via the WAC and NAC when the S/C is on its 4-6 km orbit. This model is used during the intermediary orbit and matched at various moments (t_i , t_{i+1} , etc.) with WAC images in order to estimate the initial S/C position and velocity in an asteroid relative reference frame. This matching is done on ground and therefore the S/C has to propagate the state estimation at the start of descent due to communication time.

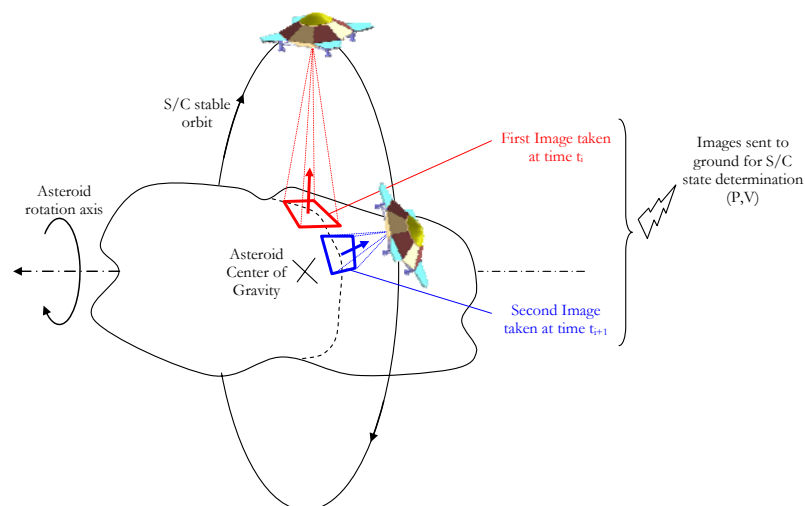


Figure 32: Position estimation via comparison with DEM model on ground

The across and along-track position and velocity errors after matching with the asteroid model can be derived. At first order, the position error depends on the navigation camera Line Of Sight Error (1 pixel at 500 m).

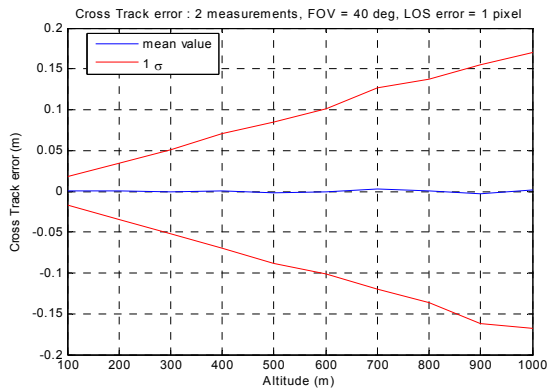


Figure 33: Cross-track error

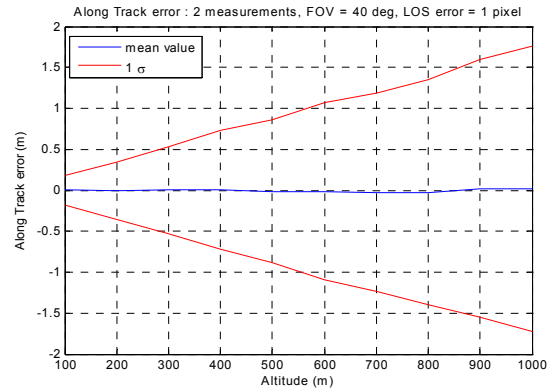
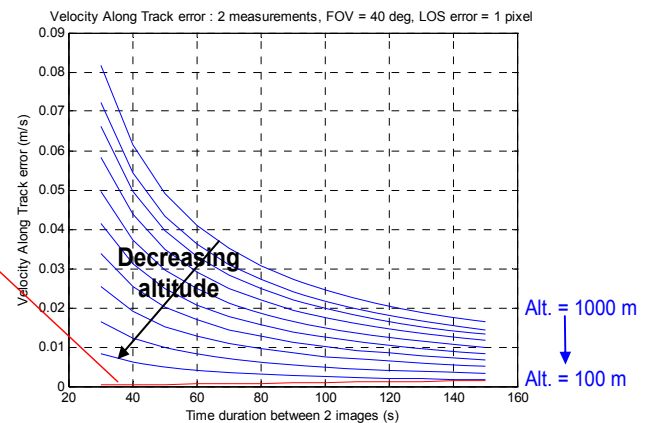
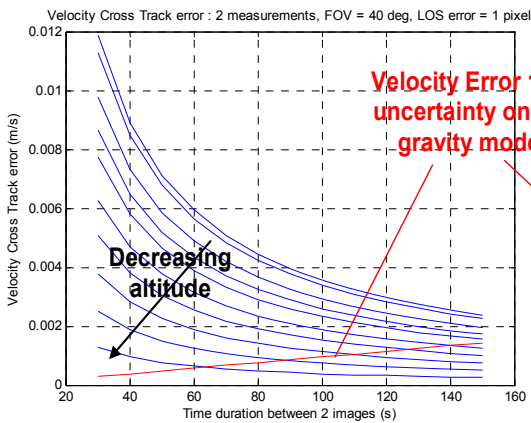


Figure 34: Along-track error

The velocity can be estimated and depends on the time between two consecutive images. The error on its estimation depends on the error due to position estimation (too short duration between 2 images) and on the uncertainty on the gravity field (too long duration between 2 images).

Figure 35: Velocity error - cross-track (left), along-track (right)



The filter needs to be initialised at the beginning of descent. This supposes that the onboard computer of the S/C needs to propagate the position error taking into account the communication time with the Earth. The summary of the expected errors at the beginning of descent is give below for a 40 min communication delay and a 50 s delay between 2 images.

Table 31: Navigation accuracy at landing departing from 500 m orbit

	Navigation accuracy from intermediary orbit at altitude 500 m	
	position error	velocity error
Along track	30 m (1σ)	0.012 m/s (1σ)
Cross track	4.5 m (1σ)	1.85 mm/s (1σ)

6.6.2.3 Navigation for landing during descent

The errors which will impact the final S/C state at touch-down with a vision-based system are the following: asteroid surface knowledge, shadow motion due to asteroid rotation, camera tracking errors. In order to minimize the first error, a DEM map has to be built with a ~ 35 cm accuracy (WAC resolution at 500 m), which is achievable with the specified NAC from 5 km altitude. The second contribution disturbs the tracking of the feature points used to estimate the velocity. It can be estimated as follows.

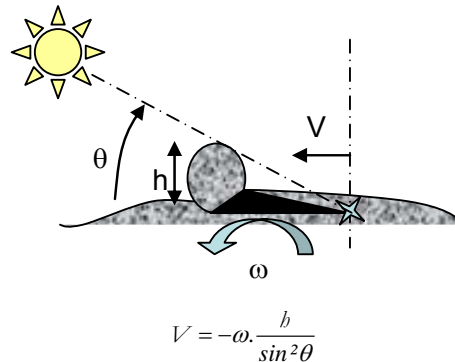


Figure 36: Shadow motion

ω is the asteroid rotation period

In a worst case 2 m rock, 20° Sun elevation angle and 2.5 h rotation period, it leads to a 1.2 cm/s velocity error. With boulder size smaller than 1 m and $\theta > 20^\circ$, the across-track velocity error is lower than 1 mm/s.

Lastly, the vision-based navigation relies on the tracking of a given set of feature points. When the points go out of the field of view, new points are tracked. During the tracking phase, the track of these feature points slowly drifts with respect to their initial positioning. This induces errors in the propagation of the vehicle states. In addition, the lateral position is controlled based on these estimated states. In order to limit the measurement noise, only 3 to 5 manoeuvres during the descent are implemented. In order to decrease the uncertainty on the position error (which would get thus worse over the descent than the initial 4.5 m error shown in Table 31), the states of the vehicle can be updated using real-time image recognition of known feature points with reference images coming from the DEM over the descent itself. This is a new feature with respect to the development performed in the frame of the NPAL development [Polle03]. This requires to store reference images and also places a high processing load on the CPU. Therefore, only 1 to 3 updates are done over the final descent which leads to very good landing performances. The process is illustrated on the graph below.

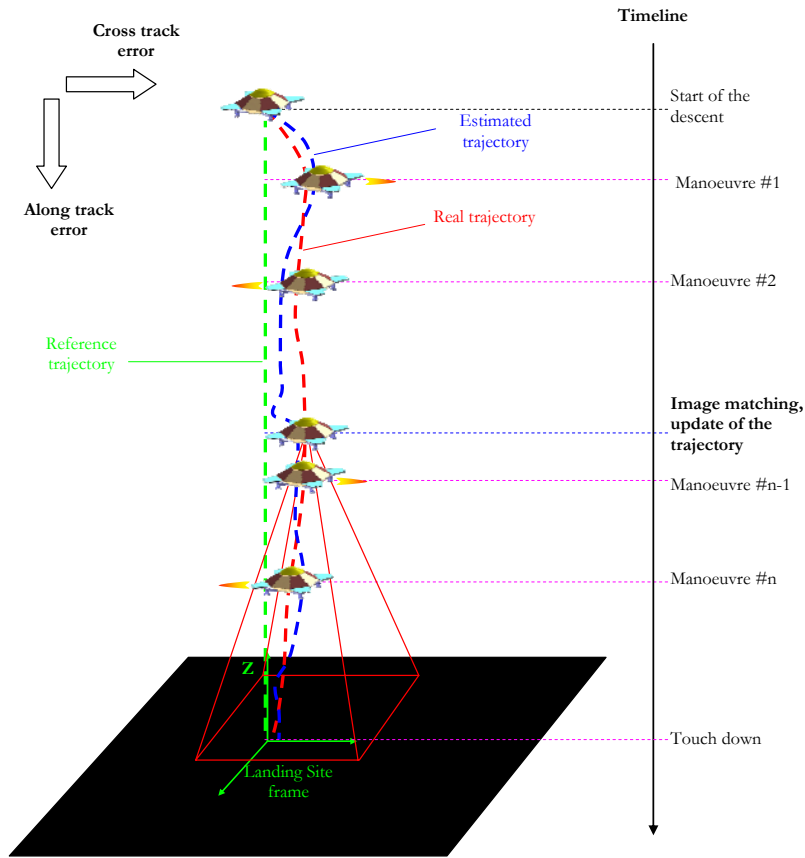


Figure 37: Descent vision-controlled trajectory

A Monte-Carlo simulation has been performed to obtain the final navigation performances at touch-down, using the following set of parameters:

Parameter	Value	
Initial position error	Along-track = 30 m (1σ)	Across-track = 4.5 m (1σ)
Initial velocity error	Along-track = 2 cm/s (1σ)	Across-track = 2 mm/s (1σ)
Thrust error	10% of thrust magnitude (1σ)	
Measurement error	0.1 pixel	
Camera features	FoV = 40°	1024x1024 matrix
Update of the vehicle state	One update at 1600 s	
Control manoeuvres	2 at 1100 s and 1620 s	
Visual measurement frequency	0.1 Hz	
Number of tracked points	2	
Number of simulation runs	1000	

Table 32: Monte-Carlo GNC simulation parameters

	Position Error	Velocity Error
Along-Track Error (1σ)	NA	1.7 cm/s

Cross-Track Error (1 σ)	3 m	5.4 mm/s
--	-----	----------

Table 33: Simulations results

These preliminary results show that the selected scenario is suitable for the given application. They could even be improved by increasing the number of tracked feature points or by implementing a Kalman filter to estimate the state of the vehicle. An altimeter would provide robustness and faster convergence of the estimation at the beginning of the descent and is selected because it also provides a direct collision avoidance capability but is not mandatory. The attitude estimation is entirely based on a classical dual gyroscope/STR measurement technique. In case of unavailability of STR measurements due to occultation by the asteroid, the long-term drift of the gyroscopes is limited such that its measurements are accurate enough throughout the whole descent and ascent phases to comply with a 10° maximum attitude angle at landing and the ascent operations. Attitude control over descent is provided by the RW.

6.7 Mechanisms

6.7.1 LANDING LEGS

6.7.1.1 Design

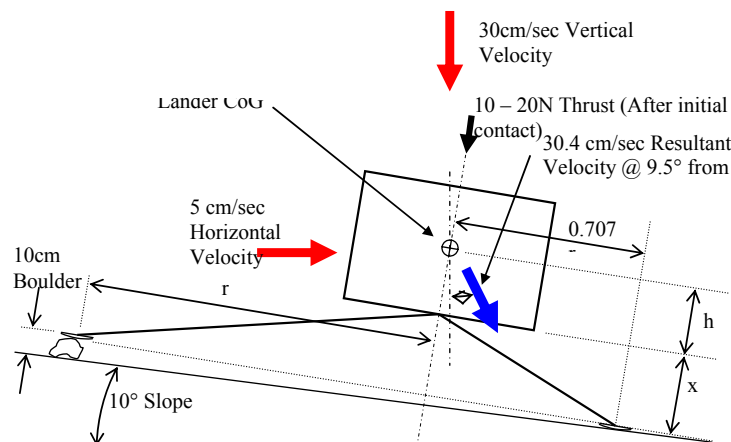


Figure 38: Worst case landing scenario

The schematic above illustrates the worst landing case with which the landing system has to cope with. The figures are derived from the requirements. Three landing legs options were assessed and analysed: Honeycomb damper, Philae landing leg type, ratcheting leg system. Honeycomb damping legs (Viking, Apollo) are more suited for planetary landings with harsher landing conditions due to their high damping capability. The drawback for this application, which needs to be further looked into is that it may not be able to cope with the multi-attempt requirement due to its high plastic behaviour. Philae landing legs are suitable for a 100 kg Philae-type of lander but may require large adaptation to the 700 kg lander which is here considered and also prevents the use of the selected sampling mechanism due to the central location of its main attachment point.

The ratcheting leg concept is well-suited and selected for the baseline concept. It can adjust its height on the surface, can rotate the lander in x and y direction, is compatible with the sampling mechanism and likely has the lowest mass of all. It is also able to cope with the worst case landing conditions while keeping the legs relatively short which avoids the use of a deployment mechanism. Its main drawbacks are the lack of heritage and its possible non-compatibility with an extended stay. Below is presented a graph illustrating the stability of the S/C at landing. It calls for a low CoG so that the footprint radius can be kept small and no deployment is needed.

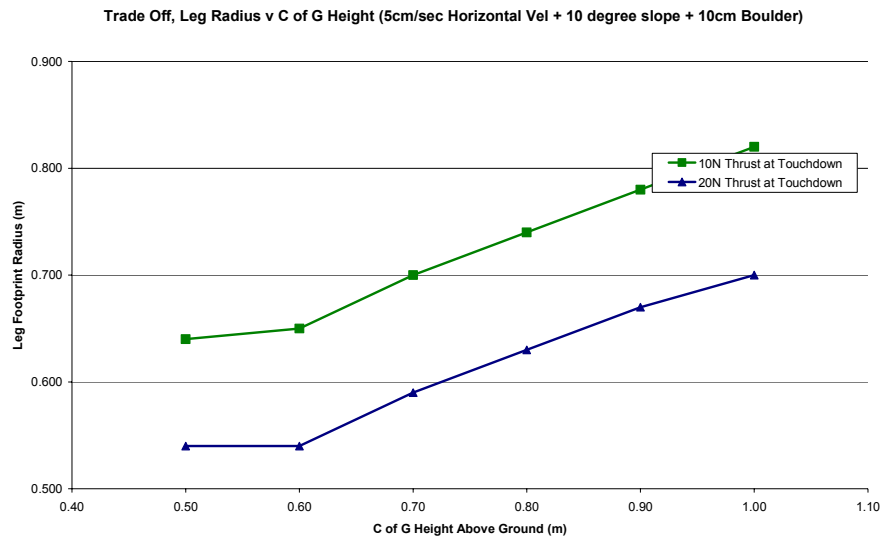


Figure 39: Landing legs required footprint to ensure stability at landing

The above graph shows that for a 1 m CoG height, the footprint radius must be > 0.8 m. The leg angle with respect to the vertical must be $> 15^\circ$ in order to avoid toppling torques considering the landing velocity orientation. These considerations lead to a footprint radius of 1.3 m.

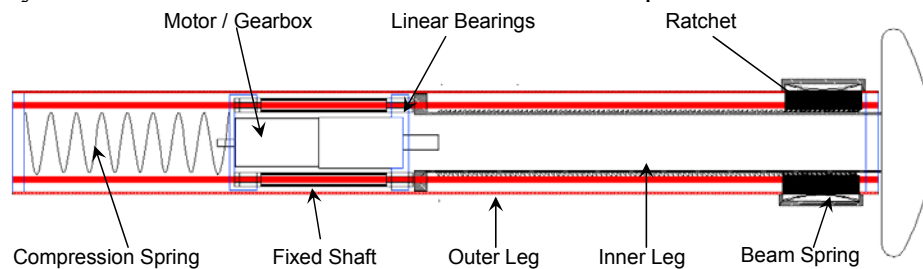


Figure 40: Ratcheting landing leg design

This system makes use of a spring and ratchet system to absorb and store the impact energy at landing. The energy of the impact pushes the inner leg up, compressing the spring and causing the ratchet mechanism to jump over the pitches. The motor may then be used to rotate the inner leg and level the lander to a proper attitude. It is also used to reset the inner leg to the deployed position for further landing attempts. Because the ratchet mechanism is a discrete system, the amount of energy stored in the spring between two pitches could be released after compression leading to a rebound and toppling. During compression, the spring is compressed until the springs equal the down-thrust force and the landing gear reaches equilibrium.

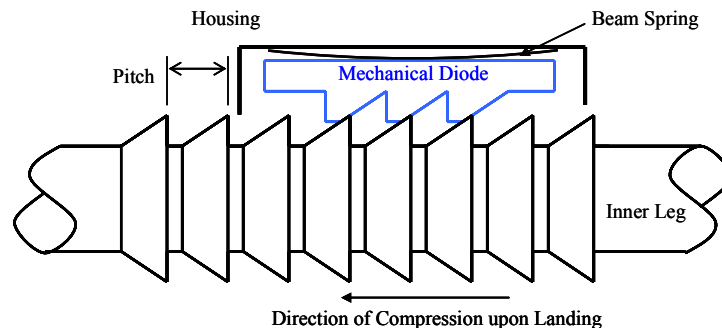


Figure 41: Worst case condition for bouncing-off the surface

The sizing of the legs is given by the worst case conditions (Figure 38). 11 cm spring compression is defined in order to limit the leg length. A landing leg dynamics has been modelled in Simulink allowing to size the springs in order to absorb the kinetic impact energy of 32.35 J. With a 450 N/mm beam spring constant and a 1250 N/m leg spring constant, the leg compresses by approximately 96mm in 0.6 seconds (with a constant down-thrust of 4x20 N). The total leg length is 529 mm. A 200 mm ground clearance is taken into account (400 mm in the vicinity of the sampling mechanism). In order to avoid the legs to be buried into the upper surface, proper design of the landing pads is also required. The motor needed to reset the leg for multiple landing requires a torque of ~ 6 Nm with margins to overcome the spring strength. For an input voltage of 6.3 V, the motor will reset the leg in 124 seconds and will consume 30 W. The leg materials used are mainly Aluminium alloy, stainless steel. The ratchet may use Phosphor Bronze. The total mass of the landing system is 29.3 kg with margins.

6.7.1.2 Stability analysis

In the worst landing case conditions (the thrusters being on at landing), the energy required to topple the lander is 3.18 J which is 3.5 times higher than the energy that the maximum horizontal velocity would bring to the lander at impact. A worst case scenario for toppling is when two legs store this energy and the two others do not have any pitch displacement. The energy stored in the spring (compression + beam) is 2.88 J in that case. This value is lower than the energy required to topple (3.18 J) but is relatively close to it, so attention shall be paid on this and pitch displacement should be possibly reduced. Nevertheless, the possible toppling situations cannot occur with the selected mechanism characteristics. In the presence of 20 N down-thrust and gravity, the maximum rebound height of the lander would be 28.7 cm if the 4 legs all have a maximum pitch displacement of 4 mm. This corresponds to an energy of 5.76 J.

6.7.2 SAMPLING MECHANISM

Following the selection of the sampling mechanism principles, the final design is presented here. The autonomous sampling acquisition payload is located at the bottom of the S/C and can operate within a few minutes and acquire up to 100 g at a time and up to 300 g in total by implementing multi-head corers. It consists of 3 corers, an articulated 4 dof arm equipped with a mandrel, drive electronics and cabling shown in the stowed configuration on the following figure. The coring tools are already in the sample container where the arm comes to pick it up or put it back after successful sampling.

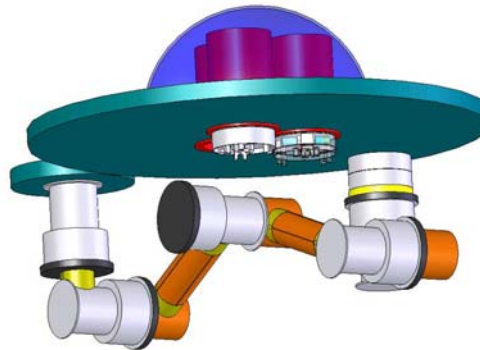


Figure 42: Sampling mechanism design

The tip of the mandrel is a latching interface and the connection to the coring tool is done via a motorized hook. The coring tool itself is 50 mm diameter x 100 mm height.

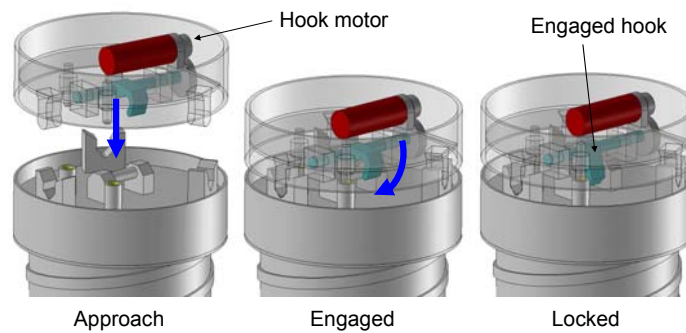
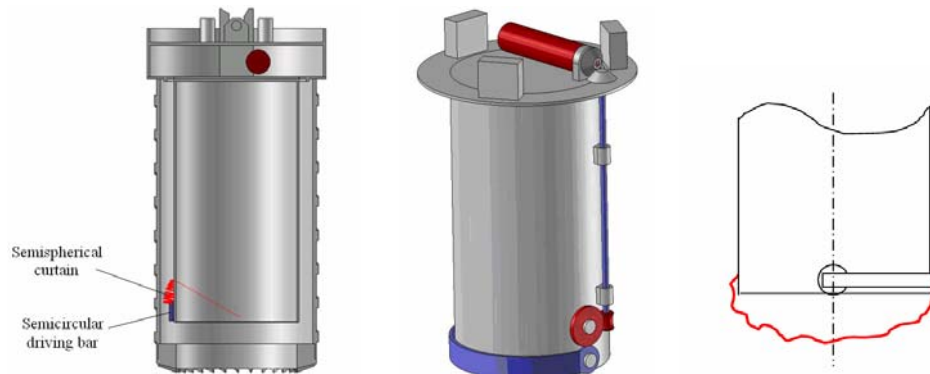


Figure 43: Sampling - Interface design of the coring tool

Three options are investigated for the closing device. One of them, an active “spherical iris” is presented here. When the sampling depth is reached, a motor is engaged. It mechanically rotates, via a shaft and a series of gears, a semi-circular bar which drives a curtain (initially folded) ensuring any kind of material (including loose regolith) remains in the tool. The curtain can be made of Tedlar for instance.

Figure 44: Corer closing mechanism – a possible design option



This particular system allows easy implementation of a verification system such as thin electrical wires or miniature optical diodes which can be inserted in the tool itself. The following figure illustrates the full sampling sequence. The initial positioning of the tool can be readily done in orbit.

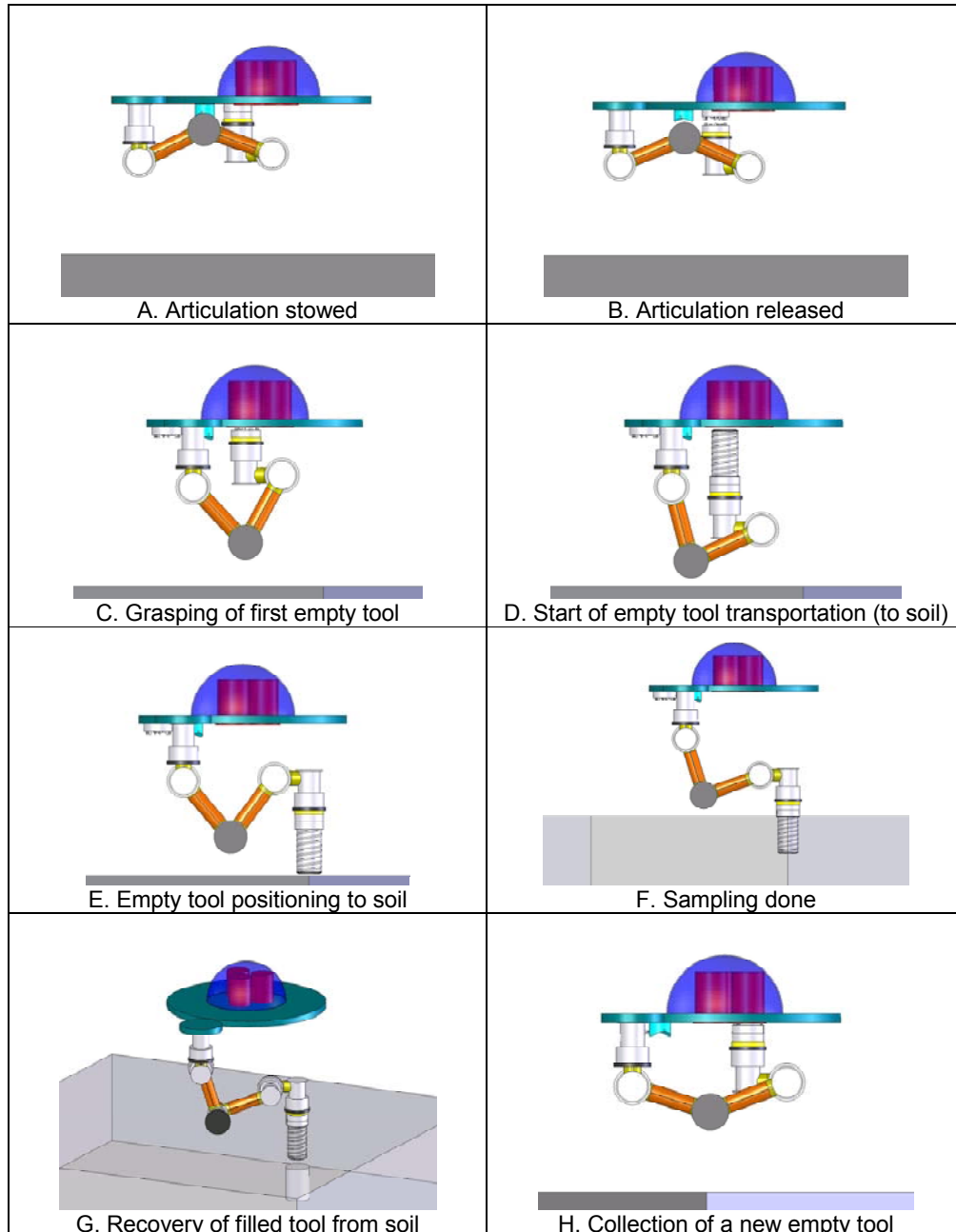


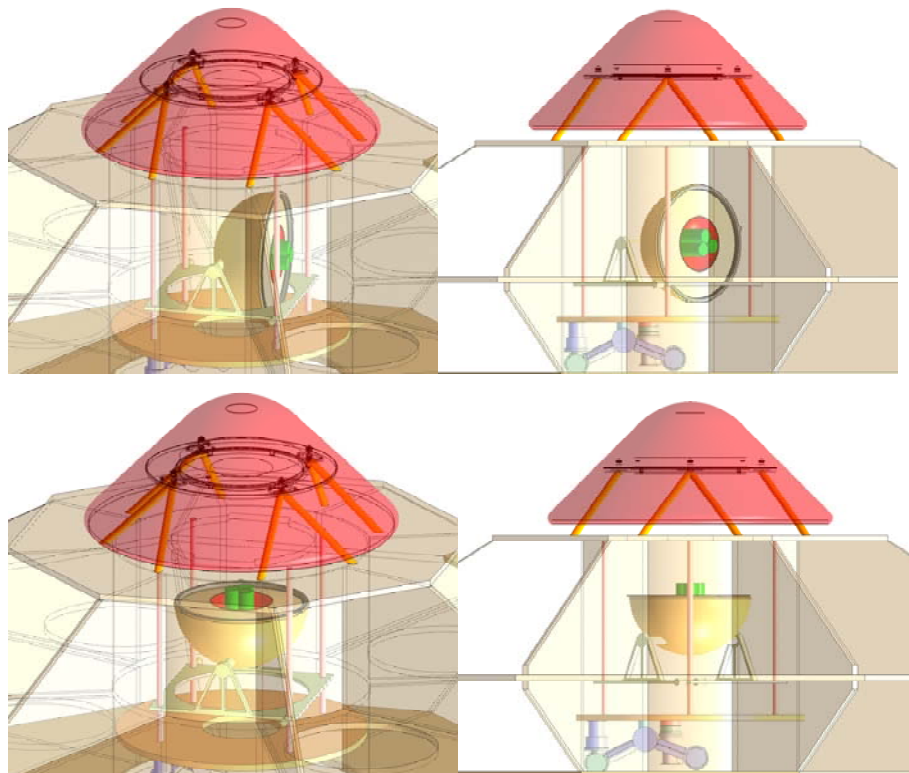
Figure 45: Sampling mechanism - deployment and sampling steps

The total required time for the previous operations is about 19.7 minutes (Sum of the actual sampling time (which can be 1-2 minutes) and the articulation moving time which depends on the specific design issues of the articulation). The total mass of the system is ~ 7.5 kg and its power

consumption is 9 W for tool free translation only and 20 W for coring operations at an advancing speed of 20 mm/min. The total required vertical thrust is well below 20 N.

6.7.3 SAMPLE CONTAINMENT AND TRANSFER

The three cylindrical corers are placed into a 200 mm spherical sample container due to the higher loads that can be withstood by a sphere-shaped body upon Earth hard-landing. No bio-hazard is expected as stated in [NRC98] and therefore no bio-sealing is required. The back-shell of the ERC is part of the sample transfer mechanism since it already contains the upper part of the container and the coring tools. When all coring tools are filled in, the back-shell of the ERC is translated for clearance, rotated by 180° and further translated up to the ERC where the multiple passive sprung loaded latches are actuated to seal the back-shell onto the ERC.



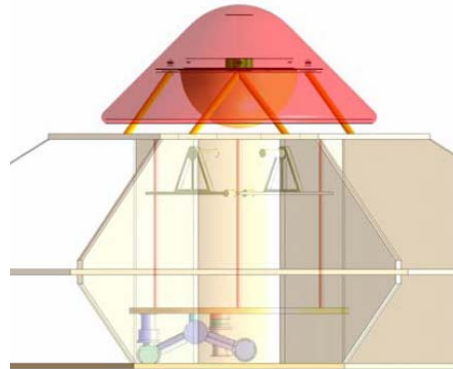


Figure 46: Sample transfer system - design and operations

The total mass and peak power of the transfer mechanism are ~ 24.8 kg and 48 W including margins.

6.8 *Earth Re-entry Capsule*

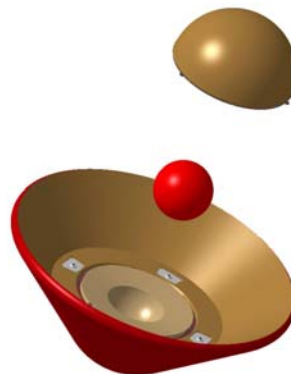


Figure 47: Earth Re-entry Capsule design

The Earth re-entry capsule contains the sample container to be returned to the Earth surface. It is designed as a passive spin-stabilized (by the OLERV) platform. The high-speed Earth re-entry calls for a deceleration system in order to decrease the loads at impact. Two options are available: active parachutes (Stardust approach) or passive inner shock absorber. A mass analysis was performed showing that parachutes do not bring any mass reduction to the system and are less reliable than a fully passive capsule which is designed for a hard landing. Therefore this latter option is selected making necessary the use of shock absorbing foam. This approach is under development for the MSR project. Simulations of the impact were used to size the overall shape, the energy absorbing foam and the TPS material. This is done for typical conditions of $V_{\text{entry}}=12.8$ km/s and $\gamma_{\text{FPA}}= 11^\circ$. One of these simulations is shown below.

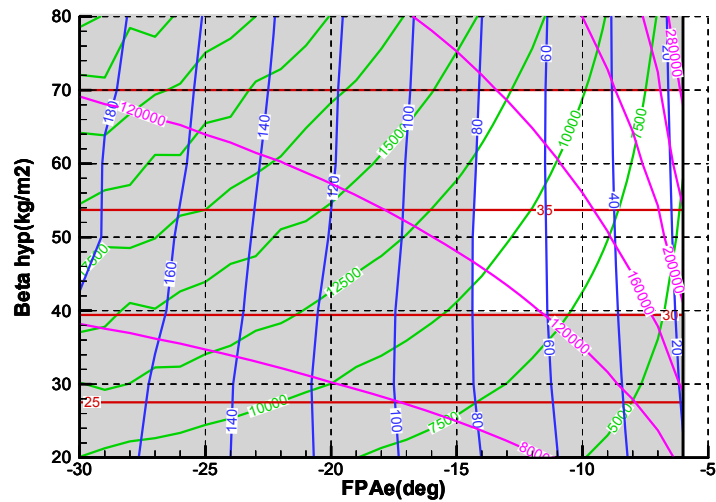


Figure 48: Sensitivity analysis of ERC entry parameters

Table 34 summarizes the characteristics of the ERC and the value of typical parameters during re-entry.

Table 34: ERC technical features

Characteristic	Value	Comment
Mass incl. 20 % margin	57 kg	
Diameter	1 m	
Nose radius	250 mm	
Shoulder radius	25 mm	
ERC half-cone angle	45°	
ERC CoG	24.8 %	If low density ablators are used, the CoG backs-up
Ballistic coefficient β	70 kg/m ²	
ERC interface	4 brackets	Also provides the required impulse to eject the ERC
Front-shield TPS material	Aléastrasil	Lightweight European PICA-like material is a possibility but requires new development and ballast of the ERC due to the backing of the CoG
Front-shield TPS thickness	18.75 mm on the nose, 12.5 mm on the cone	
Back-cover TPS material	Norcoat Liège	10 mm thickness on the lid and rear side
Landing velocity	~ 38.4 m/s	
Max acceleration during entry	~ 57 g	
Max total heat flux	~ 11 MW/m ²	
Max heat load	165 MJ/m ²	
Maximum landing load	2000 g	Achieved after 3 ms
Energy absorbing material	PU foam	
Foam thickness	100 mm	
Foam density	205 kg/m ³	! 52 kg/m ³ on the back-side

A 2 mm Norcoat Liège layer is inserted in between the front TPS and the main structure to limit the temperature of the energy absorbing material to 200°C. The front structure is a sandwich (carbon skins and aluminium honeycomb) while the impact shell structure is made of carbon skins.

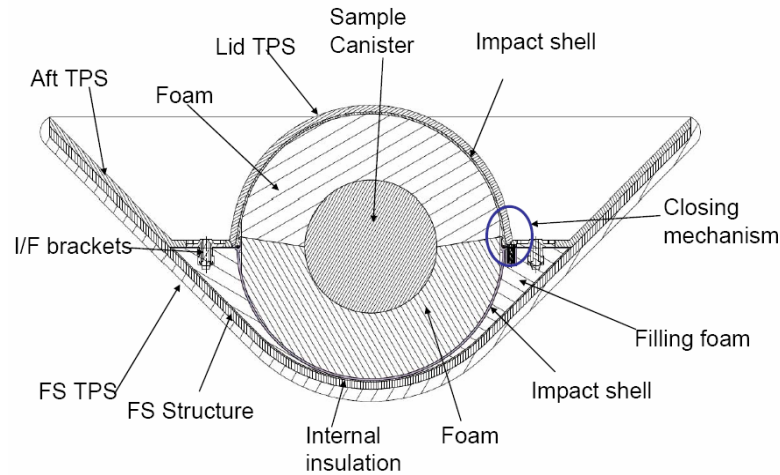


Figure 49: ERC accommodation and structure

Due to the arrival conditions, the landing site latitude is constrained to be $\pm 35^\circ$. A site such as the Woomera desert in Australia is suitable ($\sim 31^\circ\text{S}$). The site is constrained to be on ground rather than on the sea due to less complex and costly recovery operations and design of the capsule. The recovery time has to be short enough not to increase the temperature of the inner container above 40°C to preserve organics (critical for the envisaged landing in summer).

6.9 Thermal

For the baseline scenario, the driving requirements of the thermal control system are the landing operations on a sub-solar point of the surface, the thermal control of externally mounted units (thrusters, sampling mechanism) and a night stay on the asteroid (5.3). On one hand the spacecraft equipment has to be kept warm during cruise and observation phase. On the other hand, the spacecraft has to release thermal flux from the equipments (high emissivity) while not absorbing flux from the Sun (mainly visible) while on the surface. It can partly cope with this problem by selecting the appropriate radiator technology which minimizes absorption of the visible flux while have a high rejection ratio of the IR flux coming from the equipment. Silverised Teflon tape (emissivity: 0.81, absorptivity: 0.11) has suitable optical properties, with increased performance obtained using mirror tiles. However, these radiators will in turn absorb more of the asteroid IR flux on the surface. The UFO-like design of the S/C minimizes this flux since radiators are inclined away with respect to the vertical. Overall, the consequences are an over-sizing of the radiators for surface operations. The radiators will also thus cause under-cooling of the spacecraft in orbit, which in turn leads to larger heating requirement or a more complex radiator design with blind or thermal switches to reduce radiated power. The dissipating units within the spacecraft are mounted to the internal surfaces of the external panels. The spacecraft equipment temperature shows a proper behaviour through the selected thermal control system. The design leads to a radiator surface area of 1.74 m^2 which covers 17% only of the spacecraft angled area. The upper part of the spacecraft is covered with aluminised MLI Kapton (emissivity: 0.79, absorptivity: 0.49) while the bottom part is covered with VDA MLI Kapton (emissivity: 0.05, absorptivity: 0.14) to minimize IR flux from the asteroid.

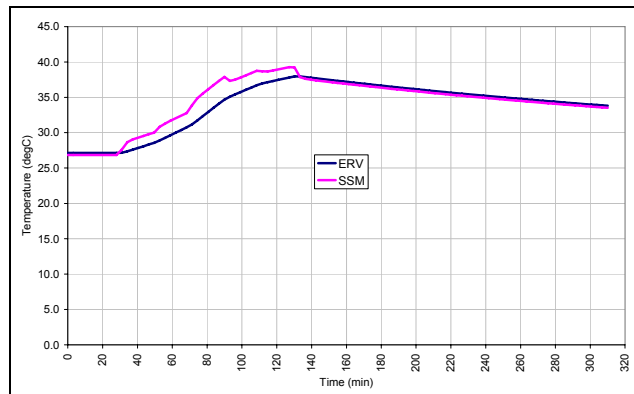


Figure 50: Internal spacecraft temperature variation with baselined thermal control

The geological features present on the body also have an impact on the thermal design due to the larger asteroid surface (in presence of hills for instance as discovered by the Apollo missions) exposed to the S/C.

The last but not least issue concerns the externally mounted equipment. For example the thrusters will be located at the edge of the spacecraft, away from the radiating surfaces, and the sampling equipment will be in the middle of the – z side of the spacecraft, exposed to the highest asteroid flux and the furthest from the spacecraft radiators. Their location makes it impossible to install radiators within their vicinity. An alternative is to use parabolic shaped radiators as used on the Apollo surface experiments ([Harris72]). The Apollo equipment thermal design for operating on the Moon had a thermal environment similar to that of an asteroid landing mission. The ALSEP radiator configuration reflects IR flux away using low emissivity parabolic surface and rejects S/C heat using high emissivity surface facing away from the asteroid as illustrated on the following schematic. This device is recommended for all thrusters. For the sampling mechanism, due its very close proximity to the asteroid surface and its mobility requirement the implementation of such a system is deemed difficult and it would be desirable to qualify the mechanism for the high temperatures it will be exposed to (~ 137°C), if possible. The total mass of the thermal control sub-system is ~ 24 kg. The power requirement to keep units within operational temperature range in orbit is 168 W.

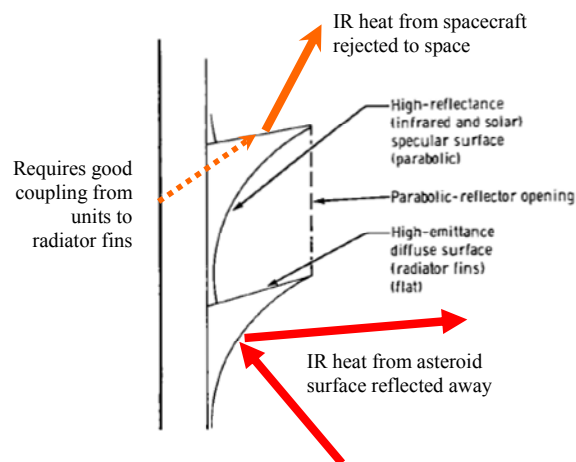


Figure 51: Parabolic-shaped radiators for externally-mounted equipment

6.10 Power

The spacecraft is equipped with 4 fixed solar array wings which can be deployed on one axis to provide power over most operational phases. They are covered with GaAs triple junction solar cells (BOL - EOL efficiency of 31% - 28% and radiation hardness >91%/year) and supplemented by Li-Ion batteries for launch (60 minutes), descent, surface and ascent operations (~ 2 h) and potential asteroid eclipses (4.5 h). The peak, on, Standby and off status for each equipment is analysed for 13 different “power” modes and lead to the power system budget presented in Figure 57. A maximum eclipse time of 4.5 h is defined at a 6-7 km altitude for the battery sizing even though it should not occur in current design (terminator orbit) but may happen if the S/C switches to safe mode. The required mass of the battery is thus 25 kg. The required battery mass for descent, landing and ascent operations is 13 kg. Therefore, the sizing provides plenty of margins for the surface operations (~ 2.5 h extra).

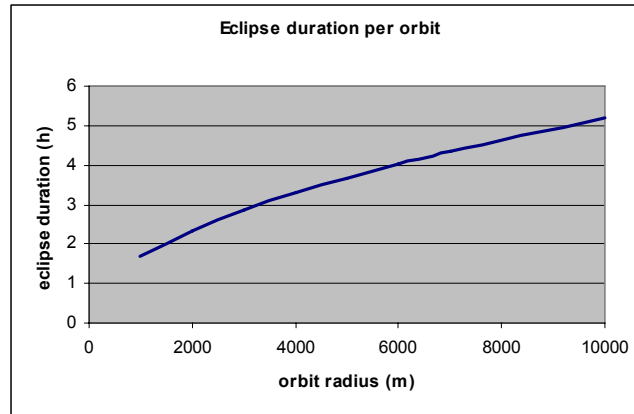


Figure 52: Variation of eclipse duration wrt orbit radius

It is assumed that in the arrays will be pointed at the sun (except in battery powered mode), with 2 degrees uncertainty, and will be the primary power source for operations and battery charging. The power system characteristics are listed below. An issue which ought to be kept in mind with the spacecraft configuration is that even partial shadowing of the arrays by the HGA could lead to complete down-power of one wing since the solar cells are mounted in row series on one panel.

Table 35: Power system characteristics

	Fixed Arrays	Units
Asteroid Orbit	Terminator	
Array Sizing Mode	Safe mode (At furthest location from the Sun during cruise)	
Array Area	3.47	m ²
Array Mass	11.8	kg
Battery Sizing Mode	Safe mode (Eclipse about the asteroid)	
Battery Energy	2465	Wh
Battery Mass	24.7	kg
Battery Volume	10500	cm ³

6.11 Data handling

The avionics system makes use of the technologies under development for the next generation of ESA solar system missions (BepiColombo, SOLO, ExoMars). For the 2016 and 2020 opportunities (respectively 1.03 and 2.87 years in solar maximum), a thin 2 mm Aluminium structure is sufficient to keep the radiation dose levels below 5 and 20 krads, which is a typical specification for space equipment and does not require rad-hard components. The data handling system (DHS) consists of the onboard computer, the mass memory system and the electronics necessary to communicate with and control the spacecraft.

The DHS consists of two LEON2 based computers. The internal and external data bus is based on MIL-STD1553 to re-use existing computer architectures. For the payload a SpaceWire network is proposed that will provide a flexible high speed interface that is capable of supporting all the instrument data rates, including the demanding vision-based camera requirements. The SpaceWire network can support the acquisition of raw instrument data enabling the science teams more flexibility in how the data can be processed. The TMTC units allow the ground segment to control the power and reset conditions of the equipments within the data handling system independently of the processors. The data processing rates involved with the NPAL system are high compared to earlier space missions. However in the low gravity environment of an asteroid the control loop for the AOCS system can be reduced from initially 20Hz to 1Hz (leading to a requirement of 45 MIPS), making suitable the LEON2 processor. Care must be taken to ensure that the NPAL system always receives prioritised access to the processor. During stages other than the descent, the processor may be switched into a low power mode to save power as it is not expected that the full performance of the processor will be required to service the instruments and AOCS system.

The mass memory must be sized to accommodate the data generated during imaging operations and housekeeping functions. The spacecraft will have an 8 hour timeslot each day to downlink data. The science operations must be sized to fit the available telemetry rate which is assumed to be 5.46 kbit/s for 24 hours. It is assumed that the number of images per day is limited to ensure that they can be down-linked at the next available downlink session and therefore minimise the mass memory requirements. In addition images will be stored at regular intervals during the descent. Based on calculation, this is not considered to be a driving requirement. The minimum mass memory size needed to ensure the telemetry windows are fully occupied will be 472 Mbits. In order to cope with burst measurements and to provide some margin the design a mass memory of 1 Gbit is proposed. When utilised for navigation image storage this provides the capability to store 85 raw uncompressed images in addition to the telemetry data for the day. The proposed mass memory size of 1Gbit will be defined as a size requirement and End of Life (EoL). The need to protect the memory from SEU adds 20% and to provide protection from single point failures, it will then be doubled. This yields a required mass memory of approximately 2.5Gbit.

The mass and power of the data handling system is mainly attributed to the implementation of the IO interfaces. The total mass of the OBDH is about 19.3 kg and the power requirement when operating in a non active mode is approximately 55W, which can increase to 70W during peak load, e.g. during science acquisition and processing of vision-based navigation.

6.12 Telecommunications

The sizing case for the communications system is the remote sensing phase where a data downlink rate of between 16.4kbps and 43.8kbps is required depending on the ground station contact duration (8 hours or 3 hours). An actively 1-axis pointed parabolic High Gain Antenna is used for direct X-band telecommunications with the Earth. A Ka-downlink is also implemented but only used for radio science but could also be used for data downlink if necessary. This could be revisited since Ka-band would provide a decrease in antenna mass (<10kg), in required communication downlink time (can be limited to 3 h) or in power requirements (36 W) or a combination of these. With the current configuration of the OLERV spacecraft the maximum diameter of the HGA is limited to ~ 1m. Otherwise, the HGA would interfere with solar panel deployment. It is in this case necessary to use 8 hours downlink and a high RF power for a feasible X-band link. The contact time can be reduced during other mission phases where the data rate is lower, for example for the cruise phase the day's data can be transmitted in 1.5 hours. The HGA is ~ 13kg. A LGA is also implemented for back-up. The X/X band transponder is 8 kg while the Ka band downlink only transponder is 1.5 kg. The total mass of the communication system is ~ 36.87 kg and requires an input power of 153.7 W (peak during landing and descent operations to transmit real-time data which is a requirement in order to understand where and how a potential failure could have occurred).

6.13 Ground segment and equipment

In terms of ground-tracking facilities, the 15-m dish of Perth can for example be used for LEO operations. A 34m ground station is assumed for the deep space operations (e.g. 2.4 AU when landing occurs). Cebreros (Spain) could be used thanks to its Ka-band receiving capability. New Norcia (Australia, near Perth) could also be envisaged since its upgrade to Ka-band is scheduled for Bepi-Colombo. A permanent science operations centre is needed to analyse data in real-time as of data reception, for fast science planning and immediate TC transmission (for instance for landing go decision, a very quick processing of data is required). This centre could be build upon the heritage which will have been gained for Philae's or Exomars operations. Another point to be mentioned and which has to be considered is the necessary ground recovery (UHF stations, containment truck, etc.) and receiving facilities to analyse science data from the sample. No bio-hazard containment facility (MSR) is required.

7 CONCLUSION

The present TRS concentrated on a technically feasible and scientifically meaningful mission profile for a cost-efficient sample return from a Near Earth Asteroid. This has resulted in a mission concept comprising of three building blocks: an outbound transfer propulsion module, a combined Orbiter-Lander-Earth Return vehicle which carries the last element, the Earth Re-entry Capsule. For cost-efficiency reasons, the system design study has put a strong focus on reducing the number as well as the complexity and technology horizon of the critical technologies, and to baseline existing technologies whenever available. The key enabling technologies listed in Table 36 are the ones which presently have a low TRL and require a proper development approach in order to fit with the overall mission programmatic with in particular a mission launch date in December 2016. Enhancing or elements under development are not listed here (e.g. highly efficient triple junction GaAs solar cells (31%), Space wire architecture, etc.).

Table 36: Enabling technologies for the selected asteroid sample return mission concept

Space element	Technology	Current TRL	Comment
Thermal control system	Parabolic shaped radiators or alternative technology	8 (US)	For externally mounted sub-systems (e.g. thrusters)
Landing GNC	Navigation camera and algorithm	4	The feature tracking algorithms as well as the hardware are under development to reach TRL 5 by 2009 [PLGTF05]
	Image processing algorithms for on-board real-time image recognition	2	Necessary new development for a vision-based navigation system to increase position accuracy
Landing mechanism	Overall leg concept (incl. landing pads)	2	No individual new technologies are needed. Design and development effort is required for the whole innovative concept (in particular stability analysis)
Sampling mechanism	Lightweight articulation	3	4 DOF arm + mandrel + slip ring + latching effector
	Coring tool	3	Actual sample cylinder
	Occluding mechanism	2	Need to bring about this element to the same level as the overall SM
Sample containment and transfer	Overall concept	2	No individual new technologies are needed. Design and development effort is required for the whole innovative concept
	Sample container	3	No bio-sealing functionality. In development for MSR (TRL 5 by 2009)
Earth re-entry capsule	Impact absorption device	2	(Only if the design was mass constrained, development of lightweight TPS material would also be required)

Many alternative mission objectives (e.g. extended surface stay) or targets (e.g. Wilson-Harrington 4015) can be envisaged, which raise other constraints resulting in different mission concepts. The NEA-SR TRS should therefore be considered as a reference concept, which aims to assist mission designers in assessing the technological complexity and challenges for NEA sample return concepts that need tailoring to fulfil an alternative set of objectives.

8 LIST OF ABBREVIATIONS

ACS	Attitude Control System
AIS	Asteroid In-Situ mission (e.g. no return leg)
AOCS	Attitude and Orbit Control System
APS	Active-Pixel Sensor
APXS	Alpha Particle X-Ray Spectrometer
ARD	Atmospheric Re-entry Demonstrator
ASR	Asteroid Sample Return
AU	Astronomical Unit
BOL	Beginning Of Life
CCD	Charge-Coupled Device
CDF	Concurrent Design Facility
COSPAR	COMmittee on SPACe Research
CPS	Chemical Propulsion System
CSG	Guiana Space Centre
CV	Cosmic Vision
DEM	Digital Elevation Model
DHS	Data Handling System
DOF	Degree of Freedom
DSM	Deep Space Manoeuvre
EGA	Earth Gravity Assist
EOL	End Of Life
ERC	Earth Re-entry Capsule (the capsule which actually performs the Earth atmosphere re-entry)
ERV	Earth Return Vehicle
ESS	Earth-Spacecraft-Sun
FDIR	Failure Detection, Isolation and Recovery
FOV	Field of View
GNC	Guidance, Navigation and Control
GSR	Ground Spatial Resolution
GTO	Geostationary Transfer Orbit (defined here as 200 km × 35,622 km altitude)
H&G	Hover&Go
HEO	Highly Elliptical Orbit
HGA	High Gain Antenna
HIPS	Highly Integrated Payload Suite
ICE	International Cometary Explorer
IEO	Interior-to-the-Earth Object
IR	Infra-red
ISAS	Institute of Space and Astronautical Science
ISS	In-situ Surface Science
LEO	Low Earth Orbit
LGA	Lunar Gravity Assist

LIBS	Laser-Induced Breakdown Spectrometry
MLI	Multi-Layer Insulation
MOID	Minimum Orbital Intersection Distance
MR	Mission Requirement
MSR	Mars Sample Return
NA	Not Applicable
NAC	Narrow Angle Camera
NEA	Near-Earth Asteroid
NEO	Near-Earth Object
NIR	Near-InfraRed
NPAL	Navigation for Planetary Approach and Landing
NRC	National Research Council
PHA	Potentially Hazardous Object
PRF	Pulse Repetition Frequency
PRM	Propulsion Module
OBDH	On-Board Data Handling
OLERV	Orbiter-Lander-Earth Return Vehicle
P/L	Payload
RCS	Reaction Control System
RSE	Radio Science Experiment
SA	Solar Array
S/C	Spacecraft
SEP	Solar Electrical Propulsion
SM	Sampling Mechanism
SoI	Sphere of Influence
SOW	Statement Of Work
SR	Sample Return
SRP	Solar Radiation Pressure
SSM	Surface Sampling Module
STR	Star TRacker
T&G	Touch & Go
TBC	To be confirmed
TBD	To be determined
TC	TeleCommand
TM	Transfer Module (or TeleMetry as per context)
TPS	Thermal Protection System
TRL	Technology Readiness Level
TRP	Technology Research Programme
TRS	Technology Reference Study
UV	Ultra-violet
WAC	Wide Angle Camera
WSB	Weak Stability Boundary
XRD	X-Ray Diffractometer
XRF-PIXE	X-Ray Fluorescence Particle-Induced X-ray Emission
ΔV	Delta-V

9 REFERENCES

- [Agnolon07I] Agnolon D., “Payload Definition Document”, ESA internal working document, draft 1.5, 12 April 2007
- [Agnolon07II] Agnolon D., “NEA-SR TRS: Mission analysis annex”, ESA public document, May 2007
- [Andersen03] Andersen A.C. & Al., “Bering: The first deep space mission to map asteroidal diversity origin and transportation”, RAST 2003: Proceedings of the International Conference on Recent Advances in Space Technologies, 20-22 November, 2003, Published by the Institute of Electrical and Electronics Engineers, Inc., 2003, p.241
- [Atzei06] Atzei A., “Margin philosophy for assessment studies”, SCI-A/2003/302/AA, issue 3.2, 11 December 2006
- [Ball02] Ball A.J. & Al, “SIMONE: near-Earth asteroid rendezvous microsattellites with solar-electric propulsion”, Proceedings of Asteroids, Comets, Meteors - ACM 2002, ESA Publications Division, 2002, p. 87 - 90
- [Bottke02] Bottke W.F. Jr. & Al., “The effect of Yarkovsky thermal forces on the dynamical evolution of asteroids and meteoroids”, Asteroids III, Bottke W.F. Jr, Cellino A., Paolicchi P., Binzel R.P. (editors), The University of Arizona Press, 2002, pg. 395-408
- [Britt05] Britt D.T. & the Gulliver team, “Sample return from Deimos: The Gulliver mission”, Lunar Planetary Institute, 68th annual meteoritical society meeting, 2005
- [Bus02] Bus S.J., Vilas F., Barucci M.A., “Visible wavelength spectroscopy of asteroids”, Asteroids III, Bottke W.F. Jr, Cellino A., Paolicchi P., Binzel R.P. (editors), The University of Arizona Press, 2002, pg. 169-182
- [Chapman04I] Chapman C.R., “The hazard of near-Earth asteroid impacts on Earth”, Earth and planetary science letters 222 (2004), 1-15
- [Chapman04II] Chapman C.R., “Space weathering of asteroid surfaces”, Annual Review of Earth and Planetary Sciences 32, P 539-567.
- [Chapman75] Chapman C. R., Morrison D., Zellner B., “Surface properties of asteroids: A synthesis of polarimetry, radiometry, and spectrophotometry”, Icarus, Vol. 25, pg. 104, 1975
- [CNES06] Presentation given on CNES NEA mission study concept at Near Earth Object Sample Return workshop, 29-30 March 2006
- [COSPAR05] COSPAR Planetary Protection rules, COSPAR/IAU Workshop on Planetary Protection, available at <http://www.cosparhq.org/Scistr/Pppolicy.htm>, updated 2005

[CV05] “Cosmic Vision, Space Science for Europe 2015-2025”, ESA brochure BR-247, 15 October 2005, available at <http://sci.esa.int/science-e/www/object/index.cfm?fobjectid=38542>

[Dainese06] Dainese C. & Al., “A cometary soil drill and sampler device”, *Aerotecnica Missili e Spazio* Vol. 85 4/2006

[Darrigo03I] D’Arrigo P. & Al., “APIES: a mission for the exploration of the main asteroid belt using a swarm of microspacecraft”, *Proceedings of the Fifth IAA International Conference on Low-Cost Planetary Missions*, 24-26 September 2003. ESA Publications Division, 2003, p. 55 - 62

[Darrigo03II] D’Arrigo P. & Al., “The Ishtar Mission: Probing the Internal Structure of NEOs”, *Physical Properties and Morphology of Small Solar System Bodies*, 25th meeting of the IAU, 23 July 2003

[DePater06] De Pater I. & Lissauer J.J., “Planetary Sciences”, Cambridge University Press, 4th printing, 2006, Chapter 9: Asteroids, pg. 331-365

[DonQuijote03] Don Quijote study team, “Don Quijote mission executive summary”, Executive summary of ESA study contract, 14 March 2003

[Gaffey89] Gaffey M., J. Bell and D. Cruikshank, “Reflectance Spectroscopy and Asteroid Surface Mineralogy”, *Asteroids II*, R. Binzel, T. Gehrels, M. Matthews (editors), The University of Arizona Press, 1989, pg. 98-127

[Goddard07] Information available on the NASA Goddard website at <http://www.nasa.gov/centers/goddard/news/topstory/2007/osiris.html>, updated 09 March 2007

[Gorevan06] Gorevan S., “Comet and Asteroid Sample Acquisition, Containerization, and Transfer for Sample Return”, *Spacecraft reconnaissance of asteroid and comet interiors*, 2006

[Harris72] Harris R. S., “Apollo Experience report – Thermal design of Apollo lunar surface experiments package”, NASA Technical Note, NASA TN D-6738, March 1972

[Harris98] Harris A. W., “A thermal model for near-Earth asteroids”. *Icarus* 131, pg 291–301, 1998

[Huber90] Huber M.C.E., Schwehm G., “Comet nucleus sample return: plans and capabilities”, *Space Science Reviews*, vol. 56, 1991, pg 109-115

[Jeffrey06] Jeffrey L. & Al., “Small body Sampling Techniques being developed at John Hopkins University Applied Physics Laboratory”, *International Astronautical Conference*, 2006, IAC-06-A3.5.04

[JPL07] JPL small body data base browser, available at <http://ssd.jpl.nasa.gov/sbdb.cgi>

[Kubota05] Kubota T. & Al. "Robotics and Autonomous Technology for Asteroid Sample Return Mission", Advanced Robotics, ICAR '05. Proceedings, 12th International Conference, 18-20 July 2005, pg 31-38

[Marov04] Marov M.Y., "Phobos-Grunt: Russian sample return mission", Advances in Space Research, Vol. 33, Issue 12, 2004, pg. 2276-2280

[MSRCDF03] CDF team, "MSR CDF study", internal ESA report, August 2003

[NEO] NASA's Near-Earth Object Program website, <http://neo.jpl.nasa.gov/neo/life.html>, last updated 2007

[NEOMAP05] "Target selection for the Don Quijote mission", Report to ESA, February 2005

[Noble05] Noble S.K., "Space weathering on asteroids", Workshop on Oxygen in Asteroids and Meteorites, held June 2-3, 2005 in Flagstaff, Arizona, LPI Contribution No. 1267., p.25, June 2005

[NRC98] National Research Council, Task group on sample return from small solar system bodies, "Evaluating the biological potential in samples returned from planetary satellites and small solar system bodies: framework for decision making", National Academy Press, Washington DC 1998

[Nygren00] Nygren W.D., "Rapid Remote Sample Collection Mechanism for Near-Earth Asteroid Sample Return", Near-Earth Asteroid Sample Return Workshop, p. 32, January 2000

[Pieters99] Pieters C., "Aladdin: exploration and sample return from Phobos and Deimos", Lunar Planetary Institute, Lunar Planetary Science, 1999

[PLGTF05] Statement of work of the "Precision Landing GNC test facility", ESA TRP activity, issue 1.1, 07 June 2005

[Polle03] Polle B. & Al., "Autonomous On-Board Navigation for Interplanetary Missions", 26th Annual AAS Guidance and Control Conference, Breckenridge, CO, USA, 5-9 Feb. 2003

[Rafeek00] Rafeek S., "NEA touch and go surface sampler", NEA sample return workshop, 2000

[Renton06I] Renton D., "Deimos Sample Return TRS executive summary", ESA-ESTEC, Executive summary of ESA study contract, 08 February 2006

[Renton06II] Renton D., "NEA-SR TRS Mission objectives", SCI-A/2005/300/NEA, issue 1.0, 17 January 2006

- [Renton06III] Renton D., “NEA-SR TRS Mission Requirements Document”, SCI-A/2005/30/NEA, issue 2.2, April 2007
- [Romstedt06] Romstedt J., “NEA-SR TRS Science Requirements Document”, SCI-A/2005/301/NEA, issue 2.1, 24 March 2007
- [Rivkin02] Rivkin A.S. & Al., “Hydrated minerals on asteroids: The astronomical record”, Asteroids III, Bottke W.F. Jr, Cellino A., Paolicchi P., Binzel R.P. (editors), The University of Arizona Press, 2002, pg. 235-253
- [Scheeres97] Scheeres D.J. & Al., “Rosetta mission: satellite orbits around a cometary nucleus”, Planetary Space Science, vol. 46, No 6/7, pg. 649-671, 1998
- [Scheeres02] Scheeres D.J., Marzari F., “Spacecraft dynamics in the vicinity of a comet”, Journal of the Astronautical Sciences, Vol. 50(1), pg. 35-52, 2002
- [SCI_A04] ESA SCI-A website available at <http://sci.esa.int/science-e/www/area/index.cfm?fareaid=65> , “Science Payload Instrument Section”, 2004
- [Sears04I] Sears D., “ The HERA mission: multiple NEA sample return”, Advances in Space Research, Vol. 34, Issue 11 , 2004, pg. 2270-2275
- [Sears04II] Sears D., “ The HERA NEA sample return mission: science requirements of the sample return collector”, Advances in Space Research, Vol. 34, Issue 11 , 2004, pg. 2276-2280
- [Soyuz01] User manual for Soyuz-Fregat, ST-GTD-SUM-01, issue 3, revision 0, April 2001.
- [Spohn01] Spohn T. & Al., “A heat flow and physical properties package for the surface of Mercury”. Planet Space Sci., pg 1571-1577, 2001
- [Sykes06] Sykes M.V., “PSI proposes a distant asteroid mission”, Planetary Science Institute Newsletter, Vol. 7, No. 2, Summer 2006
- [Tholen89] Tholen D.J. and Barucci M.A., “Asteroid taxonomy”, Asteroids II, R. Binzel, T. Gehrels, M. Matthews (editors), The University of Arizona Press, 1989, pg. 298-315
- [Vrancken06] Vrancken D. & Al., “Sealing and Sealing Monitoring System for Mars Sample Return”, 36th COSPAR Scientific Assembly, 16 - 23 July 2006, pg.1475
- [Yano06] Yano H. & Al., “Touchdown of the Hayabusa spacecraft at the Muses sea on Itokawa”, Science vol. 312, 2 June 2006
- [Yoshikawa06] Yoshikawa M., “Technologies for future asteroid exploration: what we learned from Hayabusa mission”, Lunar Planetary Institute, Spacecraft reconnaissance of asteroid and comet interiors, 2006

ANNEXES

OLERV dimensions and equipment accommodation

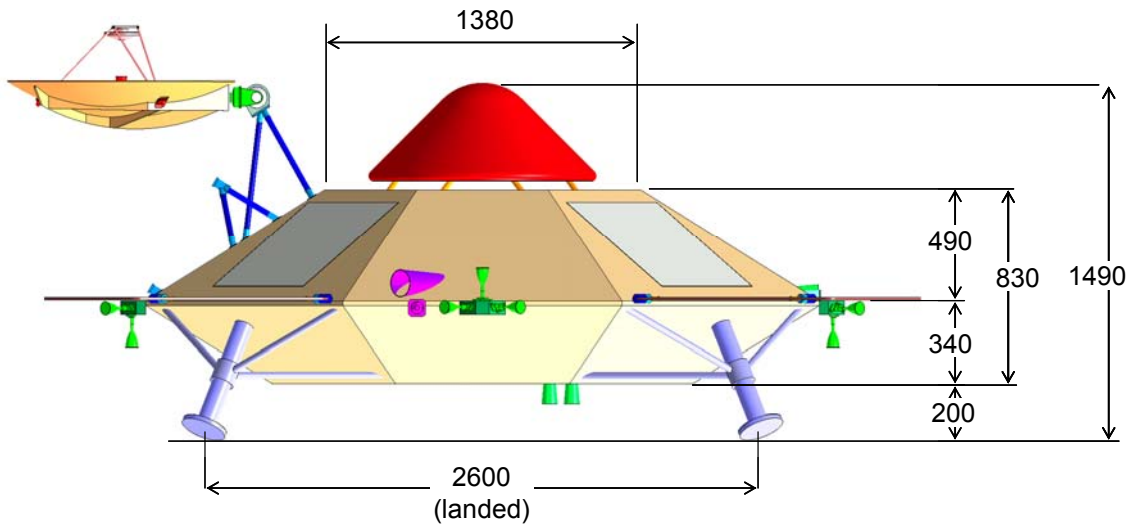


Figure 53: OLERV dimensions (side view)

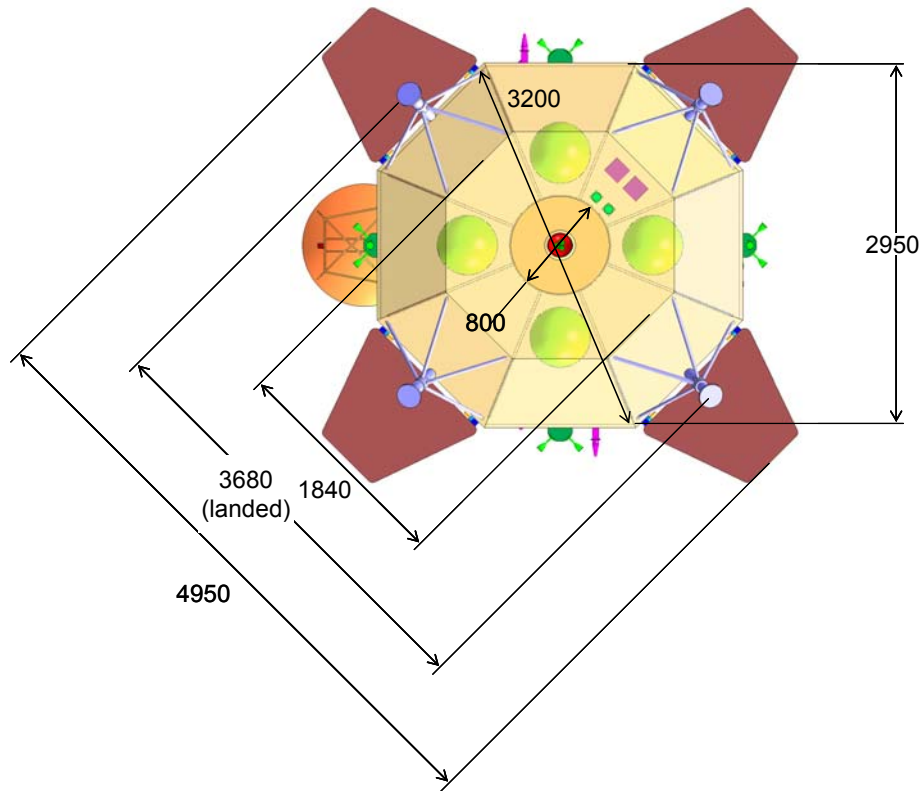


Figure 54: OLERV dimensions (top view)

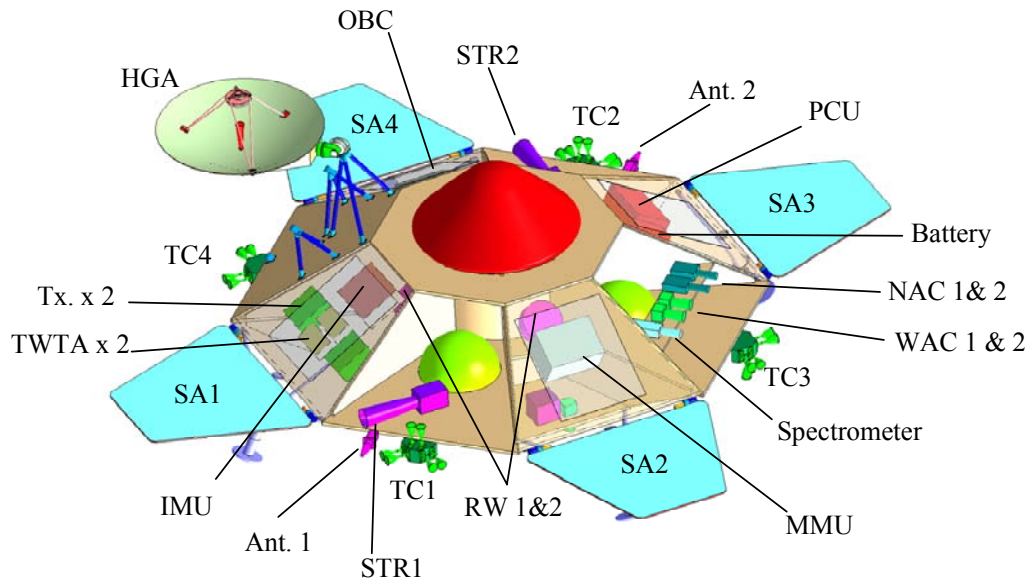


Figure 55: OLERV internal and external equipment accommodation

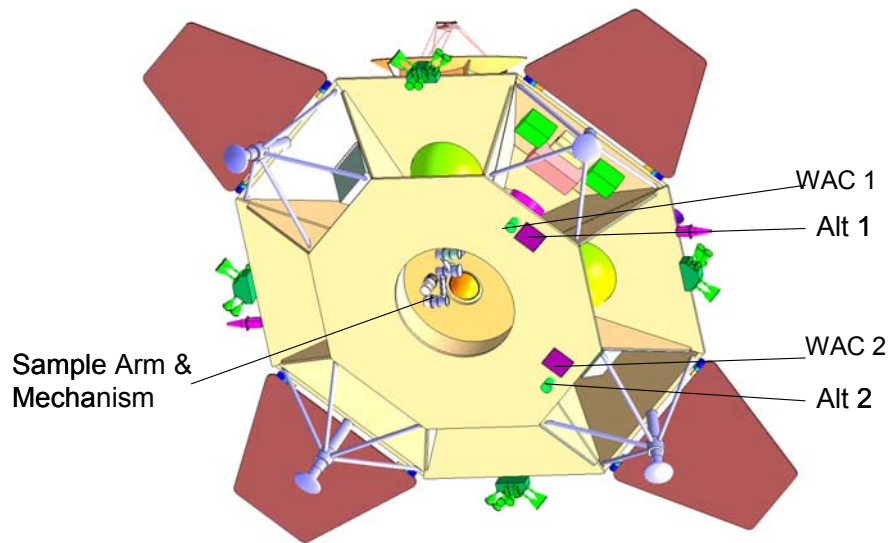


Figure 56: OLERV sampling and landing GNC equipment accommodation

Vega launch

Table 37: VEGA Launch margins

SAMPLE RETURN	Targets		199ju3 C	+Nereus C	+2002AT4 D	+1996FG3 C (binary)	+Wilson C
	C1 LSC-SEP	Capacity, Margin Mass Sco	617 -30% 0	617 -32% 0		617 -69% 0	617 -77% 0
C2 LSC-CP	Capacity, Margin Mass Sco	617 -89% 0	617 -224% 0		NP 0 0	NP 0 0	
C3 CPM/ERV	Capacity, Margin Mass Sco	617 -91% 0	617 -216% 0		NP 0 0	NP 0 0	
C4 SEPM/ERV	Capacity, Margin Mass Sco	617 -50% 0	617 -52% 0		617 -893% 0	617 -50% 0	
C5 pSEPM/ERV	Capacity, Margin Mass Sco	617 -61% 0	617 -63% 0		617 -904% 0	617 -61% 0	
C6 aSEPM/ERV	Capacity, Margin Mass Sco	617 -66% 0	617 -68% 0		617 0 0	617 -66% 0	
C7 OSC/ERV	Capacity, Margin Mass Sco	617 -87% 0	617 -89% 0		617 -930% 0	617 -87% 0	

TRL levels

Table 38: ESA TRL levels

TRL Level	Definition
1	Basic principles observed and reported
2	Technology concept and/or application formulated
3	Analytical and experimental critical function and/or characteristic proof of concept
4	Component and/or breadboard validation in laboratory environment
5	Component and/or breadboard validation in relevant environment
6	System/subsystem model or prototype demonstration in a relevant environment (Ground or space)
7	System prototype demonstration in an operational (space) environment
8	Actual ground system completed and (flight) qualified through test and demonstration (Ground and Space)
9	Actual system (flight) proven through successful mission operations